Fall 2012

Synthesis and characterization of new light emitting probes for sensitive detection of bio-molecules and live cells

Shyamala Pravin Pillai
New Jersey Institute of Technology

Copyright Warning & Restrictions

The copyright law of the United States (Title 17, United States Code) governs the making of photocopies or other reproductions of copyrighted material.

Under certain conditions specified in the law, libraries and archives are authorized to furnish a photocopy or other reproduction. One of these specified conditions is that the photocopy or reproduction is not to be "used for any purpose other than private study, scholarship, or research." If a, user makes a request for, or later uses, a photocopy or reproduction for purposes in excess of "fair use" that user may be liable for copyright infringement,

This institution reserves the right to refuse to accept a copying order if, in its judgment, fulfillment of the order would involve violation of copyright law.

Please Note: The author retains the copyright while the New Jersey Institute of Technology reserves the right to distribute this thesis or dissertation

Printing note: If you do not wish to print this page, then select "Pages from: first page # to: last page #" on the print dialog screen

ABSTRACT

SYNTHESIS AND CHARACTERIZATION OF NEW LIGHT EMITTING PROBES FOR SENSITIVE DETECTION OF BIO-MOLECULES AND LIVE CELLS

by
Shyamala Pravin Pillai

A variety of contemporary analytical platforms in technical and biological applications take advantage of labeling the objects of interest with fluorescent or luminescent tracers. Luminescent tracers take advantage of the unique property of some lanthanide metals to absorb and emit light. Long lifetime of lanthanide emission allows temporal gating of the signal, which avoids the short-lived background of interfering sample components. This property in combination with large Stokes shift contributes to extreme sensitivity of detection (ca. 10^{-13}-10^{-14} M), which makes lanthanide-based probes suitable for large variety of challenging tasks (e.g., intracellular detection of single DNA/RNA, or protein molecules, microbial pathogen detection in human specimens, tracing analysis, etc.). Luminescent probes include antenna fluorophore that absorbs light and transfers the excitation energy to a lanthanide metal tethered to antenna through chelation. The probe also contains crosslinking group that allows covalent labeling of the molecule of interest.

Despite great potentials of lanthanide-based tracers the wide spread of the technology is impeded by very high price of commercially available probes to their complex structure. The goal is to develop novel approaches for the synthesis of lanthanide probes with improved quantum efficiency. This work discusses development of new strategies for synthesis of antena-fluorophores, development of new methods for introduction of the crosslinking groups in the luminescent probes and elucidates the mechanisms of chemical reactions leading to principal synthetic intermediates.

New quinoline and quinolone based fluorescent compounds were synthesized, whose light emission can be conveniently tuned by simple structural modifications. Developed probes represent high-quantum yield, large Stokes shift fluorophores with amine-reactive and click-reactive groups convenient for conjugation. Some of these compounds can be used as sensitizers for lanthanide emission in design of highly sensitive luminescent probes. Obtained probes demonstrate efficient derivatization reactions allowing introduction of amine- or click-reactive crosslinking groups into the fluorophores. The reactivity of synthesized compounds is confirmed in reaction with low molecular weight nucleophiles as well as with click-reactive DNA-oligonucleotide counterparts. These reactive derivatives can be used for covalent attachment of the fluorophores to various biomolecules of interest including nucleic acids, proteins, live cells and small cellular metabolites. Synthesized compounds were characterized using NMR, steady-state and time-resolved fluorescence spectroscopy, as well UV absorption spectroscopy.

This work also discusses the development of fluorescent derivatives of the antifungal drugs, posaconazole and caspofungin, for diagnostic imaging of fungal cells. Invasive fungal infections (IFI's) are a growing threat to human health particularly, with increase in the number of immune-compromised patient population, such as organ transplant recipients, allogeneic BMT, hematologic cancers; AIDS etc. The diagnosis of fungal infections is a complicated task and requires a combination of clinical observations, laboratory investigation, and radiological or other diagnostic imaging methods. Only 25% of IFI cases are diagnosed pre-mortem due to the current diagnostic challenges, which justifies the development of express diagnostic procedures. To address the issue fluorescent derivatives of the antifungal drugs, posaconazole and caspofungin,

were synthesized. The fluorescent derivatives retained strong and highly specific binding to their cellular targets rendering the cells fluorescent. This new affinity-based approach strongly facilitates the detection of fungal pathogen thereby overcoming the current diagnostic challenges and can be used for clinical diagnostics. The power of this approach is not limited to fungal pathogens, but in fact represents a broader platform useful for detection of other classes of infections, both in the biological specimens and in the whole body using contemporary 3-D imaging approaches like fluorescence based *in vivo* imaging, luminescence imaging, positron emission tomography approach, and computer-assisted X-ray tomography.

SYNTHESIS AND CHARACTERIZATION OF NEW LIGHT EMITTING PROBES FOR SENSITIVE DETECTION OF BIO-MOLECULES AND LIVE CELLS

by
Shyamala Pravin Pillai

A Dissertation
Submitted to the Faculty of
New Jersey Institute of Technology
in Partial Fulfillment of the Requirements for the Degree of
Doctor of Philosophy in Chemistry

Department of Chemistry and Environmental Science

January 2013

APPROVAL PAGE

SYNTHESIS AND CHARACTERIZATION OF NEW LIGHT EMITTING PROBES FOR SENSITIVE DETECTION OF BIO-MOLECULES AND LIVE CELLS

Shyamala Pravin Pillai

Dr. Lev N. Krasnoperov, Dissertation Co-Advisor — Date
Professor of Chemistry and Environmental Science, NJIT

Dr. Arkady Mustaev, Dissertation Co-Advisor — Date
Assistant Professor of Public Health Research Institute Center, UMDNJ

Dr. Edgardo T. Farinas, Committee Member — Date
Associate Professor and Chair of Chemistry and Environmental Science, NJIT

Dr. Tamara Gund, Committee Member — Date
Professor of Chemistry and Environmental Science, NJIT

Dr. Haidong Huang, Committee Member — Date
Assistant Professor of Chemistry and Environmental Science, NJIT

BIOGRAPHICAL SKETCH

Author: Shyamala Pravin Pillai

Degree: Doctor of Philosophy

Date: January 2013

Undergraduate and Graduate Education:

- Doctor of Philosophy in Chemistry
  New Jersey Institute of Technology, Newark, NJ, 2013
- Master of Science in Chemistry,
  New Jersey Institute of Technology, Newark, NJ, 2008
- Master of Science in Physical Chemistry,
  University of Mumbai, Mumbai, India, 1995
- Bachelor of Science in Chemistry and Biochemistry,
  University of Mumbai, Mumbai, India, 1993

Major: Chemistry

Patents:

1. Simple no-chromatograph procedure for amine-reactive Eu^{3+} luminescent probes convenient for bioconjugation. Patent filed, 2012 (NJM 12-30).
2. Fluorophore chelated lanthanide luminescent probes with improved quantum efficiency. Published 07/21/2011, (WO2011088193), patent pending.

Publications:

Pillai, S., Krasnoperov, L., and Mustaev, A. "Simple no-chromatography procedure for amine-reactive Eu^{3+} luminescent chelates optimal for bioconjugation". *J. Photo chemistry and Photobiology B,* (2012). Accepted.

Pillai, S., Kozlov, M., Marras, S. A. E., Krasnoperov, L., Mustaev, A. "New Crosslinking Quinoline and Quinolone Derivatives for Sensitive Fluorescent Labeling", *J. Fluorescence,* (2012). Vol. 22, pp. 1021-1032.

Pillai, S., Kozlov, M., Marras, S. A. E., Krasnoperov, L., and Mustaev, A. "Synthesis and Characterization of New Cross-linkable Quinolone and Quinoline-based Luminescent Lanthanide Chelates". *J. Progresses in Nanotech and Nano Mat*, (2012). Accepted.

Pillai, S., Wirpsza, L., Kozlov, M., Marras, S. A. E., Krasnoperov, L., and Mustaev, A. "New Cross-linking Quinoline and Quinolone based Luminescent Lanthanide probes for Sensitive Labeling", *SPIE Photonic West proceedings* conference on Reporters, Markers, Dyes, Nanoparticles, and Molecular Probes for Biomedical Applications, Proc. SPIE 8233, 82331C, (2012).

Wirpsza, L., Pillai, S., Batish, M., Marras, S., Krasnoperov, L., and Mustaev, A. "Highly bright avidin-based affinity probes carrying multiple lanthanide chelates", *J. Photo chemistry and Photobiology B,* (2012). Vol. 116, pp. 22-29.

Pratt, A., Garcia-Effron, G., Zhao, Y., Park, S., Mustaev, A., Pillai, S., and Perlin D.S. "Evaluation of fungal-specific fluorescent labeled enchinocandin probes as diagnostic adjuncts", *J. Medical Mycology*, (2012). Accepted.

Pillai, S., and Bozzelli J.W. "Computational study on structures, thermochemical properties, and bond energies of disulfide oxygen (S–S–O)-bridged CH_3SSOH and $CH_3SS(=O)H$ and radicals", *J. Physical Organic Chemistry*, (2011). Vol.25, 6, pp. 475-485.

Oral Presentations:

"Fluorescent Derivative of Caspofungin and Posaconazole for Diagnostic Imaging of Fungal Pathogens", *244th ACS National Meeting,* August 19th -23rd, 2012, Philadelphia, PA.

"Highly Bright Avidin-based Affinity Probes Carrying Multiple Lanthanide Chelates for Ultrasensitive Detection of Biopolymers", *244th ACS National Meeting,* August 19th - 23rd, 2012, Philadelphia, PA.

"Novel Luminescent Lanthanide Probes - A Paradigm Shift in Labeling and Diagnostic Imaging", *TechConnect World, Summit and Innovation Showcase*, June 18th -21st 2012, Santa Clara, CA.

"Fluorescent Derivative of Caspofungin and Posaconazole for Diagnostic Imaging of Fungal Pathogens", *57th Annual Meeting of the New Jersey Academy of Science,* April 21st, 2012, East Orange, NJ.

"New Cross-linking Quinoline and Quinolone based Luminescent Lanthanide Probes for Sensitive Labeling", *BIOS SPIE Photonic West conference,* Jan 21st - 26th, 2012, San Francisco, CA.

Poster Presentations:

Wirpsza, L., Pillai, S., Marras, S., Kozlov, M., Krasnoperov, L., and Mustaev, A. "Development of long lived luminescent probes for ultrasensitive detection of biopolymers", *244th ACS National Meeting,* August 19th - 23rd, 2012, Philadelphia, PA.

Pillai, S., Pratt, A., Garcia-Effron, G., Zhao, Y., Park, S., Perlin, D.S., Krasnoperov, L., and Mustaev, A. "Fluorescent Derivative of Caspofungin and Posaconazole for Diagnostic Imaging of Invasive Fungal Pathogens*", International Society of Pharmaceutical Engineering,* April 19th, 2012, New Jersey Chapter.

Pillai, S., Pratt, A., Garcia-Effron, G., Zhao, Y., Park, S., Perlin, D.S., Krasnoperov, L., and Mustaev, A. "Fluorescent Derivative of Caspofungin and Posaconazole for Diagnostic Imaging of Invasive Fungal Pathogens*", Dana Knox Research Showcase,* April 4th, 2012, Newark, NJ.

Pillai, S., Wirpsza, L., Marra, S., Krasnoperov, L., and Mustaev, A. "Synthesis of New Highly Sensitive Light Emitting Probes for Biological and Technical Applications", Middle Atlantic Regional Meetings of The American Chemical Society, *42nd Annual Meeting on International Year of Chemistry,* May 21 - 24th, 2011, College Park, MA.

Krasnoperov, L., Wirpsza, L., Pillai, S., Marras, S., Kozlov, M., and Mustaev, A. "Development and Characterization of Novel Lanthanide-ion Based Luminescent Probes for Ultrasensitive Detection of Biopolymers", NACON, *8th International Meeting on Recognition Studies in Nucleic Acids,* Sept 12 - 16, 2010, UK.

Wirpsza, L., Pillai, S., Marras, S., Kozlov, M., Krasnoperov, L., and Mustaev, A. "Development and Characterization of Novel Lanthanide-ion Based Luminescent Probes for Ultrasensitive Detection of Biopolymers", *240th ACS National Meeting*, August 22 - 26, 2010, Boston, MA.

Additional Accomplishments:

1. Presented NJIT-UMDNJ's innovation Project, "Fluorescent and Luminescent Labels for Diagnostic Imaging and Sensitive Detection of Biopolymers" in a two day booth showcase at the *TechConnect World Conference*, 2012, Santa Clara, CA.

2. Presented the capstone project, "Fluorescent Derivative of Caspofungin and Posaconazole for Diagnostic Imaging of Invasive Fungal Pathogens", at *Alumni Reunion* Weekend, May 19th 2012.

3. Won 1st place in ISPE (New Jersey Chapter) Poster Competition for the project, "Fluorescent Derivative of Caspofungin and Posaconazole for Diagnostic Imaging of Invasive Fungal Pathogens".

To my beloved son, Mayaank and husband, Pravin
for their continuous support, encouragement and patience without which
this work would not have been accomplished

ACKNOWLEDGMENT

As I started this journey, I knew I was not walking alone. I take this opportunity to thank all who joined me, walked beside and helped me along the way. I take immense pleasure to express my deepest appreciation to Dr. Lev N. Krasnoperov and Dr. Mustaev Arkady, who not only served as my research advisors, providing valuable and countless resources, insight, but also constantly gave me support, encouragement, and reassurance. I wish to express my deep sense of gratitude for their consistent encouragement and support.

I would like to thank my dissertation committee members, Dr. Tamara Gund, Dr. Edgardo Farinas and Dr. Haidong Huang for their critical review and comments that contributed to this final dissertation. The author is exceptionally appreciative of Dr. Lev's research group; Laura Wirpsza, Manuvesh Sangwan and Beidi He for a very friendly atmosphere and encouraging conversations during my studies.

I would like to thank Dr. David Perlin from the Medical School of UMDNJ for allowing me to work with him in the development of a novel approach for the detection of invasive fungal infections.

I would like to deeply thank Ms. Clarisa Gonzalez-Lenahan for her timely advice and guiding me all the way to the completion of dissertation. Clarisa, thanks for being with me.

I would also like to thank Dr. Salvatore A. E. Marras from Public Health Research Institure, UMDNJ for helpful technical discussions and for allowing me to use their Quanta-Master 1 (Photon Technology International) digital fluorometer and nanodrop spectrophotometer.

I would like to extend my deepest gratitude to the coffee club at Public Health Research Institute, UMDNJ for their friendship and endless rounds of coffee and Lindt chocolates from Dr. Arkady. I will always miss those candy treats!

I would also like to thank my colleagues from Colgate Palmolive Co. Harsh Trivedi, Mahmoud Hassan and Sergio Leite for their friendship and mentoring. Harsh and Mahmoud, thanks for constantly reminding of my goal post.

Finally, I am forever indebted to my family members for their understanding, endless patience and encouragement when it was most required.

TABLE OF CONTENTS

TABLE OF CONTENTS
(Continued)

TABLE OF CONTENTS
(Continued)

TABLE OF CONTENTS
(Continued)

Chapter **Page**

TABLE OF CONTENTS
(Continued)

TABLE OF CONTENTS
(Continued)

LIST OF TABLES

LIST OF FIGURES

TABLE OF FIGURES
(Continued)

TABLE OF FIGURES
(Continued)

TABLE OF FIGURES
(Continued)

Figure **Page**

TABLE OF SCHEMES
(Continued)

LIST OF CHARTS

CHAPTER 1

INTRODUCTION

1.1 Background and Previous Studies

Fluorescent probes enable researchers to detect particular components in a complex biomolecular assembly with exquisite sensitivity and selectivity. Over the past few decades there has been remarkable growth in the use of fluorescence techniques in the biological sciences. Fluorescence spectroscopy and time-resolved fluorescence are considered to be primary research tools in biochemistry and biophysics (1). Fluorescence labeling is now a widely used technique in biotechnology, medical diagnostics, DNA sequencing, forensic science etc. There has been remarkable emphasis in the use of fluorescence for cellular and molecular imaging. In these applications, the fluorophore reporter groups are illuminated by visible or UV light, which leads to the absorption of light quantum and excitation of the molecule. The excited state is unstable and tends to relax either through dissipation of the absorbed energy by collision with other components in the medium or by emission of light. This light can be subsequently detected. Detection sensitivity is proportional to the number of the light quanta emitted by the fluorophore, which in turn is a linear function of the intensity of the excitation light. Therefore, for sensitive detection, high intensity light sources are employed. This creates the problem of discrimination of excitation and emission light, since even a small fraction of the excitation light that reaches the detector can cause significant background and decrease in detection sensitivity. This problem can be alleviated by using fluorophores with large spectral distances between excitation and emission light (Stokes shift). Commonly used organic fluorescent probes include fluorescein, rhodamine

101 (2), quinine bisulfide (2), Bodipy Fl and aminocoumarin.

Luminescent lanthanide chelates are valuable alternate probes to conventional fluorophores. Most lanthanide chelates possess the unique spectral property known as Luminescence (3, 4). The two most useful lanthanides, terbium and europium, have unusual spectroscopic characteristics, including millisecond lifetime, sharply spiked (few nm) emission spectra, and large (>150nm) Stokes shifts (5). Lanthanide emission results from transitions involving *4f* orbital, which are forbidden. As a result, the absorption coefficients are very low, less than 10 M^{-1} cm^{-1}, and emissive rates are slow, resulting in long lifetimes. The lanthanides behave like atoms and display line spectra (6). These characteristics enable temporal and spectral discrimination against background fluorescence, leading to the detection sensitivities of 10^{-12} – 10^{-15} M (7). Due to their weak absorption, lanthanides are usually not directly excited. In fact in luminescent lanthanide chelates, an organic chromophore acts as an antenna or sensitizer, absorbing excitation light and transferring energy to the lanthanide. This overcomes the inherently weak absorption cross section of the lanthanide. The excited lanthanide then loses energy either by emitting a photon or producing heat (phonons). The chelate serves several purposes: it provides a scaffold for covalently attaching the antenna in close proximity to the lanthanide, thereby facilitating the transfer of energy from antenna to lanthanide; it displaces water from the primary coordination sphere of the lanthanide, which would otherwise quench the lanthanide luminescence; and it also provides a scaffold for attaching a reactive group for coupling to biomolecules (5).

In some of the commonly known lanthanide probes like cryptase, LANCE, and terpyridine probes, the antenna is involved in binding the lanthanide; where as in polyaminocarboxylate chelates the antenna fluorophore and the chelating group are

separate entities. Nevertheless, all these four sets of probes are useful as detection agents and replace either conventional fluorescent probes or radioactive probes where subpicomolar detection limits have been achieved (8-12,5). Europium (Eu) and terbium (Tb) chelates are the most useful lanthanide probes. Dysprosium (Dy) and Samarium (Sm) are the other two lanthanides that emit in the visible region but with much weaker intensity (13).

Previous Studies

Coumarins in general are known to have widespread applications as photosensitizers (14), laser dyes (15-19) or pH indicators in biochemistry and medicine (20, 21). Consequently, a wealth of experimental and theoretical data on spectral-luminescence characteristics, photophysics and photochemistry of coumarin derivatives is available (14-41). However, considerably less attention has been paid to carbostyrils (2(1H)-quinolones) which are the aza-analogues of coumarins (15,23). Carbostyrils (aka cs124) has shorter absorption and emission wavelength as well as lower sensitivity to substituent effects. On the other hand, carbostyrils offer the advantage of greater chemical and thermal stability (42). Besides other applications, this makes them a possible candidate as wave-shifting fluorophores in high energy particle detection. This further encourages the use of carbostyrils such as 7-amino-4-methyl-2(1H)-quinolone (cs 124) as a sensitizing chromophor for lanthanide chelates. Carbostyril 124 is reported to allow a more sensitive determination of enzyme activity than other fluorophors (43). Selvin et al. (44), studies present the syntheses of DTPA conjugated with cs124 derivatives substituted on the 1-, 3,-, 4-, 5-, 6-, and 8-position. Among them, the DTPA chelate of cs124-6-SO_3H has been reported to have similar lifetime and brightness for both Tb^{3+} and Eu^{3+} compared to the

corresponding DTPA−cs124 complexes, yet it is significantly more soluble in water. The Tb^{3+} complex of DTPA−cs124-8-CH_3 has significantly longer lifetime compared to DTPA−cs124 (1.74 vs 1.5 ms), indicating higher lanthanide quantum yield resulting from the elimination of back emission energy transfer from Tb^{3+} to the antenna molecule.

As noted earlier, in contrast to coumarins only little systematic work concerning the spectral-luminescence characteristics of carbostyrils was done. Photophysical data of a reasonably large number of analytes can be found in work published by Ponomarev et al. (40,41). However, considering the increasing importance of tailor-made dyes in analytical, medicinal and biochemical applications we found it worthwhile to investigate the prospects of this important class of heterocycles as fluorophors in a more systematic manner. This work presents synthesis schemes, simplified synthetic strategies, reaction mechanisms and absorption and fluorescence spectral characteristics and quantum efficiency of the newly synthesized fluorophors and their lanthanide chelated probes.

The research focus further branches out to explore the possibility of coupling BODIPY fluorescent dye with fungal drug molecules like Posaconazole and Caspofungin in the diagnosis of **I**nvasive **F**ungal **I**nfection (IFI). Fungal tests are used to help diagnose fungal infections and also at times to determine the effectiveness of the treatment and in most case the test are either time consuming or not so accurate. In case of superficial skin and yeast infections, a clinical examination of the patient may be sufficient to determine the presence of fungal infection. Fungal culture test is recommended when there is a need to identify specific fungi present in persistent fungal infections and in those that penetrate into deeper tissues, affect the lungs, or cause systemic infections. In fungal culture test, the nutrient media used to recover fungal cells need to inhibit bacterial

growth and must support fungal growth. This takes several weeks before the antifungal treatment is administered.

Blood tests for fungal antigens and antibodies are considered faster than fungal cultures; and can test for a specific fungal species, so the doctor has to know what fungal organism to test for. Yet another drawback of blood examination is that many people have fungal antibodies from a prior exposure to the organism so that a single antibody test may not confirm the presence of a current infection.

Thus, successful diagnosis of IFI is a complicated task and required and requires a combination of clinical observations, laboratory investigation, and radiological or other diagnostic imaging methods. It is reported that only ¼ of IFI cases are diagnosed pre-morten due to the current diagnostic challenges. This gap in the diagnosis of fungal infection can be bridged by the use of highly fluorescent dye like 4,4-difluoro-4-bora-3a,4a-diaza-s-indacene (commonly referred as BODIPY, a trademark of Molecular Probes Inc) and coupling with target specific fungal drug.

BODIPY (4,4-difluoro-4-bora-3a,4a-diaza-s-indacene) is a class of fluorescent dye, known for their uniquely small Stokes shifts, fluorescence excitation maxima from 500 nm to ~650 nm and emission maxima from 510 nm to ~665 nm (45), high environment-independent fluorescence quantum yields, often approaching 100% even in water, and sharp excitation and emission peaks contributing to overall brightness and high molar absorptivity, ε_{max} typically >80,000 $cm^{-1}M^{-1}$ (46). The combination of these qualities makes BODIPY fluorophore an important dye molecule in variety of imaging applications. The BODIPY fluorophore is intrinsically lipophilic and intensely fluorescent, unlike most other long-wavelength dyes. As a result, probes incorporating this BODIPY fluorophore are more likely to mimic the properties of natural lipids. This

makes them effective tracers of lipid trafficking, as well as useful in general purpose membrane probes.

1.2 Objectives of the Current Study

Despite great potentials of lanthanide-based tracers the wide spread of the technology is impeded by very high price of commercially available probes, which is due to their complex structure. The goal of this research is development of new strategies for the synthesis of luminescent probes. The present research relates to development of new light emitting probes, which includes fluorescent and luminescent traces that can be used for ultrasensitive detection of biopolymers as well as for invasive and non-invasive determination of the composition of multicomponent mixtures. The research objective is identified in two parts; A) Synthesis and characterization of new cross-linking quinoline and quinolone based fluorescent derivatives and their luminescent lanthanide chelates for sensitive labeling and B) Development of fluorescent derivatives of anti-fungal drug, posaconazole and caspofungi for diagnostic imaging of Invasive Fungal Infections.

Research Strategy

Part A: *Synthesis and Characterization of New Cross-linking Quinoline and Quinolone based Fluorescent Derivatives and their Luminescent Lanthanide Chelates for Sensitive Labeling*

Development of new luminescent probes is challenging, since the transfer of energy from the antenna to the lanthanide is complex (a process not yet well understood) and very sensitive to subtle structural variations in the fluorophore. Another challenge is the necessity of combining three functional units within the same reporting probe: an antenna, a chelated lanthanide, and a cross-linking group (for attachment to the

biomolecule of interest) as shown in Figure 1.1. This requires a complex synthetic strategy; eventually leading to compounds whose size often exceeds 1,000 Da. Attachment of different reactive groups, chelating components and other chemical modifications of the fairly small dye molecule could lead to a large collection of valuable fluorescent probes.

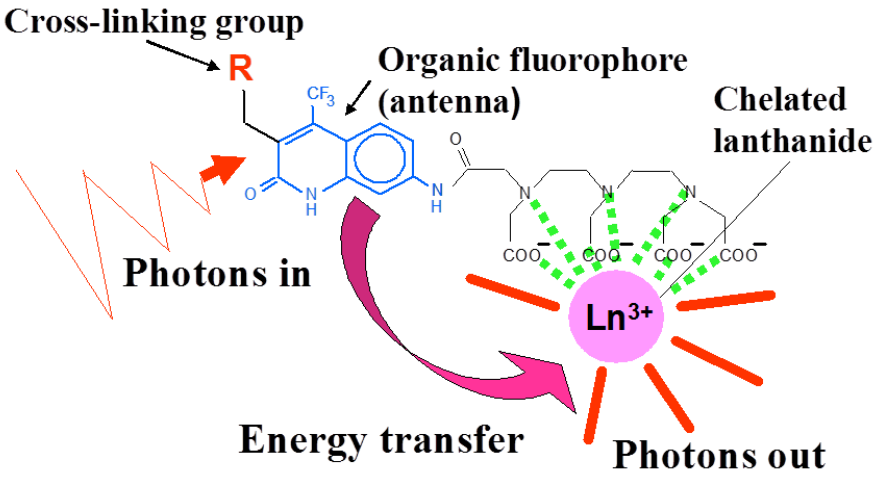

Figure 1.1 Design and operational principle of the lanthanide probe.

Two commonly used classes of lanthanide chelates are diethylenetriaminepentaacetic acid (DTPA) and tetraethylenetetraminohexaacetic acid (TTHA). These chelates attach to 7 amino quinolones, which are known as DTPA and/or TTHA-cs124 derivatives. The advantage of these classes of compounds is their high quantum yield, high solubility in water, and the possibility of introducing chemical modifications in the fluorophore to spectrally optimize the transfer of energy to the lanthanide, and to enable the attachment of a cross-linking group. A number of methods for the conjugation of these chelates to biomolecules have been suggested. One of them is to use the dianhydride form of DTPA, in which one of the anhydrides modifies the amino group of the chromophore, while the other anhydride reacts with amino group of

the biomolecule. Even though this approach is technically simple, it raises concerns about the side reactions (modification of other nucleophilic groups) due to the high reactivity of anhydrides. The second approach takes advantage of the conjugation of one of the DTPA anhydride groups with the cs124 moiety, followed by reaction of the remaining anhydride with the diamine. The unmodified amino group of the resulted adduct can then be converted to an amino-reactive isothiocyano or thiol-reactive groups. This mode of attachment of the cross-linking group weakens the retention of the lanthanide within the chelate by eliminating one ligating carboxylate, and it also reduces the brightness of the lanthanide (30 to 1,000%) due to the quenching effect of the additional coordinated water molecule. These factors restrict *in vivo* applications where high concentration of metal scavengers is an issue (e.g., intracellular imaging). Analogous derivatives of the fluorophore coumarine have been suggested and used in biophysical studies. However, compared to their quinolone counterparts, they are less bright and do not support terbium (Tb) luminescence.

The unique photon emission properties of lanthanide-based probes render them suitable for a wide variety of applications that require ultrasensitive detection of biomolecules. Progress in this field depends on the availability of efficient probes. The complexity of energy pathways in luminescent lanthanide chelates is not fully understood, leaving much room for improvement in their applications as labels for probes. The development of more efficient probes is highly desirable, because new more challenging applications have arisen (e.g., for the detection of rare pathogens in environmental samples and detection of single molecules in cells).

In the course of this work, new antena-fluorophores were synthesized, new methods have been developed for introduction of crosslinking groups in the luminescent

probes and mechanisms of the chemical reactions leading to principal synthetic intermediates have been elucidated. Novel quinoline-based fluorophores with useful fluorescent properties were obtained and their derivatives coupled to DNA oligonucleotides using click chemistry to obtain sensitive hybridization probes. Several luminescent lanthanide probes were also developed and their suitability to label biomolecules was tested using click reaction and proteomic studies with whole cell lysates of *E.coli*. These reactive derivatives can be used for covalent attachment of the fluorophores to various biomolecules of interest including nucleic acids, proteins, live cells and small cellular metabolites. Synthesized compounds were characterized using NMR, steady-state and time-resolved fluorescence spectroscopy, as well as UV absorption spectroscopy.

Part B: ***Development of Fluorescent Derivatives of Anti-Fungal Drug, Posaconazole and Caspofungi for Diagnostic Imaging of Invasive Fungal Pathogens***

Caspofungin and Posaconazole are broad spectrum antifungal drugs. Both caspofungin and posaconazole shows activity against infections with Aspergillus and Candida. In caspofungin the mode of action involves disturbing the integrity of the fungal cell wall by inhibiting the enzyme β(1,3)-D-Glucan synthase.

Posaconazole is a triazole antifungal drug and is active against Candida, Aspergillus, Zygomycetes: (47) (48). Posaconazole inhibits the growth of fungi by disrupting the close packing of acyl chains of phospholipids thereby impairing the functions of certain membrane-bound enzyme in fungi. Posaconazole is significantly more potent at inhibiting 14-alpha demethylase than itraconazole (49) (50) and is administered orally.

As the fungal drugs (posaconazole and caspofungin) exhibit affinity binding to the specific enzyme in the fungal cells, pathogen specific targeting probes, (a.k.a. affinity based approach) can be utilized in the development of the diagnostic tool for detecting fungal infections. The BODIPY Fl dye is successfully coupled with the drug molecule without losing its anti-fungal activity. In its conjugate form the Bodipy Fl-drug complex is severely quenched due to intramolecular stacking interactions. However, on binding to the target fungal cell, the intramolecular stacking is destroyed and fluorescence is observed signaling the presence of fungal infection.

CHAPTER 2

BASICS OF FLUORESCENCE

2.1 Introduction

Emission of light from electronically excited state of any substance is referred as Luminescence. Depending on the nature of excited state, luminescence can be divided into two categories viz. fluorescence and phosphorescence. In Phosphorescence, emission of light occurs from triplet excited states, in which the electron in the excited orbital has the same spin orientation as the ground-state electron. As transition to the ground state is forbidden, emission rates are slow such that emission lifetimes are in the order of millisecond to seconds or even longer. It should be noted that phosphorescence is not observed in fluid solutions at room temperature due to several processes that compete with light emission, such as non-radiative decay and quenching. On the other hand, in case of fluorescence, the electronic transition from excited state to the ground state is spin allowed and occurs rapidly by emission of photon. In fluorescence, the emission lifetimes are in the order of nanoseconds.

Quinine, the first known fluorophore was responsible for the development of the spectrophotometers that appeared in 1950's. During the World War II, the department of war was interested in monitoring antimalarial drugs, including quinine. This early drug assay resulted in a subsequent program at the NIH (National Institute of Health) to develop the first practical spectrofluorometer (51).

Fluorescence emission spectra are a plot of fluorescence intensity vs wavelength (nm) or wavenumber (cm^{-1}). The emission spectra are dependent upon the chemical structure of the fluorophore and the solvent in which it is dissolved. The sensitivity of

fluorescence was used in 1877 to demonstrate that the rivers Danube and Rhine were connected by underground stream (52).

Jablonski Diagram

Basic principles of molecular photophysics can be understood with the help of the Jablonski diagram, named after the Polish physicist Aleksander Jablonski.

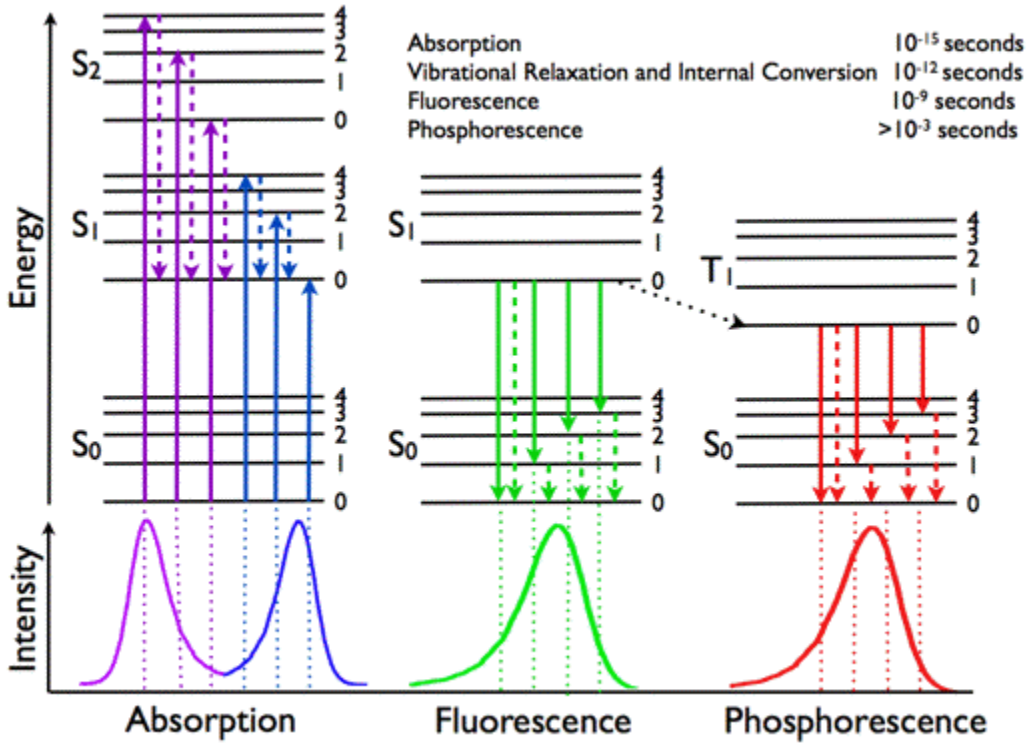

Figure 2.1 Jablonski diagram representing energy level and spectra.
[Source: photobiology.info-VisserRolinski]

The Figure 2.1 illustrates the electronic states of a molecule and the transitions between them. The electronic states are arranged vertically by energy. They are grouped horizontally by spin multiplicity. In the left part of the diagram three singlet states with anti-parallel spins are shown: the singlet ground state (S_0) and two higher singlet excited states (S_1 and S_2). Singlet states are diamagnetic, as they do not interact with an external magnetic field. The triplet state (T_1) is the electronic state with parallel spins. A molecule

in the triplet state interacts with an external magnetic field. Transitions between electronic states of the same spin multiplicity are allowed. Transitions between states with different spin multiplicity are formally forbidden, but may occur owing to a process called spin-orbit coupling. This transition is called intersystem crossing. Superimposed on these electronic states are the vibrational states, which are of much smaller energy.

In the above Figure 2.1, solid arrows indicate radiative transitions due to absorption (violet, blue) or emission (green for fluorescence; red for phosphorescence) of a photon. Dotted arrows represent non-radiative transitions (violet, blue, green, red). Internal conversion is a non-radiative transition, which occurs when a vibrational state of a higher electronic state is coupled to a vibrational state of a lower electronic state. In the notation of, for example, $S_{1,0}$, the first subscript refers to the electronic state (first excited) and the second one to the vibrational sublevel (v = 0). In the diagram, the following internal conversions are indicated: $S_{2,4} \rightarrow S_{1,0}$, $S_{2,2} \rightarrow S_{1,0}$, $S_{2,0} \rightarrow S_{1,0}$ and $S_{1,0} \rightarrow S_{0,0}$. The dotted arrow from $S_{1,0} \rightarrow T_{1,0}$ is a non-radiative transition called intersystem crossing, because it is a transition between states of different spin multiplicity.

2.2 Fluorescence

In 1852, the British scientist Sir George G. Stokes coined the term "fluorescence" after observing blue luminescence in the mineral fluorite. Stokes also discovered the redshift in band maximum of the fluorescence spectrum relative to the band maximum of absorption (Stokes shift).

The lowest vibrational level of S_1 is the starting point for fluorescence emission to the ground state S_0, non-radiative decay to S_0 (internal conversion), and transition to the

lowest triplet state (intersystem crossing) (Figure 2.1). Fluorescence takes place on the nanosecond timescale (1 ns = 10^{-9} s) and, depending on the molecular species, its duration amounts to 1-100 nanoseconds. It is clear from the Jablonski diagram that fluorescence always originates from the same level, irrespective of which electronic energy level is excited. The emitting state is the zeroth vibrational level of the first excited state $S_{1,0}$. It is for this reason that the fluorescence spectrum is shifted to lower energy than the corresponding absorption spectrum (Stokes shift). From the sketched spectra in Figure 2.1, it can be concluded that vibrational fine structure in a fluorescence spectrum reports about vibrations in the ground state, and vibronic bands in an absorption spectrum provides information on vibrations in higher electronic excited states (53).

Another factor that has to be considered in fluorescence spectroscopy is the Franck-Condon factor. Referring to the Jablonski Scheme in Figure 2.1, it can be seen that the fluorescence transition $S_{1,0} \rightarrow S_{0,0}$ is not the most intense one. The Franck-Condon principle states that the most intense vibronic transition is from the vibrational state in the ground state to that vibrational state in the excited state vertically above it (Figure 2.2, blue arrow).

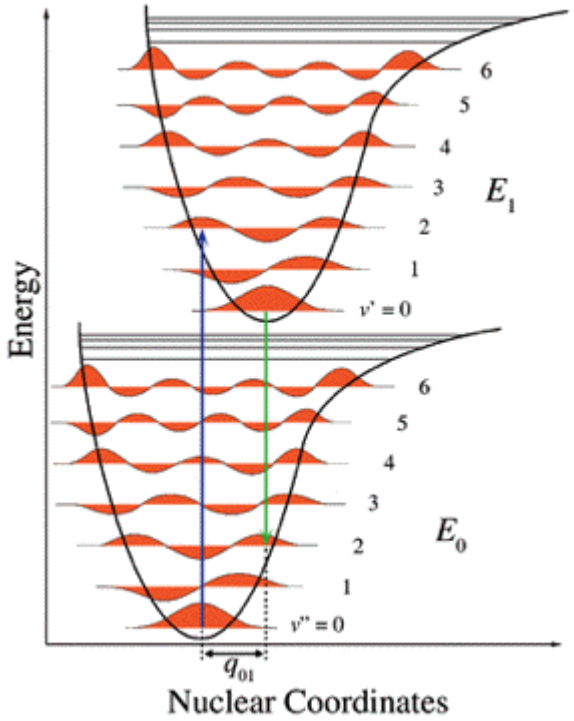

Figure 2.2 Energy diagram for explanation of the Franck-Condon principle. The potential wells show favored transitions between vibrational sublevels ν = 0 and ν = 2 both for absorption (blue arrow) and emission (green arrow).
[Source: Wikipedia: Franck-Condon Principle]

2.3 Characteristics of Fluorescence

2.3.1 Absorption Spectrum

The measurement of an absorption spectrum (Figure 2.3) is based on the Lambert-Beer law, and shows the ability of the investigated sample to absorb light at different wavelengths. As light absorption occurs almost always from the lowest vibrational level of the electronic ground state, the absorption spectrum characterizes the energetic structures of the electronic excited states of an aromatic molecule.

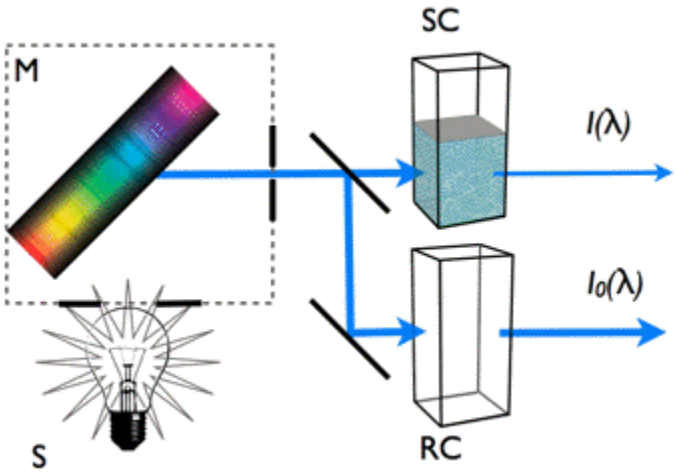

Figure 2.3 Measurement principle of light absorption spectra.
[Source: photobiology.info-VisserRolinski]

The values measured directly in the spectrophotometer are the intensities of light transmitted through sample and reference cuvettes. The light source S generates a broad spectrum of light and the dispersion device (grating or prism) M selects a monochromatic light of specific wavelength λ. The light is then divided into two identical beams directed to two cuvettes, a sample cuvette, SC, containing the solution of the aromatic compound and a reference cuvette, RC, with solvent only. Changing the wavelength over the required range enables measuring the intensities of the light transmitted through both cuvettes, $I(\lambda)$ and $I_0(\lambda)$ (53).

The absorbance A_λ at wavelength λ is then defined as:

$$A_\lambda = \log[I_0(\lambda) / I(\lambda)] \tag{2.1}$$

and is equal according to the Lambert-Beer law to:

$$A_\lambda = \varepsilon(\lambda)cd \tag{2.2}$$

where ε(λ) is the extinction coefficient at wavelength λ for the particular molecule, c its concentration, and d the path length of the cuvette, for instance 1 cm.

2.3.2 Fluorescence Spectrum

In fluorescence spectrum, $I_{flu}(\lambda)$ represents the intensity of the fluorescence light emitted by the sample as a function of emission wavelength (Figure 2.4). As fluorescence transitions start in most cases from the lowest vibrational level of the first electronic excited state, $I_{flu}(\lambda)$ characterizes the energetic structure of the electronic ground state (53).

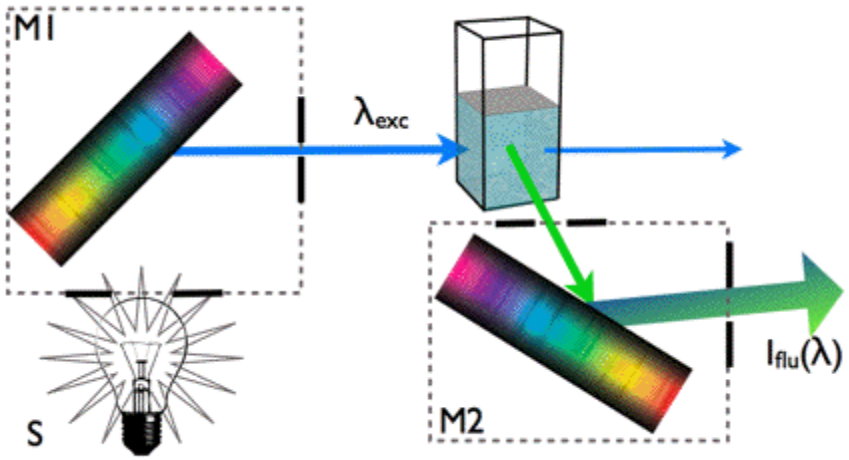

Figure 2.4 Schematic of fluorescence measurement.
[Source: photobiology.info-VisserRolinski]

As presented in Figure 2.4, fluorescence is detected at right angle to the excitation beam in order to minimize the presence of scattered excitation light in the fluorescence channel. A monochromatic light beam of selected wavelength λ_{exc} excites the molecules in the sample. Fluorescence light is emitted from the excited state of these molecules in all directions. The monochromator M2 allows measurements of fluorescence intensity as

a function of the emission wavelength. An excitation spectrum is essentially an absorption spectrum, because the fluorescence intensity $I_{flu}(\lambda)$ is proportional to:

$$I_{flu}(\lambda) \propto \varepsilon(\lambda) I_0 \Phi \tag{2.3}$$

where $\varepsilon(\lambda)$ is the extinction coefficient at excitation wavelength λ, I_0 is the monochromatic light intensity, and Φ is the quantum yield of fluorescence (see below). This equation is valid only for dilute fluorophore solutions, in which the absorbance of the aromatic compound never exceeds 0.05. Excitation spectra turn out to be useful in obtaining absorption spectra of very dilute samples (1).

2.3.3 Quantum Yield of Fluorescence

The fluorescence quantum yield is an intrinsic property of a fluorophore. It is one of the important properties used for the characterization of novel fluorescent probes. The quantum yield, $\boldsymbol{\Phi_F}$, is defined as the ratio of the number of fluorescence photons emitted by the sample $\boldsymbol{n_E}$ to the number of photons absorbed $\boldsymbol{n_A}$. It can be shown also that Φ_F is the ratio of the rate of the radiative transition ($\boldsymbol{k_r}$) to the rates of all transitions **($\boldsymbol{k_r}$+$\boldsymbol{k_{nr}}$),** in which the excited state is involved. In other words the quantum yield gives the probability of the excited state being deactivated by fluorescence rather than by another, non-radiative mechanism. Therefore, any molecular mechanism leading to a non-radiative depopulation of the excited state reduces the quantum yield:

$$\Phi_F = \frac{n_E}{n_A} = \frac{K_r}{K_r + K_{nr}} \tag{2.4}$$

Measurements of the absolute quantum yield of a fluorophore require sophisticated instrumentation. For practical reasons it is easier to determine the relative quantum yield

of a fluorophore by comparison to a reference fluorophore with a well-known quantum yield. In general, there are two methods for relative quantum yield measurements; a single-point method and a comparative method (54). Using the single-point method the quantum yield is calculated using the integrated emission intensities from a single sample and reference pair at identical concentration. This method is fast and easy and gives a good approximation of quantum yield. However, a more reliable method for recording Φ_F is the comparative method of Williams et al., which involves the use of well characterized standard samples with known Φ_F values. Essentially, solutions of the standard and test samples with identical absorbance at the same excitation wavelength can be assumed to be absorbing the same number of photons. Hence, a simple ratio of the integrated fluorescence intensities of the two solutions (recorded under identical conditions) will yield the ratio of the quantum yield values. Since Φ_F for the standard sample is known, it is trivial to calculate the Φ_F for the test sample.

In practice, the quantum yield measurement is slightly more complicated because it must take into account a number of considerations. For example:

1. Self-quenching due to concentration effect
2. Influence of the solvent system; more so when the solvent matrix for the sample is different than for the standard
3. The validity in the use of standard compound and its Φ_F value under proper conditions
4. It is important to cross-calibrate the reference standard with another, in order to ensure that both the standards are behaving as expected. This provides greater confidence in the use of their quantum yield values

Table 2.1 Standard Materials and their Literature Quantum Yields

Compounds	Solvent	Emission Range/nm	Literature Quantum Yield
Rhodamine 101	Ethanol + 0.01% HCl	600 – 650	1.00 (55)
Cresyl Violet	Methanol	600 – 650	0.54 (56)
Quinine sulfate	0.1M H_2SO_4	400 – 600	0.54 (57)
Fluorescein	0.1M NaOH	500 – 600	0.79 (58)
Chlorophyll A	Ether	600 – 750	0.32 (59)
Zinc phthalocyanine	1% pyridine	660 – 750	0.30 (60)
Tryptophan	Water	300 – 380	0.14 (61)
2-aminopyridine	0.1M H_2SO_4	315 – 480	0.60 (62)
Anthracene	Ethanol	360 – 480	0.27 (63)
9,10-diphenyl Anthracene	Cyclohexane	400 – 500	0.90 (64)

2.3.4 Fluorescence Lifetime

The fluorescence lifetime is the average time the molecule stays in its excited state before emitting a photon. Fluorescence typically known to follows first-order kinetics:

$$[\boldsymbol{S_1}] = [\boldsymbol{S_0}]\, \mathbf{e}^{-\Gamma \mathbf{t}} \tag{2.5}$$

where $[S_1]$ is the concentration of excited state molecules at time t, $[S_0]$ is the initial concentration and Γ is the decay rate or the inverse of the fluorescence lifetime. This is an example of exponential decay. Various radiative and non-radiative processes can influence the excited state. In such case the total decay rate is the sum over all rates:

$$\Gamma_{tot} = \Gamma_{rad} + \Gamma_{nrad} \tag{2.6}$$

where Γ_{tot} is the total decay rate, Γ_{rad} the radiative decay rate and Γ_{nrad} the non-radiative decay rate. If the rate of spontaneous emission or any of the other rates are fast, the lifetime is short. For commonly used fluorescent compounds, typical excited state decay times are in the order of nanoseconds. The fluorescence lifetime is an important

parameter for practical applications of fluorescence such as fluorescence resonance energy transfer (FRET).

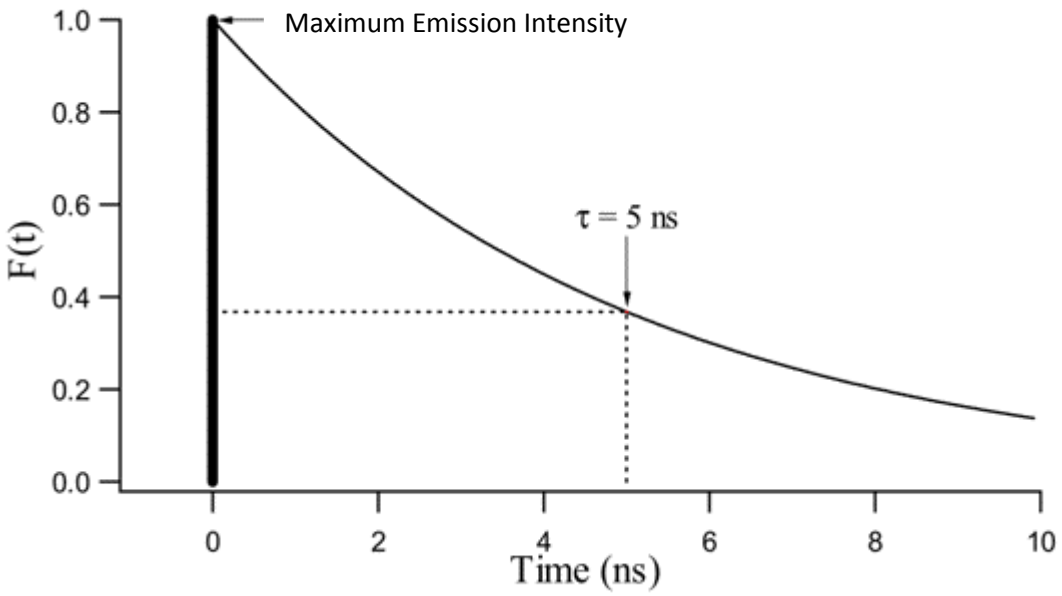

Figure 2.5 Illustration of a typical fluorescence decay profile.

2.3.5 Fluorescence Quenching

Quenching refers to any process that result in decrease of fluorescence intensity of a given fluorophore. A variety of processes such as excited state reactions, energy transfer, complex-formation and collisional quenching etc can result in quenching. Molecular oxygen, iodide ions and acrylamide (65) are some of the commonly known quenchers, while chloride ion is a well-known quencher for quinine fluorescence. (66-68).

Some fluorophores tend to form nonfluoroscent complexes with quenchers at ground state. This is referred as static quenching. The donor and acceptor molecules form an intramolecular dimer which is nonfluorescent and has unique spectral properties.

Aggregation can often lead to fluorescence quenching. Due to hydrophobic affect the dye molecules stack together to minimize contact with water. High temperatures and surfactants can help disrupt stacking interactions.

Solvent medium in which the fluorescence properties are studied are also known to cause quenching. The concept of solvation can be understood from interactions between a solute (fluorophore) and the surrounding solvent molecules. The dominating solute-solvent interactions arise from electrostatic dipole-dipole interactions, which lead to lowering the potential energies of all energy levels involved in absorption and fluorescence processes. The fluorescence spectra of the solvent-sensitive fluorophore, 2-mercapto-ethanol adduct of 6-**b**romo**a**cetyl-2-**d**imethyl**a**mino**n**aphtalene (badan) in a number of solvents are shown in Figure 2.6. Larger the dipole moment of the solvent molecule the stronger is the "red-shift" of the spectrum.

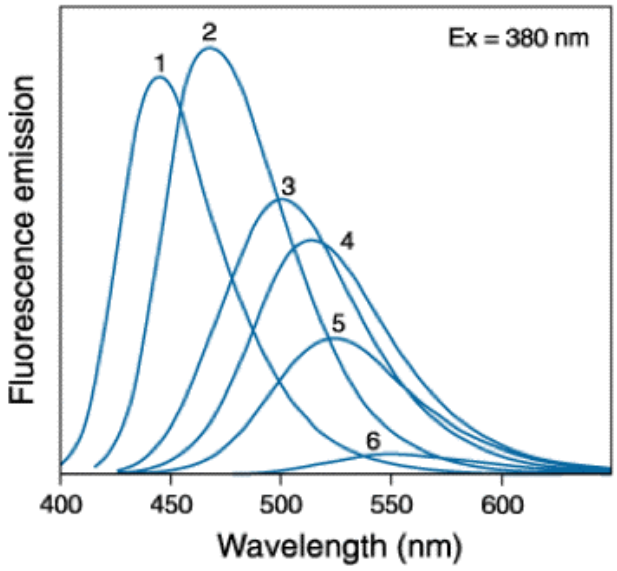

Figure 2.6 Fluorescence spectra of "badan" in: (1) toluene, (2) chloroform, (3) acetonitrile, (4) ethanol, (5) methanol and (6) water.
[Source: **Handbook of Molecular Probes**]

2.3.6 Fluorescence Resonance Energy Transfer (FRET)

It is a process of energy transfer between two chromophores. In FRET, a donor chromophore which is in its electronic excited state, may transfer energy to an acceptor chromophore in close proximity, typically less than 10 nm through nonradiative dipole–dipole coupling. This mechanism is termed "Förster resonance energy transfer" and is named after the German scientist Theodor Förster. A circumstance where both chromophores are fluorescent, the term “fluorescence resonance energy transfer” is often used instead, although the energy is not actually transferred by fluorescence. FRET is a dynamic quenching mechanism and is extremely dependent on the donor–acceptor distance, $\boldsymbol{R}$, falling off at a rate of $1/\boldsymbol{R}^6$. FRET also depends on the donor–acceptor spectral overlap and the relative orientation of the donor and acceptor transition dipole moments. FRET can typically occur over distances up to 100 Å.

2.3.7 Stokes Shift

Stokes shift is the difference in wavelength between excitation and emission maxima. It is named after Irish physicist George G. Stokes. When a molecule absorbs energy, it gets excited to higher energy level where it is unstable. It tends to relax by emitting the absorbed energy. When the emitted photon has less energy than the absorbed photon, this energy difference is the Stokes shift. If the emitted photon has more energy, the energy difference is called an anti-Stokes shift. (69) Stokes Shift influences the sensitivity of the assay, higher the Stokes Shift better is the spectral discrimination.

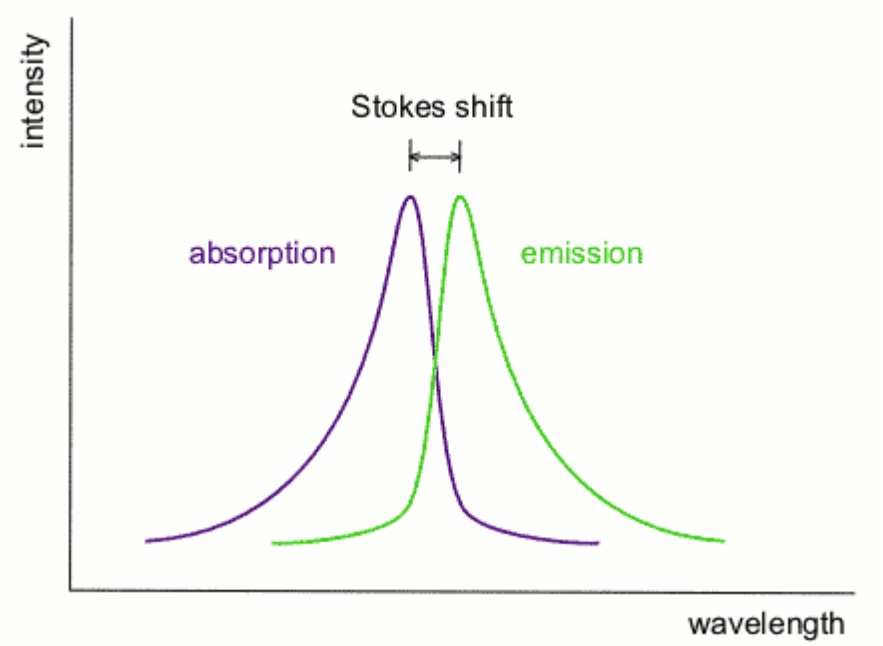

Figure 2.7 Example of Stokes Shift.
[Source: Wikipedia]

2.3.8 Isobestic Point

The isosbestic point corresponds to a wavelength at which the absorption spectra of two or more substances cross each other. A pair of substances can have several isosbestic points in their spectra. Figure 2.8 is an example of presence of isobestic points in a chemical reaction.

In chemical kinetic studies, isosbestic points are used as reference points to study reaction rates, as the absorbance at those wavelengths remains constant throughout the whole reaction. The presence of isobestic point is indicative of single pathway reaction. When a movement in the isobestic point is observed, it could be concluded that the reaction gives rise to intermediates or side reaction products.

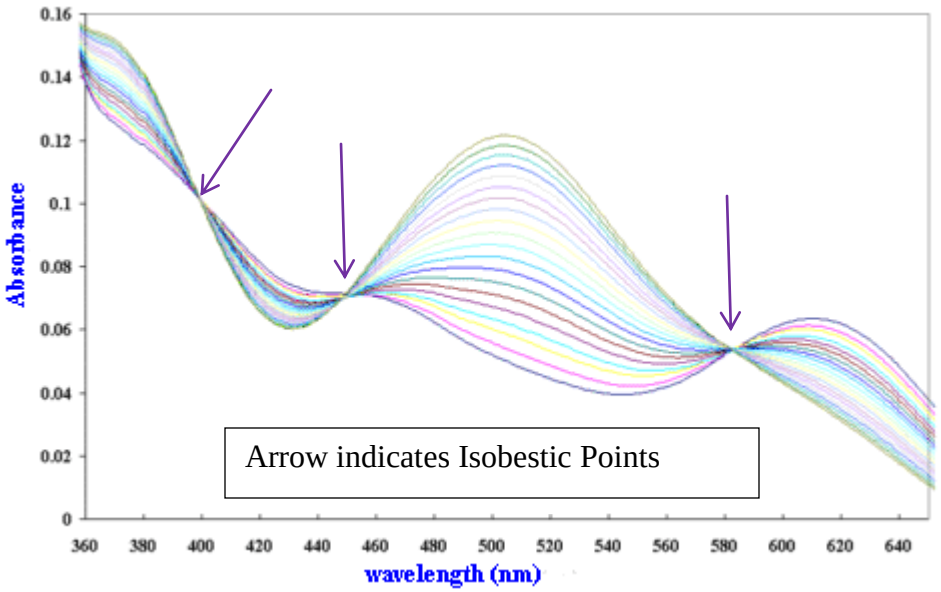

Figure 2.8 Example of isobestic point in a chemical reaction.
[Source: www.chem.uwimona.edu.jm]

In Figure 2.8 there are three isobestic points at 400 nm, 450 nm and 580 nm, respectively. The above overlap spectrum indicates that the reaction is a equimolar reaction which do not give rise to any intermediates products, the spectra are linear combination of two components and reflect an equilibrium between these two components.

CHAPTER 3

CROSS-LINKING QUINOLINE AND QUINOLONE DERIVATIVES FOR SENSITIVE FLUORESCENT LABELING

3.1 Introduction

Fluorescent labels are used in numerous applications that relay on sensitive detection of biological macromolecules (proteins, nucleic acids, polycarbohydrates, etc.), as well as for specific labeling of cells and tissues. In these applications, the fluorophore reporter groups are illuminated by visible or UV light, which leads to absorption of the light quantum and excitation of the molecule. The excited state is unstable and tends to relax either through dissipation of the absorbed energy by collision with other components in the medium or by emission of light. This light can be subsequently detected. Detection sensitivity is proportional to the number of the light quanta emitted by the fluorophore, which in turn is a linear function of the intensity of the excitation light. Therefore, for sensitive detection, high intensity light sources are employed. This creates the problem of discrimination of excitation and emission light, since even a small fraction of the excitation light that reaches the detector can cause significant background and decreases the detection sensitivity. This problem can be alleviated by using fluorophores with large spectral distances between excitation and emission light (Stokes shift). Quinolone (47) and discovered in the course of present study, quinoline fluorophores, possess the desired property. This chapter, describes the synthesis and reaction mechanisms for new derivatives of these fluorophores that are suitable for attachment to biological macromolecules. It is found that 7-aminoquinolones can be conveniently modified at either the 1-amido- or 2-oxogroup, yielding corresponding quinolone and quinoline

derivatives with preserved fluorescent properties and large Stokes shift (ca. 50-110 nm). Subsequent modification of the resulting compounds at the 7-amino group allows tuning of the fluorescence from deep blue to green emission. Using analogous modifications, amine-reactive isothiocyano-derivatives, as well as azido derivatives capable to click-react with acetylenic counterparts (48-50) were synthesized. Reactivity of the compounds were verified in reactions with cysteine and alkyne-derivatized DNA oligos. The results suggest suitability of the new reactive probes for fluorescent labeling with detection limit in the nanomolar range.

3.2 Synthesis Scheme

The following reagents were purchased from Aldrich:1,3-diiodopropane, triphenyl phosphine, triethylamine, 1,3-phenylenediamine, ethyl 4,4,4-trifluoroacetoacetate, p-toluenesulfonylchloride, *N*-trityl-1,6-diaminohexane, 4,4'-bischloromethylbiphenyl, methylbromacetate, anhydrous dimethylformamide and dimethylsulfoxide, 1-butanol, ethylacetate, chloroform, acetonitrile, ethanol, sodium, potassium, and ammonium hydroxide, lithium azide, Na_2SO_4, Na_2CO_3, acetic acid, citric acid, thiocarbonyldiimadazole, TBTA-copper complex, $TbCl_3$, $EuCl_3$, $SmCl_3$ and $DyCl_3$, silica gel TLC plates on aluminum foil (200 μm layer thick with a fluorescent indicator). All chemicals were the purest grade available. Excitation and emission fluorescence spectra in a steady-state mode were recorded using a Quanta-Master 1 (Photon Technology International) digital spectrofluorometer at ambient temperature. UV-absorption spectra were recorded on a UV-visible spectrophotometer (Cary 300 Bio, Varian). 2'-O-methyl-RNA oligos containing the following sequences were used: 5' hexynyl – CUUC GUC CAC AAA CAC AAC UCC U GAAG – BHQ2 3'; 5'hexynyl – CUAG ACC ACA CAA

CCU AC CUAG – BHQ2 3’; 5’ hexynyl – GCC UCG UCG CCG CAG CUA ACU AUC CGU GUG CGUC – NH2 3’.

3.2.1 Synthesis of 7-amino-4-triflurомethyl-quinolone (cs124-CF_3) and 7-amino-4-triflurомethyl-2-ethoxy quinoline (Qin124-CF_3)

Twenty mmol (2.16 gm) of 1,3-phenylenediamine dissolved in 10 ml DMSO were mixed with 20 mmol (3.68 gm) of ethyl 4,4,4-trifluoroacetoacetate. The mixture was incubated 1.5 h at 80 °C, supplemented with 2 ml of 10 M aqueous KOH and kept for another 20 min at room temperature. Two fluorescent products with R_f = 0.92 (green blue) and 0.44 (blue) were detected by TLC in ethylacetate. The mixture was poured into 10 ml of 0.1 M citric acid and left for 2 h on ice. The precipitate (cs124-CF_3) and Qin124-CF_3 was collected by filtration, washed with water, dried and suspended in chloroform. After filtration, the precipitate (pure cs124-CF_3) was dried under reduced pressure, while chloroform filtrate containing mostly fluorescent product with high mobility (Qin124-CF_3) on TLC was evaporated *in vacuo* and the product purified by silicagel column chromatography using hexane-acetone (3:1) as eluent. The fractions containing pure product were collected and evaporated to dryness. Yields: cs124CF_3 ~ 44% and for Qin124-CF_3 ~ 26%. UV for cs-124-CF_3: λ_{max1} = 230 nm and λ_{max2} = 270 nm λ_{max3} = 360; For Qin-124: λ_{max1} = 226 nm and λ_{max2} = 315 nm, λ_{max3} = 345 nm. 1H NMR for Qin124-CF_3 : 7.60 (dd,1H, 5H, J_1= 9.0, J_2 = 2.1), 6.94 (dd, 1H, 6H, J_1 = 9.0, J_2 = 2.4), 6.88 (s, 1H. 8H), 6.85 (d, 1H, 3H, J = 2.1), 6.0 (s, 2H, 7-amino), 4.42 (q, 2H, -OCH_2, J = 7.2), 1.35 (t, 3H, methyl, J=7.2).

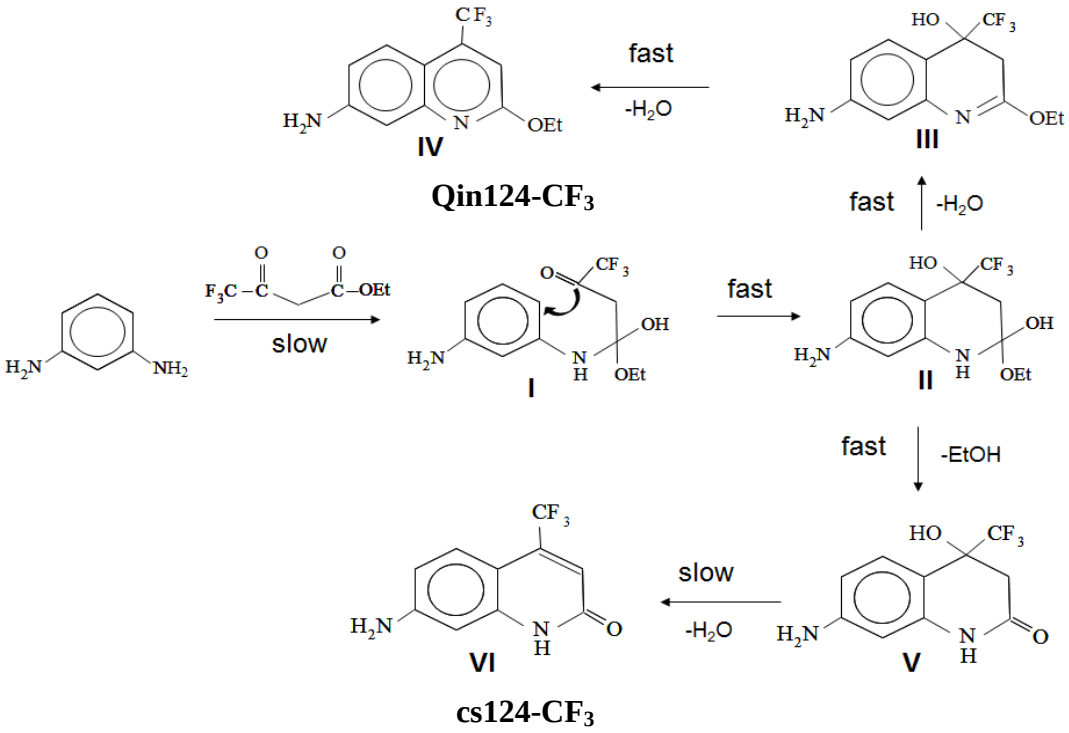

Scheme 3.1 Reaction between 1,3-diamine and 4,4,4-trifluoroacetoacetate. Structures I, II and III are hypothetical.

3.2.1.1 Analytical Syntheses at Various Incubation Conditions. In order to confirm the structure of reaction products and the reaction intermediates, 108 mg (1 mmol) of 1,3-phenylenediamine was dissolved in 0.5 ml DMSO and supplemented with 150 µl of ethyl 4,4,4-trifluoroacetoacetate. The reaction mixture was divided into equal portions ca. 370 µl each. One portion was incubated at 50 °C for 3 h, while the other half was incubated at 110 °C for 1 h. One hundred microliter aliquots of the reaction mixtures diluted with 250 µl of n-butanol were applied on TLC plates and dried in hot air flow. After separation in ethyl acetate as a developing solvent, the fluorescent products with R_f = 0.44 (cs124-CF_3) and R_f = 0.92 (Qin124-CF_3) along with non-fluorescent products with R_f = 0.62 and 0.84 were eluted by methanol and evaporated to dryness. UV for cs124-CF_3: λ_{max1} = 360 nm. For Qin124-CF_3: λ_{max} = 347 nm. Bottom Intermediate: λ_{max} = 230 nm. Top Intermediate:

λ_{max} = 310 nm. ^{1}H NMR spectra for the products with R_f = 0.44 and 0.92 were identical to cs124-CF_3 and Qin124-CF_3 correspondingly. ^{1}H NMR for the product with R_f = 0.62 (comp. V): 10.15 (s, 1H, -NH), 7.15 (d, 1H, 6H, J = 8.4) , 6.57 (s,1 H, 8H), 6.24 (dd, 1H, 5H, J_1= 8.3 , J_2 = 2.1), 6.10 (d, 1H, hydroxy H, J = 2.1), 5.4 (s,2H, 7-amino), 2.76 (q, 2H, 3H, J_1= 32.4 , J_2 = 16.5).

3.2.1.2 Incubation of Non-fluorescent Reaction Products at Various Conditions. The solutions of purified reaction products with R_f = 0.62 and 0.84 (see previous section) in DMSO (ca. 1 mg/ml, 100 µl,) were kept either at 110 ^{o}C or supplemented with 2 µl of 10 M KOH and left at room temperature. At time intervals the mixtures were analyzed by TLC in ethylacetate as developing solvent.

3.2.1.3 Alkylation of cs-124CF_3 by ethyl p-toluenesulfonate. Solution of 300 µmol of cs124-CF_3 in 500µL DMSO was supplemented with 16.8 mg of anhydrous powdered KOH and 400 µmol of ethyl p-toluenesulfonate. The reaction mixture was vortexed for 30 min and left for 4 h until completion of the reaction as confirmed by TLC in hexane-acetone (3:1) system. Two reaction products were observed. The reaction mixture was poured dropwise to 12 ml water. After centrifugation at 6000 rpm for 10 min, the precipitate was collected and dissolved in 1 ml of ethanol and subjected to TLC in hexane-acetone (3:1) solvent system. Product with R_f = 0.38 was eluted by methanol and evaporated in vacuo. UV absorption spectrum was identical to comp. IV (see above). Yield = 5.7 mg. ^{1}H NMR: 7.60 (dd,1H, 5H, J_1= 9.0, J_2 = 2.1), 6.93 (dd, 1H, 6H, J_1 = 9.0, J_2 = 2.4), 6.88 (s, 1H. 8H), 6.85 (d, 1H, 3H, J = 2.1), 6.0 (s, 2H, 7-amino), 4.42 (q, 2H, -OCH_2, J = 7.2), 1.35 (t, 3H, methyl, J=7.2).

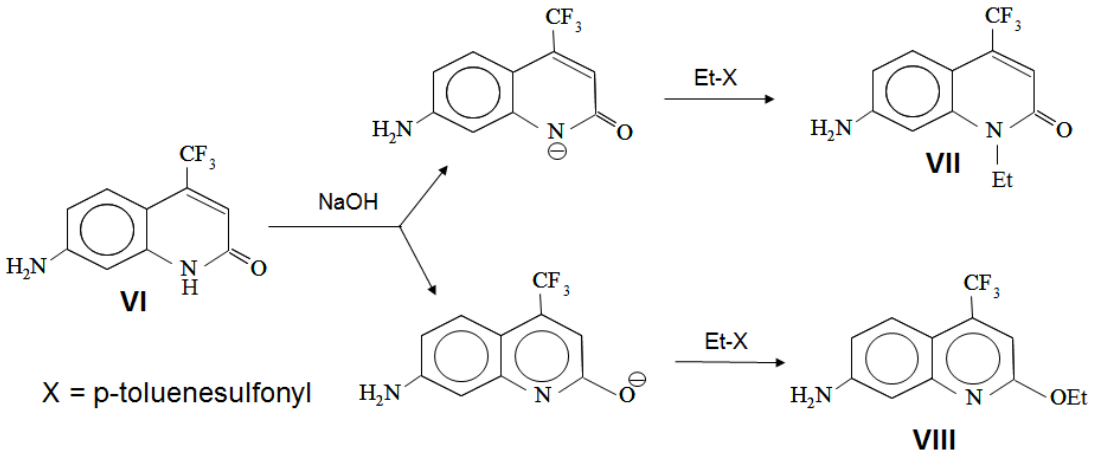

Scheme 3.2 N- and O- alkylation of quinolone fluorophore.

3.2.2 Synthetic Route for Quinolone and Quinolone Reactive Groups

3.2.2.1 Synthesis of 1-iodo-3-azido propane. Nine grams of 1,3-diiodopropane were mixed with 15 ml of DMF and supplemented with 1.5 g of lithium azide. After 1 h incubation at 37 ^{o}C, TLC analysis using hexane as developing solvent revealed one reaction product with R_f = 0.2 along with starting 1,3-diiodopropane (R_f = 0.4). The mixture was poured into 150 ml of water and extracted with an equal volume of ether. The organic layer was dried over anhydrous sodium sulfate and evaporated under reduced pressure. The residue was dissolved in hexane and subjected to silicagel column chromatography using the same solvent as eluent. The fractions corresponding to product were collected and evaporated to dryness. Yield = 2.4 g, (30%).

3.2.2.2 1-(3-azidopropyl)-cs124-CF_3 and 7-amino-4-trifluoromethyl-2-(3-azido oxy propyl) quinolone. Four-hundred fifty six milligrams (456 mg) of cs124-CF_3 dissolved in 4 ml of DMSO were supplemented with 112 mg of anhydrous KOH and 422 mg of $IC_3H_6N_3$ and left overnight at room temperature. TLC analysis in hexane-acetone (3:1) mixture revealed the presence of two fluorescent reaction products, R_f = 0.15 (blue fluorescence, azido cs124-CF_3) and R_f = 0.3 (green-blue fluorescence, azido Qin124-CF_3). The reaction products were precipitated by addition of 45 ml of water, dried under vacuo, dissolved in acetone and purified by silica gel column chromatography using hexane-acetone (3:1) as eluent. The fractions corresponding to the products migrating to R_f = 0.15 and 0.3 were collected and evaporated to dryness. 1-(3-azidopropyl)-cs124-CF_3 (compound IX): Yield = 292 mg, UV: λ_{max1} = 281 nm, $\lambda_{max2,}$ = 369 nm (ε = 17150 M^{-1} cm^{-1}). ^1H NMR chemical shifts (d) in DMSO are: 7.43 (dd, 1H, 5H, J= 8.7), 6.62 (m, 2H, 6H and 8H combined), 6.55 (s, 1H, 3H), 6.22 (s, 2H, 7-amino), 4.18 (t, 2H, α-CH_2, J=7.2), 3.48 (t, 2H, γ-CH_2, J=6.75), 1.86 (quintet, 2H, β-CH_2, J= 6.9). Compound X: Yield = 84 mg, UV: λ_{max1} = 255 nm, λ_{max2} = 350 nm (ε = 12300 M^{-1} cm^{-1} ^1H NMR chemical shifts (d) in DMSO are: 7.67 (dd, 1H, 5H), J=1.8), 6.92-6.96 (dd, 1H, 6H, J=2.4), 6.9 (s, 1H, 8H), 6.86 (d, 1H, 3H, J=2.1), 4.4 (t, 2H, γ-CH_2, J=6.3), 3.5(t, 2H, α-CH_2, J=6.6), 2.0 (quintet, 2H, β-$CH_{2,}$ J=6.4).

3.2.2.3 1-(3-aminopropyl)-cs124-CF_3. Two hundred milligrams of azido cs124-CF_3 were treated with 217 mg of triphenylphosphine in 1 ml DMF at 50 °C for 2.5 h followed by addition of 0.2 ml of ammonium hydroxide and the incubation continued at the same temperature. After 1h the reaction mixture was acidified with 1M citric acid to pH ~ 4.0 - 4.5 and extracted with ether (2 x 10 ml). The pH of the aqueous phase was

adjusted to pH 10 by NaOH and the solution was extracted with ether (3 x 20 ml). The ether extracts were collected, dried over anhydrous sodium sulfate and evaporated in vacuo. The residue was further dissolved in acetone and evaporated in vacuo to afford crystalline product. Yield = 183 mg (85 %). ^{1}H NMR chemical shifts (d) in DMSO are: 7.44(dd, 1H, 5H, J = 8.7), 6.71(s, 1H, 8H), 6.65(dd, 1H, 6H, J = 8.8), 6.56(s, 1H, 3H), 6.24(s, 2H,7-amino), 4.18(t, 2H, α-CH_2, J = 7.2), 3.24(t, 2H, terminal amine, J = 6.4), 2.6(t, 2H, γ-CH_2, J = 6.6), 1.73(quintet, 2H, β-CH_2, J = 6.9).

3.2.2.4 1-(3-isothiocyanopropyl)-cs124CF_3. The solution of 28.4 mg of compound XI (see precious paragraph) in 0.3 ml of DMSO was mixed with 21.4 mg of 1,1'-thiocarbonyldiimidazole in 0.2 ml of chloroform and incubated at ambient temperature. After 10 min, 3 μl TFA were added and the incubation continued for 1 h at 50 °C. TLC in hexane-ethylacetate (2:1) mixture as developing solvent revealed near complete conversion to isothiocyanate compound. The product was precipitated by 8 ml of water, the residue dissolved in 1.5 ml of methanol, re-precipitated by 8 ml water, and after centrifugation at 7000 rpm for 5 min dissolved in 2.0 ml of methanol and dried in vacuo. Yield = 18 mg (55 %) yellow powder. ^{1}H NMR chemical shifts (d) in DMSO are: 7.45(d, 1H, 5H, J = 8.7), 6.68(s, 1H, 6H), 6.65(s, 1H, 8H,), 6.57(s, 1H, 3H), 6.19(s, 2H,7-amino), 4.25(t, 2H, γ-CH_2, J = 6.9), 3.78(t, 2H, α-CH_2, J = 6.4), 2.04(quintet, 2H, β-CH_2, J = 6.6).

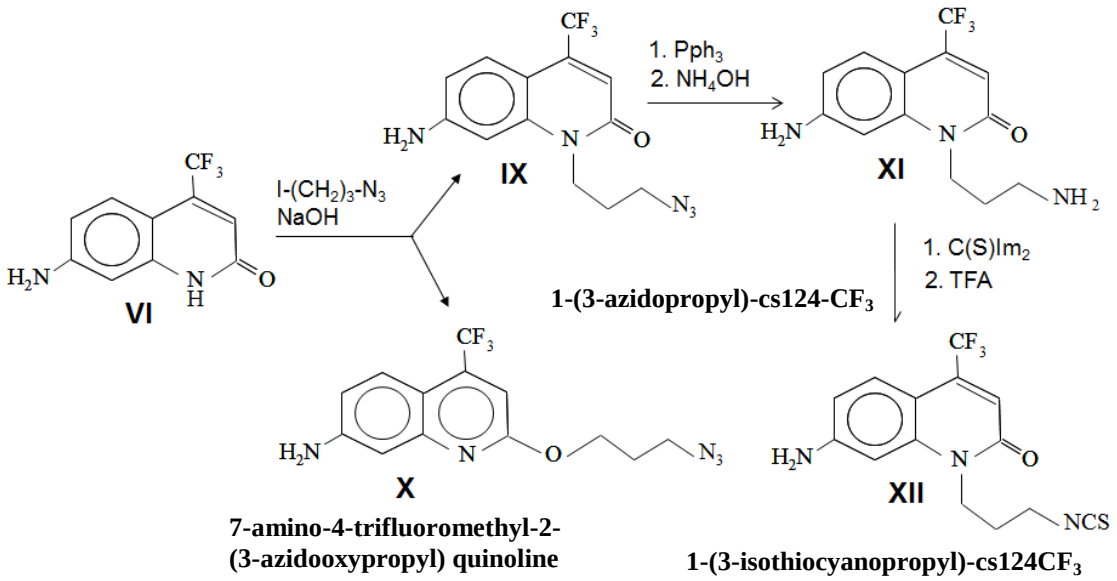

Scheme 3.3 Synthetic route for quinolone and quinolone reactive groups.

3.2.3 Synthesis of 7-amino-4-trifluoromethyl-2-[1-methyleno(4-p-methylazido) biphenyl] quinolone and 7-amino-4-trifluoromethyl-2-O-[methyleno(4-ethylazido) biphenyl]quinoline

Solution of 53 milligrams of cs124-CF_3 in 0.4 ml of DMF was consequently mixed with 36 µl of aqueous 10 M NaOH and a solution of 150 mg of 4,4'-bischloromethylbiphenyl in 1 ml DMF. After 20 min incubation at room temperature, 50 mg of lithium azide was added and incubation continued for another 20 min at 60 ^{o}C. TLC analysis in hexane-acetone 2:1 system revealed two main products with relative mobility of 0.35 (for **XIII**) and 0.45 (for **XIV**). The reaction mixture was poured in 10 ml of water, the residue precipitated by centrifugation, washed with water, dissolved in 10 ml of acetonitrile and evaporated to dryness under reduced pressure. The products were purified by silicagel column chromatography in the same system. Yield for compound **XIII** was 60 mg; for compound **XIV** - 10 mg. UV absorption spectrum, comp. **XIII**: λ_{max1} = 226 nm, λ_{max2} = 257 nm, λ_{max3} = 368 nm. λ_{min1} = 218 nm, λ_{min2} = 241 nm, λ_{min3} = 308 nm. For comp.

XIV: λ_{max1} = 258 nm, λ_{max2} = 347 nm, λ_{min1} = 238 nm, λ_{min2} = 307 nm. ^{1}H NMR chemical shifts (d) in DMSO for comp. **XIII** are: 7.66 (m, 4H, o,o'biphenyl H), 7.48 (dd overlapped, 1H, 5H, J=2.1), 7.45 (d, 2H, biphenyl m-H, J = 8.1), 7.3 (d, 2H, biphenyl-m'-H, J – 8.4), 6.7 (s, 1H, 8H), 6.62 (dd, 1H, 6H, J_1=9.0, J_2 = 1.8), 6.55 (d, 1H, 3H, J=1.8), 6.25 (s, 2H, 7 amino), 5.45 (s, 2H, -CH_2-N_3), 4.48 (s, 2H, N-CH_2). For comp. **XIV**: 7.71 (dd, 4H, o,o'biphenyl H, J_1 = 8.25, J_2 = 2.4), 7.65 (dd overlapped, 1H, 5H, J_1 = 11.85, J_2 = 2.4), 7.61 (d, 2H, biphenyl m-H, J = 8.1), 7.47 (d, 2H, biphenyl-m'- H, J – 8.1), 6.97 (d, 1H, 6H, J=2.1), 6.94 (d, 1H, 8H, J= 2.1), 6.9 (d, 1H, 3H, J=2.1), 6.04 (s, 2H, 7 amino), 5.5 (s, 2H, -CH_2-N_3), 4.5 (s, 2H, O-CH_2).

3.2.4 Synthesis of 7-amino-4-methyl-2-[1-methyleno(4-p-methylazido)biphenyl] quinolone and 7-amino-4-methyl-2-O-[methyleno(4-p-ethylazido)biphenyl]quinoline

These compounds were synthesized as corresponding trifluoromethyl-derivatives (see above). R_f for **XV** is 0.22 (in hexane-acetone 2:1 developing system). UV absorption spectra for comp. **XV:** λ_{max1} = 225 nm, λ_{max2} = 260 nm, λ_{max3} = 350 nm, λ_{min1} = 217 nm, λ_{min2} = 243 nm, λ_{min3} = 308 nm; for comp. **XVI**: λ_{max1} = 235 nm, λ_{max2} = 256 nm, λ_{max3} = 335 nm, λ_{min1} = 225 nm, λ_{min2} = 242 nm, λ_{min3} = 305 nm. ^{1}H NMR chemical shifts (d) in DMSO for comp.**XV** are: 7.65 (dd, 4H, o,o'biphenyl H, J_1 = 11.1, J_2 = 8.4), 7.45 (dd overlapped, 1H, 5H), 7.45 (dd,2H, biphenyl m-H, J_1 = 8.25, J_2 = 5.1), 7.25 (d, 2H, biphenyl-m'- H, J – 8.1), 6.49 (d, 1H, 6H), 6.44 (dd, 1H, 3H, J= 1.8), 6.21 (s, 1H, 8H), 5.8 (s, 2H, 7-amino), 5.38(s, 2H, N-CH_2), 4.4 (s, 2H, -CH_2-N_3), 2.36 (d, 3H, 4-methyl, J = 0.9).

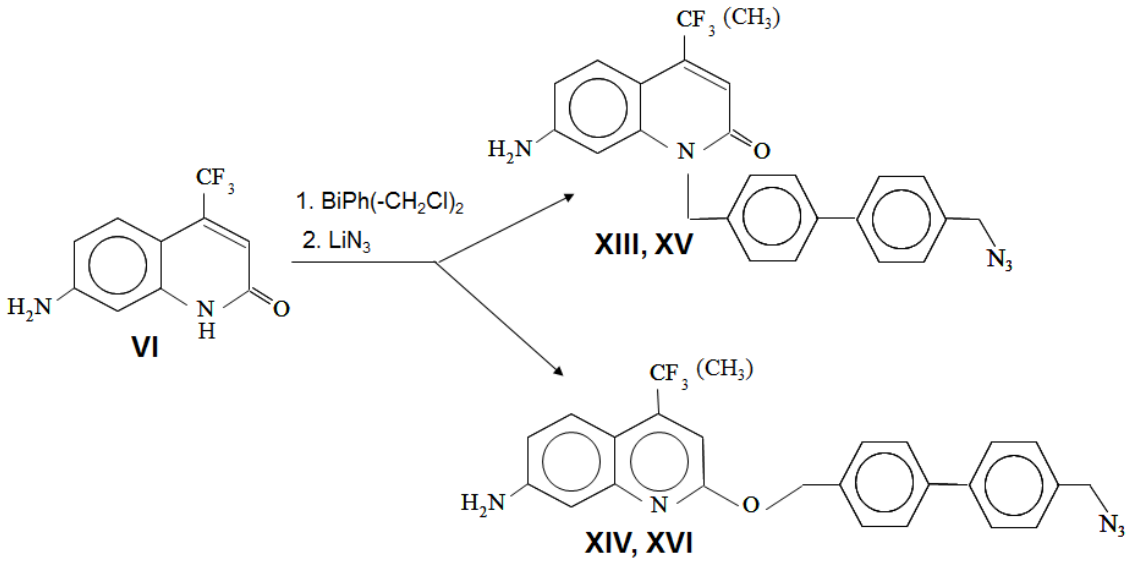

Scheme 3.4 Synthesis of cs124 reactive derivative with biphenyl spacer.

3.2.5 Synthesis of 7-methylamino-4-trifluoromethyl-2[1-(3-azidooxypropyl)] Quinolone and 7-dimethylamino-4-trifluoromethyl-2[1-(3-azidooxypropyl)]) Quinoline

Ten milligrams of 7-amino-4-trifluoromethyl-2-(3-azidooxypropyl) quinoline were dissolved in 0.1 ml of DMF and supplemented with 30 µl of iodomethane. After 1 h, 2 µl of N-,N-diiso propylethylamine was added and incubation continued for another 4 h. The alkylation products were purified by preparative TLC using hexane-acetone (3:1) mixture as developing solvent. Yield for compound **XXI (7-methylamino-4-trifluoromethyl-2[1-(3-azidooxypropyl)] quinoline** was 1 mg: UV absorption spectrum, λ_{max1} = 257 nm, λ_{max2} = 271 nm, λ_{max3} = 360 nm. λ_{min1} = 246 nm, λ_{min2} = 262 nm, λ_{min3} = 315 nm. Yield for compound **XXII (7-dimethylamino-4-trifluoromethyl-2[1-(3-azido oxypropyl)]) quinolone)** was 2.5 mg. UV absorption spectrum, λ_{max1} = 221 nm, λ_{max2} = 266 nm, λ_{max3} = 378 nm. λ_{min1} = 208 nm, λ_{min2} = 246 nm, λ_{min3} = 318 nm. ^{1}H NMR chemical shifts (d) in DMSO for comp. **XXI** are: 7.60 (dd,1H, 5H, J_1= 9.15, J_2 = 2.1), 6.97 (dd, 1H, 6H, J_1 = 9.15, J_2 = 2.1), 6.90 (s, 1H. 8H), 6.85 (d, 1H, 3H, J = 2.1), 6.69 (d, 1H, 3H,J=2.4), 6.64

(q, 1H, 7-amino, J=5.1), 4.46 (t, 2H, γCH_2, J = 6.3), 3.54 (t, 2H, αCH_2, J=6.6), 2.79 (d,3H, monomethy-NCH_3, J = 4.8, 2.05 (quintet, 2H, βCH_2, J=6.6). For comp. **XXII:** 7.74 (dq,1H, 5H, J_1= 5.1, J_2 = 2.1), 7.2 (dd, 1H, 6H, J_1 = 9.15, J_2 = 2.7), 6.99 (s, 1H. 8H), 6.9 (d, 1H, 3H, J = 2.7), 4.48 (t, 2H, γCH_2, J = 6.3), 3.54 (t, 2H, αCH_2, J=6.6), 3.07 (s, 6H, monomethyl and dimethyl group), 2.06 (quintet, 2H, βCH_2, J=6.3).

3.2.6 Synthesis of 7-acetamido-4-trifluoromethyl-2-(3-azidooxypropyl) Quinoline

Five milligrams of compound **X** were dissolved in 50 μl of DMF and 20 μl of acetic anhydride was added. The reaction was allowed to proceed at room temperature for 1h. The product was purified by preparative TLC using hexane-acetone (3:1) mixture. Yield 4.2 mg. UV absorption spectrum, λ_{max1} = 226 nm, λ_{max2} = 254 nm, λ_{max3} = 325 nm, λ_{max4} = 339 nm; λ_{min1} = 241 nm, λ_{min2} = 302 nm, λ_{min3} = 330 nm. ^{1}H NMR chemical shifts (d) in DMSO for comp. **XXIII (7-acetamido-4-trifluoromethyl-2-(3-azidooxypropyl) quinoline)** are: 10.43 (s, 1H, -NH), 8.42 (d, 1H, 8H, J=1.8), 7.9 (d,1H, 5H, J_1= 9.1, J_2 = 2.1), 7.61 (dd, 1H, 6H, J_1 = 9.0, J_2 = 2.1), 7.23 (s, 1H. 3H), 4.52 (t, 2H, γCH_2, J = 9.6), 3.56 (t, 2H, αCH_2, J=6.6), 2.13 (s, 3H, acetyl methyl group), 2.06 (quintet, 2H, βCH_2, J=6.3).

3.2.7 Synthesis of 7-amino-4-ethoxy-3-carboxamido(6-isothiocyanobutyl)-2-trifluoro methylquinoline

3.2.7.1 Synthesis of 7-amino-4-ethoxy-3-carbomethoxymethyl-2-trifluoro methyl quinolone. A mixture of 2.2 ml trifluoroacetoacetate and 1.5 ml methylbromoacetate in 7 ml DMF was placed in a round-bottom flask, cooled on ice and 1.0 g of powdered KOH was added in a few portions under intensive agitation so that the temperature of the reaction mixture is kept in the range 40 – 50 ^{o}C. After 1 h reaction the incubation continued at 60 °C for another 1 hr. The reaction mixture was then diluted with 20 ml water and extracted with chloroform. The organic layer was collected, dried over anhydrous sodium sulfate and evaporated in vacuo at 70 °C for 30 minutes to remove un-reacted components. The residue (1.9 g) was dissolved in 3.5 ml of DMSO and 0.76 g of 1,3-phenylenediamine was added, followed by incubation at 50 °C overnight. A major fluorescent product (R_f = 0.9 in ethylacetete as developing solvent) with intense green-blue fluorescence was observed. The mixture was diluted to 30 ml by 0.05 M aqueous NaOH and extracted with ether (2 x 40 ml). The organic layer was dried over anhydrous sodium sulfate and evaporated in vacuo. The residue was then subjected to silica gel chromatography on 40 ml column using hexane-acetone (4:1) mixture as eluent. The fraction corresponding to the products migrating with R_f = 0.9 in ethylacetete was collected and evaporated to dryness. Yield 400 mg (12 %). UV: λ_{max} = 350 nm (ε= 10000 M^{-1} cm^{-1}), λ_{min} = 270 nm (ε= 6300 M^{-1} cm^{-1}). ^{1}H NMR chemical shifts (d) in DMSO are: 1,33(t, 3H, 4-OCH_2CH_3, J=7.2), 3.65 (s, 3H,-OCH_3), 3.94 (q, 2H, 3-methylene, J=2.4), 4.38 (q, 2H, 4-OCH_2CH_3, J=7.2), 5.94 (2H, broad, 7 amine), 6.83 (d, 1H, 8H, J=2.4), 6.92 (dd, 1H, 6H), 7.67 (m, 1H, 5H).

3.2.7.2 Synthesis of 7-amino-4-ethoxy-3-carboxymethyl-2-trifluoromethylquinoline.

One milliliter of 1 M aqueous NaOH was added to 100 mg of product **XVII** dissolved in 2 ml dioxane. After 2 h of incubation at 50°C, the organic solvent was evaporated at reduced pressure. The aqueous solution was acidified to pH 3 – 3.5 by addition of citric acid and extracted with chloroform. The chloroform layer was collected, dried over anhydrous sodium sulfate and evaporated *in vacuo*. Yield = 60 mg. ^{1}H NMR chemical shifts (d) in DMSO are: 1,34 (t, 3H, 4-OCH$_2$C**H**$_3$, J=7.2), 3.84, (q, 2H, 3-methylene, J=2.4), 4.41 (q, 2H, 4-OC**H**$_2$CH$_3$, J=7.2), 5.9 (2H, broad, 7 amine), 6.83 (d, 1H, 8H, J=2.4), 6.92 (dd, 1H, 6H, J_1=10, J_2=2.4), 7.67 (m, 1H, 5H), 12,52 (1H, broad, carboxyl).

3.2.7.3 Synthesis of 7-amino-4-ethoxy-3-methylcarboxamido(4-tritylaminobutyl methyl)-2-trifluoromethylquinoline. Compound XVIII (60 mg, 180 µmol) was dissolved in 2 ml of THF and supplemented with 28 mg (200 µmol) of 4-nitrophenol and 100 mg (380 µmol) of dicyclohehylcarbodiimide (DCC). Following 30 min incubation, 300 µmol of N-trityl-1,4-diaminobuthane in 3 ml of methanol was added to the above mixture and incubation continued for another 60 min. The solvent was evaporated in vacuo, the residue dissolved in chloroform and extracted three times with 0.1 M aqueous sodium bicarbonate. Organic phase was evaporated in vacuo and the product purified by silicagel column chromatography using hexane/acetone (3:1) as eluent. Yield – 70 mg. ^{1}H NMR chemical shifts (d) in DMSO are: 1,2-1.8 (m, 12H,), 1,93 (q, 2H, ζ-methylene, J=7.2), 3.00 (q, 2H, α-methylene, J=7.2) 3.72 (q, 2H, 3-methylene, J=2.4), 4.38 (q, 2H, 4-OCH$_2$CH$_3$, J=7.2), 5.85 (2H, broad, 7 amine), 6.89 (dd, 1H, 8H, J_1=10, J_2=2.4), 7.17 (t, 3H, p-ArH, J=7.2), 7.28 (t, 6H, m-ArH, J=7.4), 7.39 (d, 6H, o-ArH, J=7.4), 7.67 (m, 1H, 5H), 7.84 (t, 1H, amide, J=7.2).

3.2.7.4 Synthesis of 7-amino-4-ethoxy-3-carboxamido(6-isothiocyanobutyl)-2-trifluoro methylquinoline. The product XIX was dissolved in 2 ml of 90 % acetic acid. After incubation (90 ^{o}C, 15 min) the mixture was evaporated in vacuo. The residue was suspended in 2 ml of 0.1 M aqueous HCl and extracted with chloroform. The aqueous phase was supplemented with NaOH to pH 12 - 12.5 and extracted by chloroform. The organic phase was dried over anhydrous sodium sulfate and evaporated *in vacuo.* The residue was dissolved in 2 ml of chloroform/methanol (5:1) mixture and 22 mg (120 μmol) of 1,1'-thiocarbonyldiimidazole were added. After 10 min, 150 μmol of trifluoroacetic acid was added and incubation continued for 60 min at 50 ^{o}C. The mixture was diluted with water and extracted with chloroform. The organic layer was evaporated and the product purified by silicagel column chromatography. Yield: 40 mg. ^{1}H NMR chemical shifts (d) in DMSO are: 1.2-1.5 (m, 9H), 1.62 (m, 2H, ε-CH_2, J=7.2), 3.04 (m, 2H, α-CH_2, J=7.2), 3.65 (t, 2H, ζ-CH_2, J=7.2), 3.73 (s, 2H, 3-methylene), 3.90 (q, 2H, -OCH_2CH_3, J=7.2), 5.85 (s, 2H, broad, 7 amine), 6.7 (d,1H, 8H, J=2.4), 6.89 (dd, 1H, 6H, J_1=7.2, J_2=2.4), 7.66 (m, 1H, 5H), 7.87 (t, 1H, broad, amide).

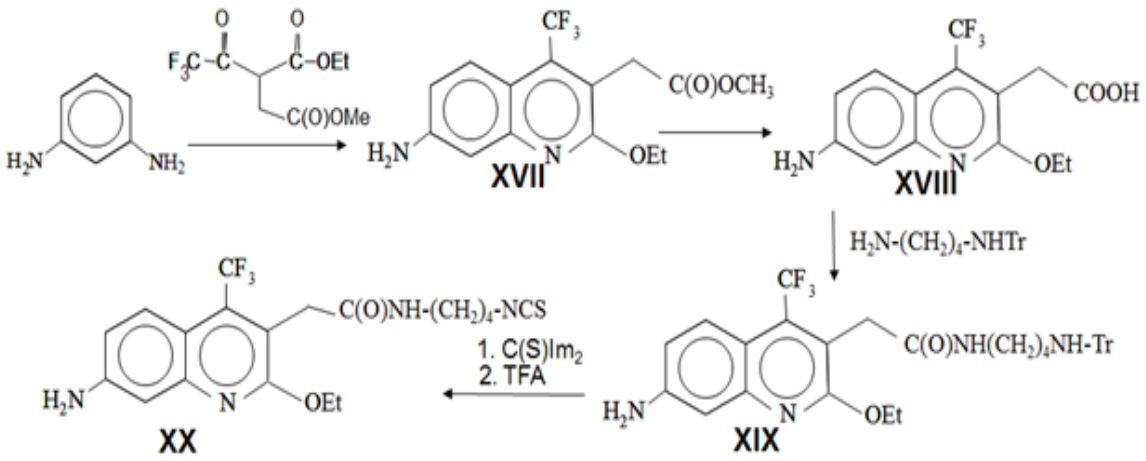

7-amino-4-ethoxy-3-carboxamido(6-isothio cyanobutyl)-2-trifluoromethylquinoline

7-amino-4-ethoxy-3-methylcarboxamido(4-tritylaminobutylmethyl)-2-trifluoromethylquinoline

Scheme 3.5 Synthetic strategy for amine reactive quinolone derivative.

3.2.8 Click Reactions

Three microliters of 2M triethylammonium acetate buffer, pH 7.0 and 15 µl of DMSO were mixed with 5 µl of 0.5 mM alkyne-modified oligonucleotide possessing, or lacking a quencher. One microliter of the 10 mM azido-fluorophore, 3 µl of 5mM ascorbic acid solution; and 3 µl of 10 mM Copper (II) – TBTA stock in 55% DMSO, were consequently added to the solution. After overnight incubation at room temperature, the mixture was supplemented with 3 µl of 3 M NaAc pH 5.5 and oligonucleotide material precipitated by addition of 300 µl of ethanol. The residue was additionally washed by 80% ethanol (2 x 0.3 ml), dissolved in water and subjected to reverse phase HPLC.

3.2.9 Reaction of Isothiocyano-Compound with Cysteine and Ethylenediamine

The reaction mixture contained 0.1 M sodium-borate pH 9.5, 10 mM cysteine, and 0.1 – 1 mM of isothiocyano compound. The mixture was incubated 5 min at room temperature and the reaction products analyzed by TLC using acetonitrile-water (3:1) as developing

solvent. The reaction with ethylenediamine was performed with 0.1 M ethylenediamine pH 8.0 at 50 ^{o}C for 1 h. The products were analyzed as described for cysteine reaction.

3.2.10 Synthesis of Reactive Quinolone and Quinoline Derivatives

The next goal was the synthesis of crosslinkable derivatives of cs124-CF_3 and newly discovered quinoline fluorescent derivative Qin124-CF_3. To this end, the possibility of chemical modification of these fluorophores was investigated. By analogy with previous observations ((53), (54)), it is reasoned that amide group of cs124-CF_3 in ionized form can undergo alkylation, thus allowing introduction of crosslinking groups into the core moiety (Scheme 3.2). Indeed, incubation of cs124-CF_3 with ethyl ester of p-toluenesulfonic acid in the presence of NaOH yielded two fluorescent products migrating with R_f = 0.44 and 0.9 in TLC in ethylacetate developing system. It is proposed that these two products originate due to alkylation at the amido group nitrogen and oxygen that can assume a negative charge (providing high reactivity) as a result of lactim-lactam tautomery (see Scheme 3.2). These alkylation reactions would afford quinolone (**VII**) and quinoline (**VIII**) compounds correspondingly. Indeed, NMR analysis confirmed the proposed structures. Next, we performed the same reaction but with 1-iodo-3-azidopropane, alkylating compound bearing azido group (Scheme 3). In the other version fluorophore was treated with bifunctional alkylating agent, 4,4'-bis(chloromethyl) biphenyl and the introduced the azido group by subsequent reaction with lithium azide. The final products (compounds **IX** and **X**) of Scheme 3.3 as well as **XIII** and **XIV** of Scheme 3.4 can be used directly for coupling to the molecules of interest via "click"-reaction with alkyne counterparts pre-attached to the molecules of interest. Alternatively, the azido group can be reduced to amino group (comp. **XI**) that can be converted to

amine-reactive isothiocyano group (comp. **XII**), or to thiol-reactive bromoacetamido group. The reduction of the azido-compound was performed with high yield by treatment with triphenylphosphine followed by incubation with ammonium hydroxide. Isothiocyano derivative was obtained by reaction of products **XI** with thiocarbonyldiimidazole, and subsequent treatment with trifluoroacetic acid. The reactivity of the resulting compounds was confirmed by reaction with cysteine using TLC analysis. Similar approaches were further used for the synthesis of biphenyl derivatives of 4-methyl- and 4-trifluoromethylquinolones **XIII** -**XVI** (Scheme 3.4).

The crosslinkable quinoline compounds could also be obtained using modified derivatives of ethyl 4,4,4-trifluoroacetoacetate by adapting the previously published protocols for the synthesis of analogous quinolone compounds (51). In this way, alkylation of ethyl 4,4,4-trifluoroacetoacetate with methyl ester of bromoacetic acid at methylene carbon (Scheme 3.5) was first performed. The resulting intermediate was incubated with 1,3-phenylenediamine at moderate temperature that favors formation of quinoline compound (product **XVII** of Scheme 3.5) that was converted to cadroxylate (compound **XVIII**) by saponification. This compound was treated with carbodiimide and 4-nitrophenole resulting in activated ester that was introduced in reaction with mono-tritylated 1,4-diaminobutane yielding compound **XIX**. Deprotection followed by treatment of the resulting amino-derivative with N,N-thiocarbonyldiimidazole and trifluoroacetic acid afforded final product – isothiocyanate **XX**.

3.3 Results

3.3.1 Investigation of the Reaction Mechanism for Quinolone and Quinoline Fluorophore Formation

In the previous study (51), during the synthesis of carbostyril derivatives along with expected quinolone compound cs-124-CF_3, a new fluorescent product which has not been described was detected. Since the compound was highly fluorescent and displayed large Stokes shift (120 nm), it was worthwhile to identify it and study the reaction mechanism in more details in order to determine the influence of the reaction conditions on the product yield. The suggested mechanism for the reaction between ethyl 4,4,4-trifluoroacetoacetate with 1,3 phenylenediamine is shown in Scheme 3.1. Chromatographic analysis revealed that incubation of starting compounds results in quick accumulation of unknown fluorescent product (compound **IV** of Scheme 3.1, which is named Qin124-CF_3) with R_f = 0.9 along with expected compound cs124-CF_3 (R_f = 0.44). Some non-fluorescent compounds (compound **V** of Scheme1, R_f = 0.62 and another product with R_f = 0.84), possibly reaction intermediates were also detected. Continued incubation of these purified non-fluorescent products in the original reaction conditions showed that the compound **V** slowly converted into fluorescent cs124-CF_3. (compound **VI** of Scheme 3.1, R_f = 0.44). At the same time, incubation of purified compound **V** in the reaction conditions did not lead to compound **IV**, suggesting that compound **IV** originates from an earlier reaction intermediate (possibly from compound **II**). This is consistent with the fact that fluorescent compound **IV** stops accumulating after intermediate **V** is formed in the course of the synthetic reaction (Figure.3.1). Finally, non-fluorescent reaction product with R_f = 0.84 was stable at the incubation conditions and therefore represented the side-product. In compound **II,** elimination of ethanol would

lead to observed precursor of cs124-CF_3 (compound **V**), while dehydration would create compound **III**, which finally converts to fluorescent product **IV**. The identity of compounds **IV**, **V**, and **VI** was confirmed by NMR spectroscopy. In addition, we have shown that product **IV** was authentic to the compound obtained by O-ethylation of cs124-CF_3 (see below) as judged by chromatographic mobility, UV absorption, fluorescence, and NMR spectroscopy. The formation of analogous to **IV** 7-hydroxyquinoline compound upon incubation of 3-aminophenol with trifluoroacetoacetate has been reported (52), reflecting common reaction mechanism. The structure of the initial reaction intermediate is more uncertain, since the only stable adduct amenable for analysis is **V**. Ethyl 4,4,4-trifluoroacetoacetate has two electrophilic centers, which are carbons of carbonyl function and esterified carboxyl group. There are also two nucleophilic centers in phenylenediamine (amino groups and carbons of the ring in positions 4 and 6) that can be potentially attacked by acetoacetate derivative. Thus initial reaction can proceed through acylation of the amino group (compound I) followed by intramolecular attack of the phenyl ring (product **II**). As indicated by UV absorption spectroscopy and chromatographic mobility the same fluorescent compounds were formed at both 50 °C and 110 °C. However, high temperature dramatically accelerates the formation of quinolone derivative (from intermediate **V**), while the amount of produced quinoline compound was not effected in accordance with proposed kinetic scheme (Scheme 3.1).

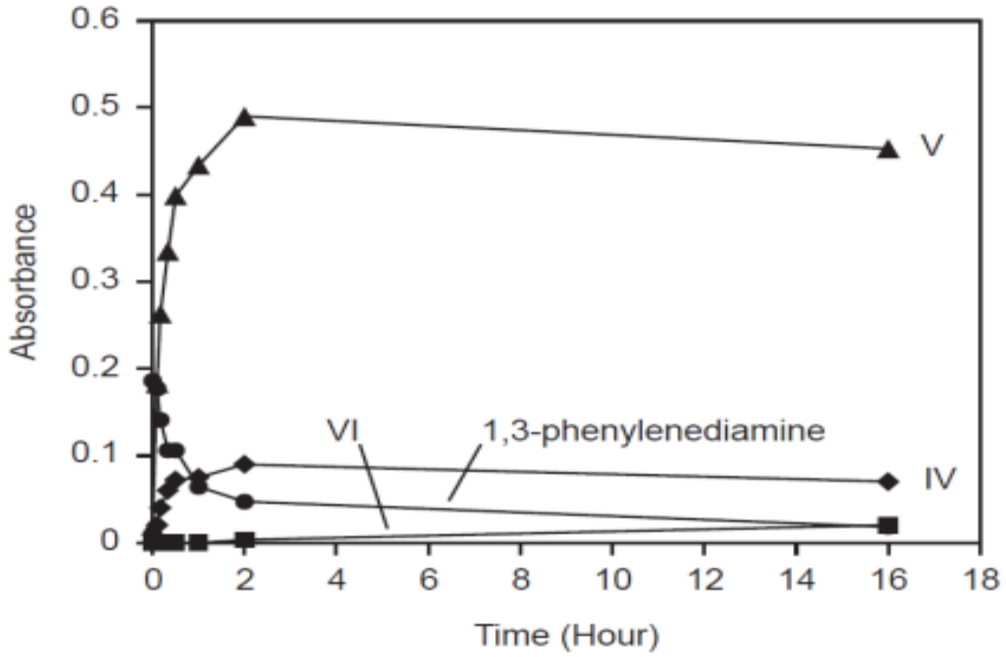

Figure 3.1 Time course for product accumulation in the reaction mixture containing 1,3-phenylenediamine and trifluoroacetoacetate. Products are numbered according to Scheme 3.1.

V-to-**VI** conversion is strongly accelerated (ca. 10^6 times) in the presence of NaOH. The same, but less pronounced effect (ca. 50 times) was observed upon the addition of catalytic amount of trifluoroacetic acid to the starting reaction mixture. These findings allow dramatic reduction of both reaction temperature and the reaction time and nearly quantitative conversion of starting compounds to fluorophores **IV** and **VI**.

3.3.2 UV Absorption and Fluorescent Spectra of the Synthesized Compounds

As seen from Table 3.1 and Figure 3.2, the synthesized compounds have absorption maxima in the register 200-300 nm as well as longer wavelength absorption (300-400 nm) optimal for fluorescence excitation. The molar extinction for the compounds in this far UV region vary from 6000 to ca. 19 000 $M^{-1}sm^{-1}$. Generally, quinolone compounds in the range 300-400 nm have extinction coefficients two-three fold greater than corresponding quinoline compounds (compare compounds **IX** and **X**; **XIII** and **XIV**).

Quantum yields for compounds **XIII** and **XIV** are comparable, while quantum yield for **X** is half of that for **IX**. Among corresponding quinolone and quinoline derivatives of 4-methyl substituted compounds, quantum yields differ insignificantly as well (compare comp. **XV** and **XVI**).

Table 3.1 Fluorescent and UV-absorption Properties of Synthesized Fluorophores and Reference Compound, 4-methylumbelliferone

Compound	Absorption $M^{-1} \times cm^{-1}$	Excitation (nm)	Emission (nm)	Stokes shift (nm)	Relative brightness	Quantum yield* (Φ)
4-Me-umb.	16 500	365	446	81	1	0.7
IX	18 900	370	450	80	0.77	0.47
X	10 000	359	463	104	0.22	0.26
XV	18 000	353	404	51	0.79	0.51
XVI	9 000	343	413	70	0.30	0.39
XIII	18 000	372	450	78	0.84	0.54
XIV	6 000	360	461	101	0.22	0.42
XXI	10 000	367	465	98	0.24	0.28
XXII	10 000	374	481	107	0.24	0.27
XXIII	10 000	339	402	63	0.12	0.14

*Calculated by comparison to the reference compound 4-methylumbelliferone.

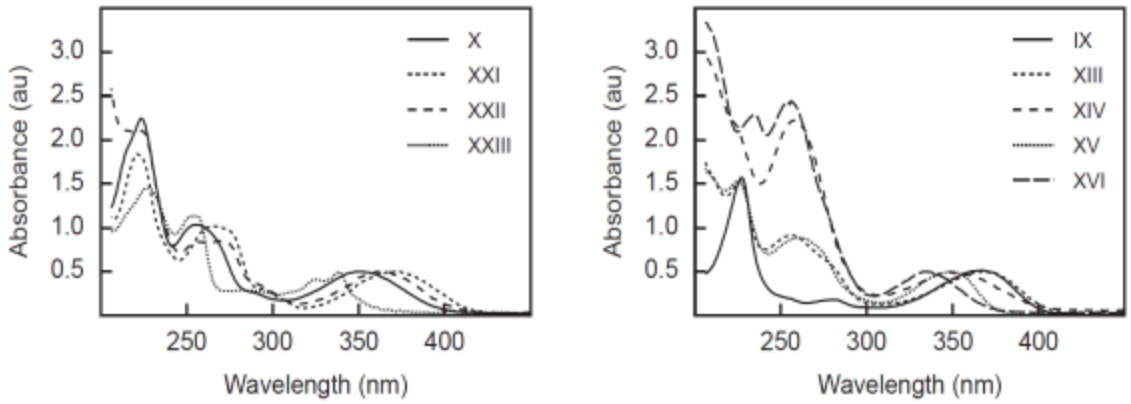

Figure 3.2 UV absorption spectra for reactive fluorophore compounds.

In order to generate fluorophores with various colors it was studied how chemical modification of 7-amino group of quinoline compounds effect their emission spectrum. Based on various modifications, mono- and dimethylamino- derivatives (compounds **XXI** and **XXII** correspondingly) and related acetamido- derivative (compound **XXIII**) were obtained. As seen from Table 3.1 and Figure 3.2 these modifications significantly changed fluorescent properties of the original fluorophore (compound **X**). Thus methylation of the amino group caused red shift, while acylation resulted in strong blue shift of the emission spectrum. While methylation did not affect quantum yield of the fluorophore, acetylation caused two fold reduction in quantum yield. Comparing to trifluoromethyl fluorophores (compounds **IX**, **X**) corresponding 4-methyl derivatives (compounds **XV**, **XVI**) displayed blue shift of fluorescence emission (Table 3.1 and Figure 3.2). In generally, it was noted that Stokes shifts were larger for 4-trifluoromethyl compounds comparing to corresponding 4-methyl fluorophores. The emission spectra of synthesized reactive fluorescent compounds cover all colors from deep blue to green (Figures 3.3 and 3.4), which makes them useful labels in biochemical and technical applications.

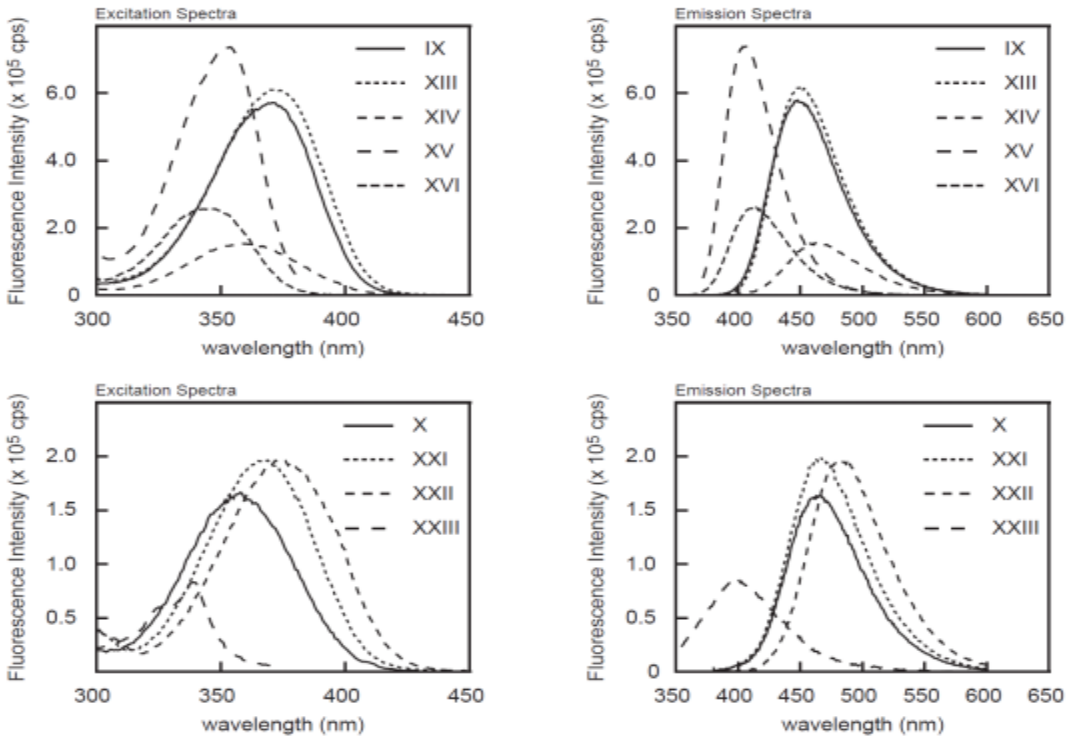

Figure 3.3 Fluorescent spectra for reactive fluorophore compounds.

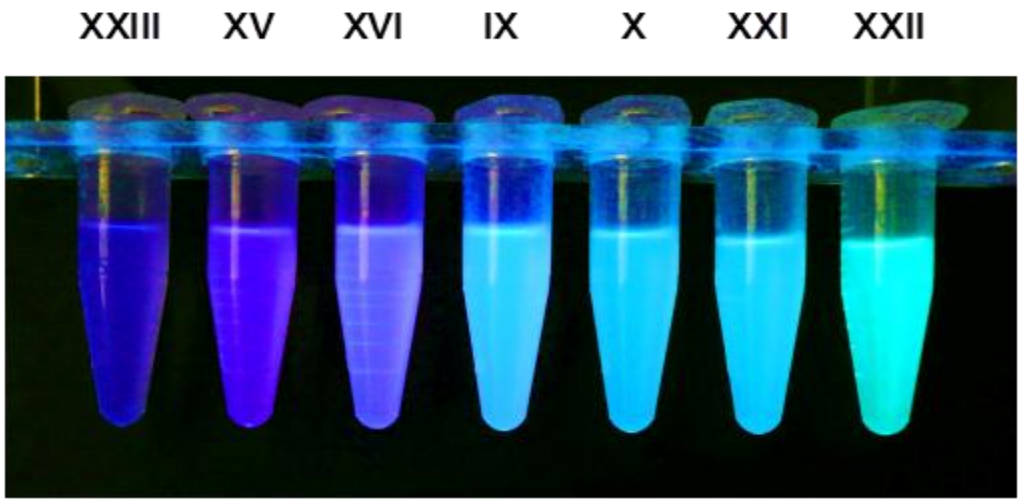

Figure 3.4 Typical fluorescence of fluorescent compounds.

3.3.3 Chemical Reactivity of Synthesized Compounds

In the present study the obtained amine/thiol-reactive isothiocyano (ITC)- as well as azido-derivatives of fluorophores, which are suitable for click-reaction with acetylenic counterparts, catalyzed by copper complexes. The reactivity of ITC compounds was examined with cysteine at weakly alkaline conditions favoring ionization of thiol group. The reaction proceeded quickly and quantitatively at room temperature, yielding dithiocarbamate derivatives as was evidenced by strongly reduced mobility of the reaction products on TLC. The same effect was observed in reaction of ITC compounds with ethylenediamine at 50 ^{o}C.

Click reactivity of azido-fluorophores was confirmed by incubation with alkyne-derivatized oligonucleotides in the presence of copper complex and ascorbate. HPLC of the reaction mixture revealed nearly quantitative coupling of the fluorophores to the oligos (Figure 3.2). These results suggest suitability of the synthesized compounds for fluorescent DNA labeling. It should be mentioned that attachment of fluorophores to DNA was accompanied by considerable quenching (Table 3.2), which was most likely due to stacking interaction of the fluorophores with DNA bases.

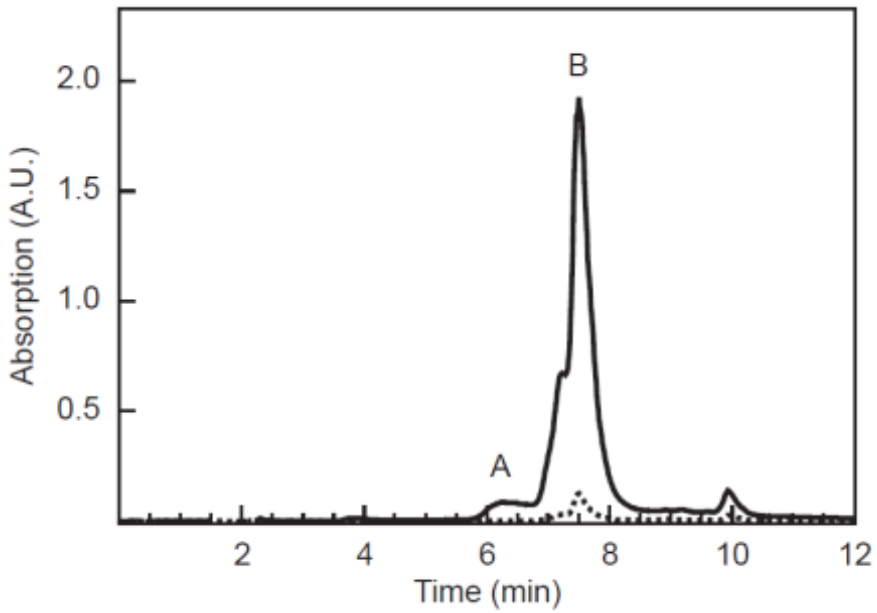

Figure 3.5 HPLC analysis of the reaction mixture after click-attachment of fluorophore X To an oligonucleotide oligo. A = starting material; B = fluoropfore-modified oligo.

Table 3.2 Fluoroscence of Free Fluorophores and the Same Fluorophores Attached to DNA

Probe	Fluorescence of free probe	Fluorescence of oligo-bound probe	Quenching factor
XIII	5.9×10^5	2.5×10^5	2.4
XV	7.5×10^5	1.1×10^5	6.8
IX	5.8×10^5	1.6×10^5	3.6

3.4 Summary

In the present research, new synthetic strategies to obtain fluorescent derivatives of quinolone fluorophores have been explored. In the course of optimization of the reaction conditions for the synthesis of 4-trifluoromethyl quinolone compound, previous observations on an unknown product with useful fluorescent properties were made. This prompted to investigate the reaction mechanism in more details. NMR spectrum, along with kinetic data of the product accumulation suggests that this new compound represents 7-amino-4-trifluoromethyl-2-ethoxyquinoline. The identity of the product was confirmed by its independent synthesis through ethylation of 7-amino-4-trifluoromethylquinolone. Further characterization of this compound (Table 3.1) revealed its valuable fluorescent properties, which are large Stokes shift (104 nm) and high quantum yield (ca. 0.3).

Furthermore, the possibility to modify quinolone compounds with the aim to introduce crosslinkable groups for fluorescent labeling was explored. At this end, it as found that quinolones can be easily modified by alkylation either at amide nitrogen, or oxygen to yield N-1 derivatives of quinolone, or O-2 derivatives of quinoline, correspondingly. The reaction proceeds with high yield in the alkaline conditions that promote ionization of the amido group. Using this reaction, crosslinkable derivatives containing isothiocyano-, or azido groups were obtained. In addition, alternative approaches were explored to introduce crosslinking group into quinoline moiety using previously described reaction of 1,3-phenylenediamine with trifluoro methylmethylethylsuccinate that proved useful for corresponding quinolone derivatives. The desired compound was obtained with reasonable yield by optimization of the reaction temperature. Structurally related 4-methyl quinolone and quinoline fluorescent derivatives were obtained using analogous derivatization reactions. These derivatives

exhibit considerable blue emission shift comparing to 4-trifluoromethyl counterparts. Synthesized fluorescent compounds can be further modified at 7-amino group, allowing tuning of fluorescence emission, so that altogether the synthesized reactive compounds span emission register from deep blue to green. These fluorescent compounds can be efficiently crosslinked to DNA and proteins, which makes them valuable probes for biochemical applications with detection limit in the nanomolar range.

CHAPTER 4

NEW CROSS-LINKING QUINOLINE AND QUINOLONE BASED LUMINESCENT LANTHANIDE PROBES FOR SENSITIVE LABELING

4.1 Introduction

Luminescent lanthanide labels possess a long emission lifetime resulting in unusually high detection sensitivity in time-resolved mode thus making them useful alternatives to conventional organic fluorophores and radioactive labels (80-87). These complex probes include an antenna-fluorophore coupled to a chelated lanthanide ion. Due to poor light absorption, lanthanide ion has to be sensitized or "pumped". This is achieved by tethering of the ion through a chelator to a light-absorbing molecule, which after photon capture transfers the energy to the lanthanide, thereby acting as an antenna. An excited Ln^{3+} ion has a unusually long millisecond lifetime, since transition from excited-to-ground state is formally forbidden. Lanthanide probe emission spectra are sharply spiked, due to the shielding effect of outer electron orbits. Another remarkable property of the emission is the large spectral distance between excitation end emission light (Stokes shift), which further contributes to high detection sensitivity.

Despite a great demand in lanthanide luminescent labels, their widespread is impeded by high price of commercially available probes, which is mostly due to laborious multi-step synthesis. Indeed, a lanthanide probes include three functional units: antenna, chelated lanthanide metal, and cross-linking group (for the attachment to the biomolecule of interest) as shown in Figure 4.1. This requires a complex synthetic strategy and eventually leads to compounds whose size often exceeds 1000 Da. The goal was to develop simple strategies for the synthesis of crosslinking lanthanide chelates that efficiently couple to biomolecules. As prototypes for the crosslinking probes, we have

chosen oligoethyleneiminocarboxylate chelates of common carbostyril fluorophores such as cs124 and cs124CF_3 (88-96). High quantum yield and solubility in water makes these compounds suitable for labeling of biomolecules and live cells.

A number of methods for the conjugation of these chelates to biomolecules have been suggested. One of them is accomplished through the dianhydride form of DTPA. This is where one anhydride function modifies the amino group of a chromophore, while the other reacts with the amino group of a biomolecule (88). Even though this approach is technically simple, it raises concerns about the side reactions (modification of the other nucleophilic groups) due to high reactivity of anhydrides. The second approach takes advantage of the conjugation of one of DTPA anhydride group with the cs124 moiety, followed by reaction of the remaining anhydride function with the diamine. The unmodified amino group of the resulting adduct can then be converted to amine-reactive isothiocyano, click reactive or thiol-reactive groups (90). However, this mode of attachment of the cross-linking group weakens the lanthanide retention in the chelate by eliminating one ligating carboxylate and also reduces brightness (91) due to quenching effect of additional coordinated water. These factors can potentially restrict *in vivo* applications where high concentration of metal scavengers is an issue (e.g., intracellular imaging). To perfect the lanthanide probes, derivatives with amine and click reactive crosslinking groups in the chromophore moiety of cs124 DTPA and cs124CF_3 DTPA chelates have been developed. This work illustrates that the synthesized luminescent probes as listed in Chart 4.1 are highly luminescent and can be successfully used as luminescent labels for nucleic acid hybridization probes (52), for imaging of bacterial and mammalian cells, and for labeling of a bacterial proteome. Chart 4.2 lists reference compounds, cs124 and cs124-CF_3 and model chelates used in the study.

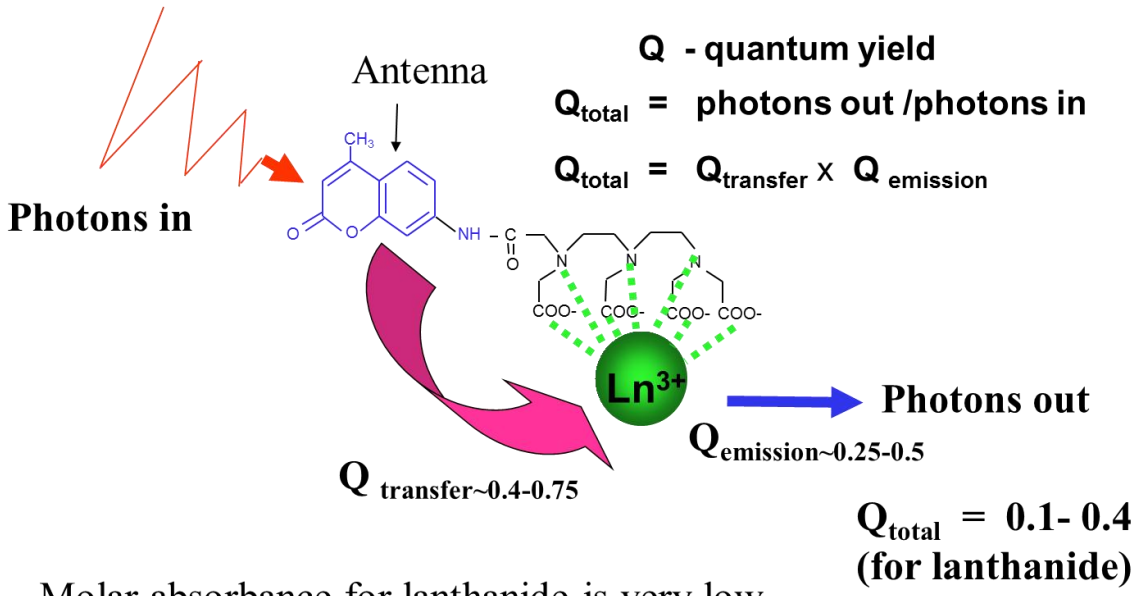

- Molar absorbance for lanthanide is very low.
- Antenna serves to sensitize the lanthanide by transferring the energy
- Q_{total} determines the brightness of the probe

Figure 4.1 Various components of lanthanide probes and operating principle. Lanthanide probe consist of a) Reactive Crosslinking Group b) Antenna Fluorophore for Excitation, and c) Chelated Lanthanide for Light Emission.

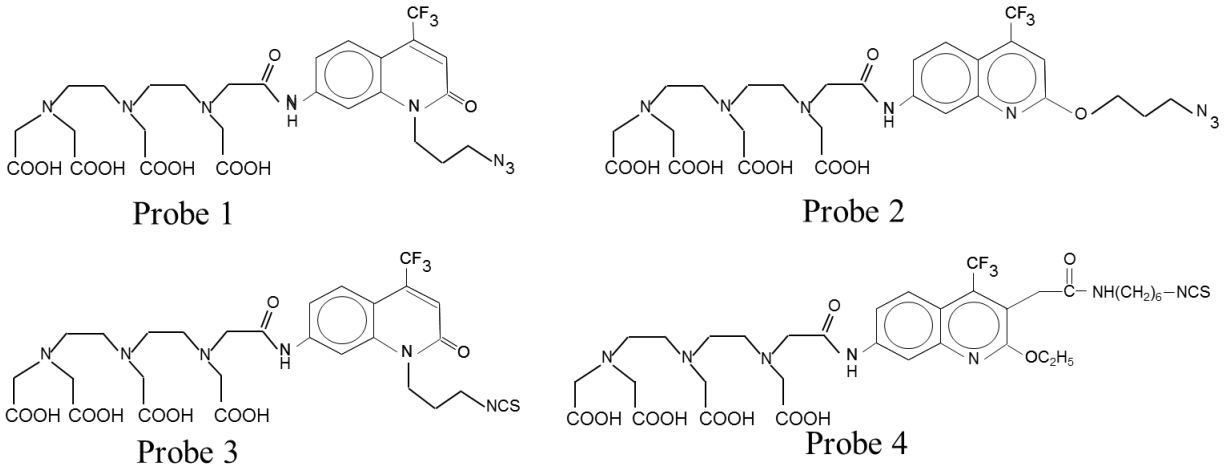

Chart 4.1: The structures of synthesized luminescent lanthanide probes.

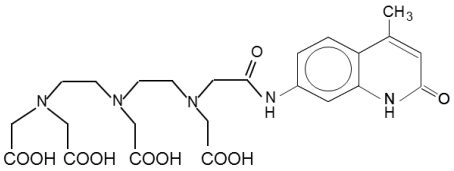

Reference Compound 1
cs124

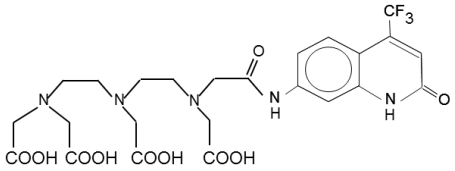

Reference compound 2
cs124-CF_3

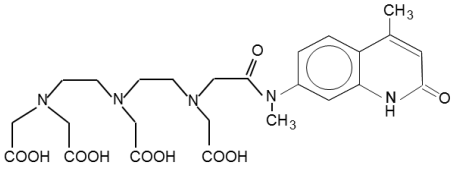

Model Compound

Chart 4.2 The structures of reference compounds, cs124, cs124-CF_3, and model chelate used in the study.

4.2 Synthesis of Lanthanide Probes and Model Chelates

The following reagents were purchased from Aldrich: diethylenetriaminepentaacetic acid dianhydride (DTPA), triethylamine, 1,3-phenylenediamine, ethyl 4,4,4-trifluoroacetoacetate, ethylacetoacetate, 1,3-dicyclohexylcarbodiimide (DCC), ethylenedianime, N-trityl-1,6-diaminohexane, methylbromacetate, anhydrous dimethylformamide and dimethylsulfoxide, 1-butanol, ethylacetate, chloroform, acetonitrile, ethanol, sodium and potassium hydroxide, Na_2SO_4, Na_2CO_3, acetic acid, citric acid, thiocarbonyldiimadazole, $TbCl_3$, $EuCl_3$, $SmCl_3$ and $DyCl_3$, silica gel TLC plates on aluminum foil (200 μm layer thick with a fluorescent indicator). Only distilled and deionized water (18 Ω cm-1) was used. All experiments, including the preparation and use of lanthanide complexes, were performed either in glassware washed with mixed acid solution and rinsed with metal-free water or in metal-free plastic ware purchased from Bio-Rad. All chemicals were the purest grade available.

Synthesized compounds (Chart 4.1) represent cs124 and cs124CF_3 derivatives with modifications in positions 1, 2, and 3 of the carbostyril ring. Three basic strategies have been used for the synthesis.

4.2.1 Synthesis of Probes 1 and 2

Compound I in Scheme 4.1 is synthesized as discussed in Section 3.2.1. Probes 1 and 2 were further obtained through alkylation of cs124CF_3 by 1-azido-3-iodopropane as shown in Scheme 4.1. Alkylation yielded two isomeric compounds – products of the alkyliodide attack on N1 nitrogen and 2-oxygen of anionic form of the starting compound in the ratio 3:1. Subsequent acylation with DTPA dianhydride produced the desired chelates.

The DTPA chelates of probe 1 and probe 2 were them divided into four equal portions. Each portion was then reacted with equimolar concentration of lanthanide salt, $EuCl_3$, TCl_3, $SmCl_3$ and $DyCl_3$ to yield respective lanthanide chelates with distinct spectral and photo-physical properties.

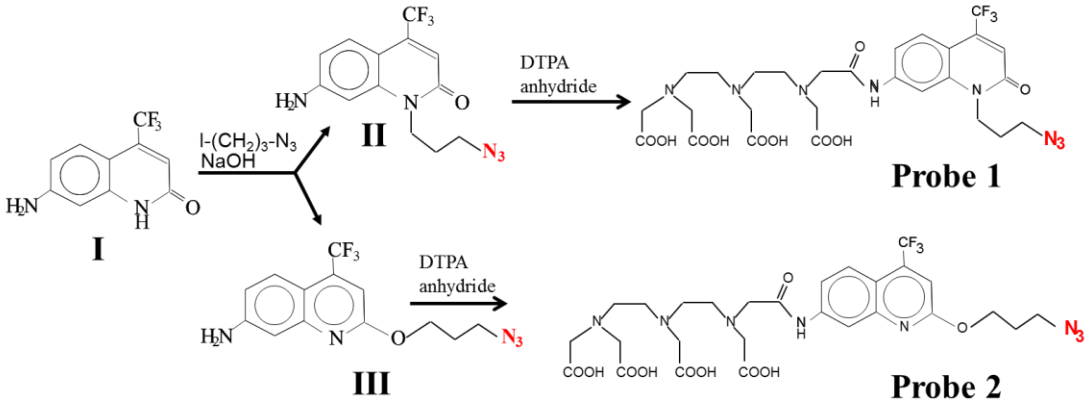

Scheme 4.1: Synthetic strategy for probes 1 and 2.

Eight milligrams (8 mg) of DTPA was dissolved in 80 µl of DMSO and reacted with 3 mg of compound **II** and **III** at 50 °C. The DTPA acylation reaction was monitored

at various time intervals. 5 µl aliquot of reaction mixture was withdrawn at various time intervals in 400 µl of acetonitrile : water (70:30) mixture. UV absorbance measurements of acylation reaction mixtures are shown in Figure 4.2 for probe **1** and in Figure 4.3 for probe **2**.

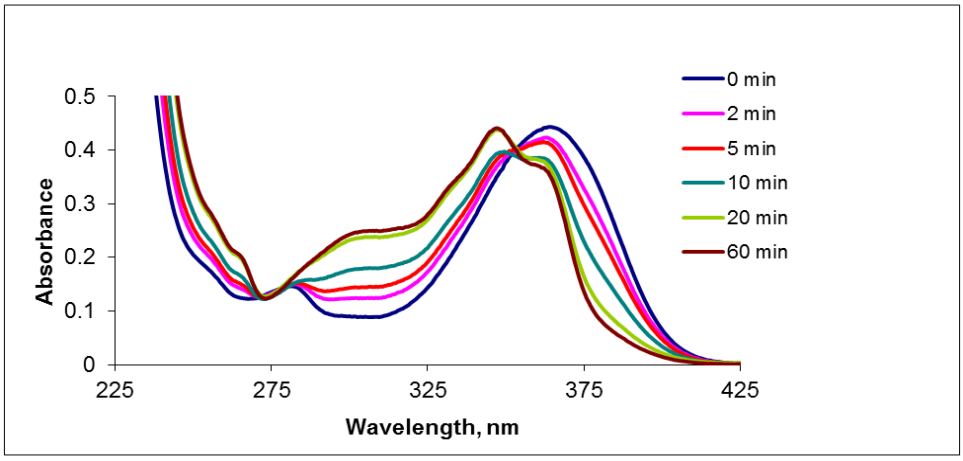

Figure 4.2 DTPA acylation kinetics of probe 1.

The DTPA acylation reaction of probe **1** takes about 60 minutes and displays two isobestic points in absorption spectra.

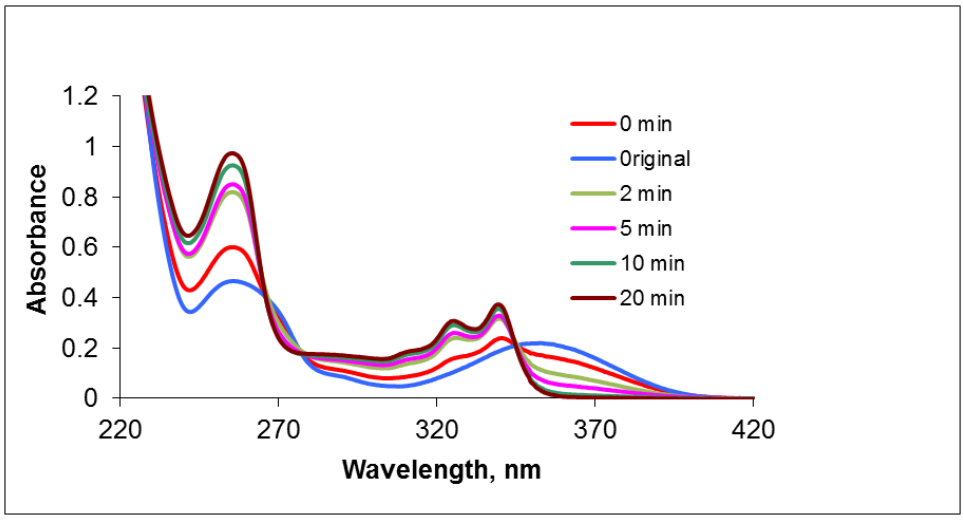

Figure 4.3 DTPA acylation kinetics of probe 2.

The DTPA acylation reaction of probe **2** is relatively faster and takes place in 20 minutes and reveals four isobestic points in the absorbance spectra. Isobestic points suggest absence of consecutive reactions in the system.

4.2.2 Synthesis of Probes 3

Probe 3 can be obtained by treating compound **II** with triphenylphosphine under alkaline conditions to yield the amino derivative. Deprotection followed by treatment of the resulting amino-derivative with N,N-thiocarbonyldiimidazole and trifluoroacetic acid afforded product compound **V**, an isothiocyanate derivative. Subsequent acylation with DTPA dianhydride produced the desired probes 3 (Scheme 4.2).

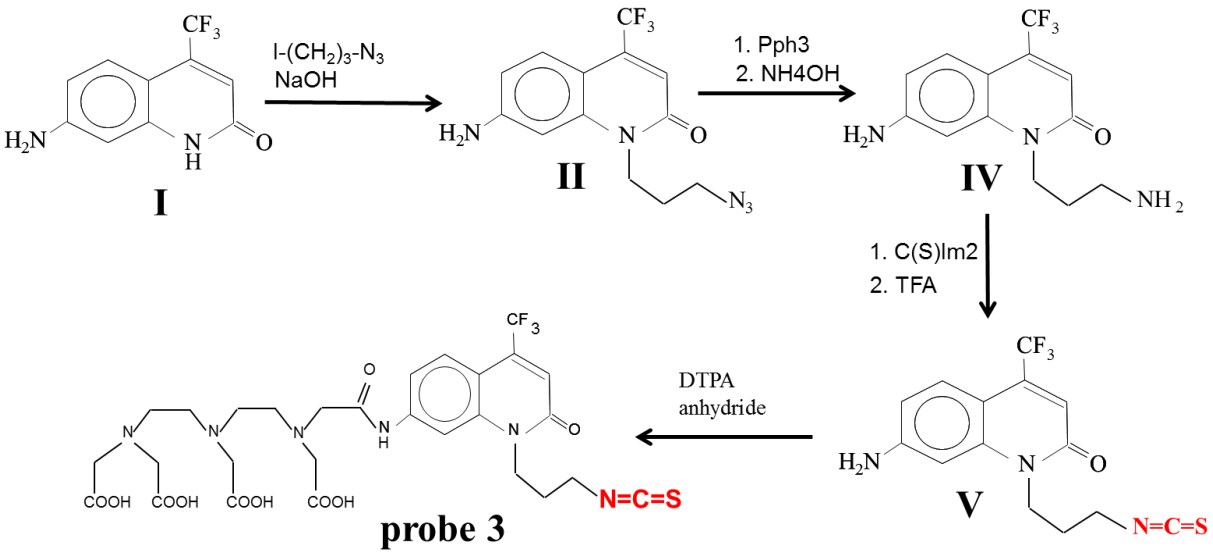

Scheme 4.2 Synthetic strategy for probes 3.

4.2.3 Synthesis of Probes 4

In the synthesis of probe 4, alkylation of ethyl 4,4,4-trifluoroacetoacetate was performed with methyl ester of bromoacetic acid at methylene carbon. The resulting intermediate

was incubated with 1,3-phenylenediamine at moderate temperature that favors formation of quinolone compound (product **VI** of Scheme 4.3) that was converted to carboxylate derivative (compound **VII**) by saponification. This compound was treated with dicyclohexylcarbodiimide and 4-nitrophenole resulting in an activated ester that was introduced in reaction with mono-tritylated 1,4-diaminobutane yielding compound **VIII**. Deprotection followed by treatment of the resulting amino-derivative with N,N-thiocarbonyldiimidazole and trifluoroacetic acid afforded product compound **IX**, an isothiocyanate derivative.

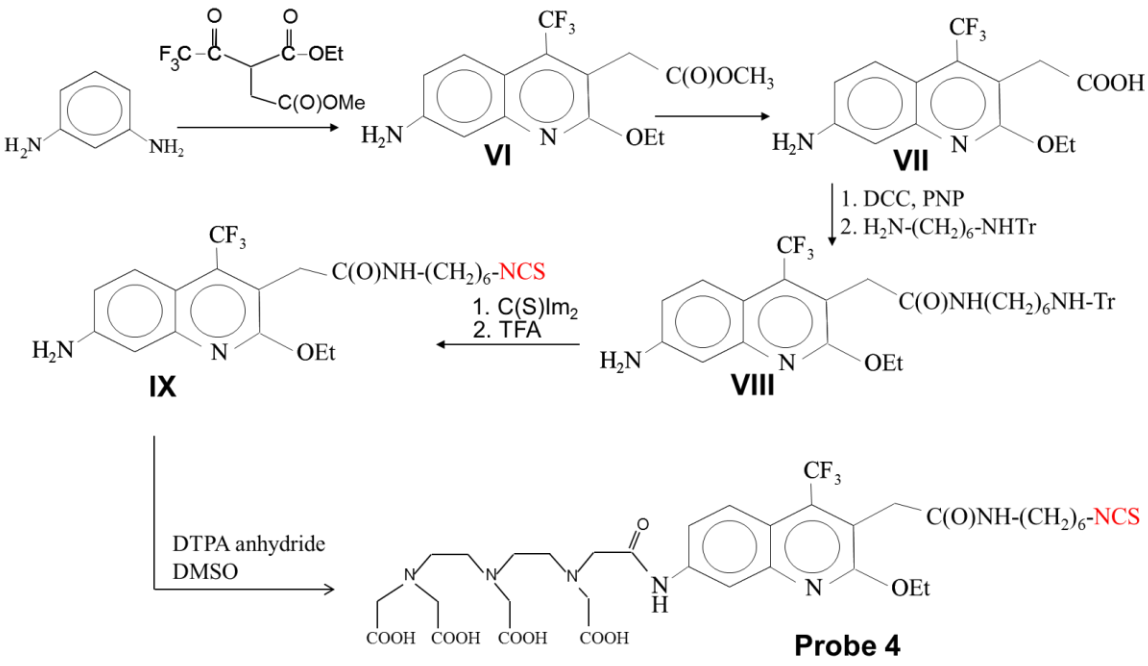

Scheme 4.3 Synthetic strategy for probe 4.

Subsequent acylation with DTPA dianhydride produced the desired probes **4**. Thirty-five milligrams (35 mg) of DTPA is dissolved in DMSO followed by reaction with 16 mg of compound **IX** at 50° C for 20 min.

4.2.4 Synthesis of 7-amino monomethyl cs124 (Model Chelate)

Thirty-four milligrams (34 mg) of cs124 is dissolved in 300 µl DMF and reacted with 15 µl iodomethane at RT for 60 min. Additional 15 µl of iodomethane was added to the reaction mixture and reaction was further continued at 40 °C for 1 hr. The progress of reaction was monitored by TLC with $CHCl_3$: ethanol (10:1) as developing system. The reaction products were precipitated by 2 x 2 mL water, residue spun down and collected by centrifugation at 6000 rpm. The residue containing a mixture of mono and di substituted methylated compound was dissolved in 1 mL ethanol. The desired product **X** was purified by preparatory TLC using $CHCl_3$: ethanol (10:1) as developing system. Yield for compound **X** was 13 mg: UV absorbance spectrum, λ_{max1}= 323nm and λ_{max2} = 346 nm. Subsequent acylation with DTPA dianhydride at 70 °C produced the desired model chelate.

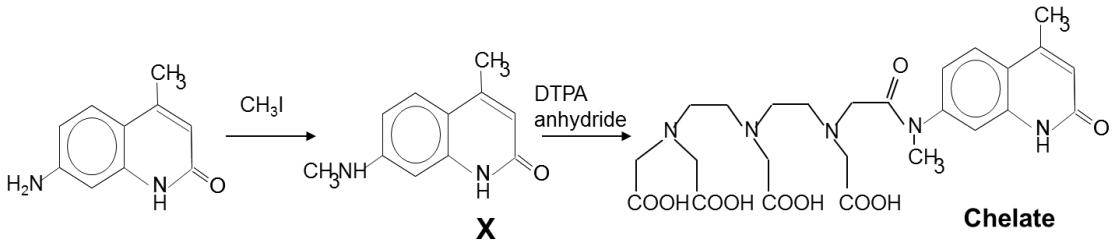

Scheme 4.4 Synthetic scheme for model chelate.

The DTPA acylation reaction was monitored at various time intervals. 5 µl aliquot of reaction mixture was withdrawn at various time intervals and mixed with 400 µl of acetonitrile : water (70:30) mixture. UV absorbance measurements of acylation reaction are shown in Figure 4.4. The acylation reaction of model chelates yielded five isobestic points, indicating that the spectra are linear combinations of two components.

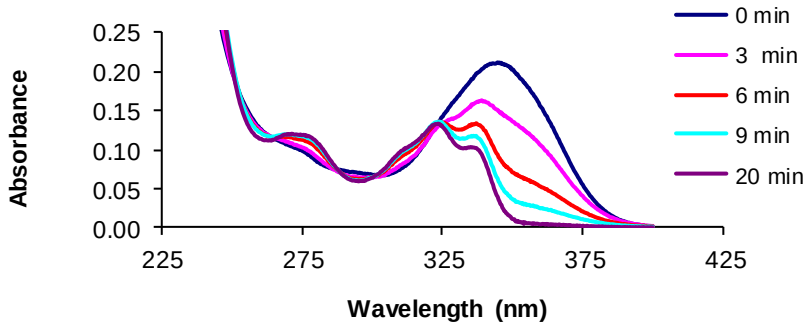

Figure 4.4 DTPA acylation kinetics of model chelate.

It was noted that the DTPA acylation reaction proceeded relatively slow with the model chelate when compared with acylation of original cs124 (reference compound, Chart 4.2). The acylation reaction in cs124 took place at room temperature while acylation reaction in case of N-methylated product was required to be carried out at 70 °C. The reactions progression was monitored by decrease in absorption, illustrated in Figure 4.5. Absorbance was recorded at 360 nm and 355 nm for Model Chelate and cs124 respectively. Based on reaction kinetics, the estimated half reaction time for cs124 at RT and Model Chelate at 70 °C was 3.5 min. The difference between absolute rate of the reactions at 70°C was about 300 fold.

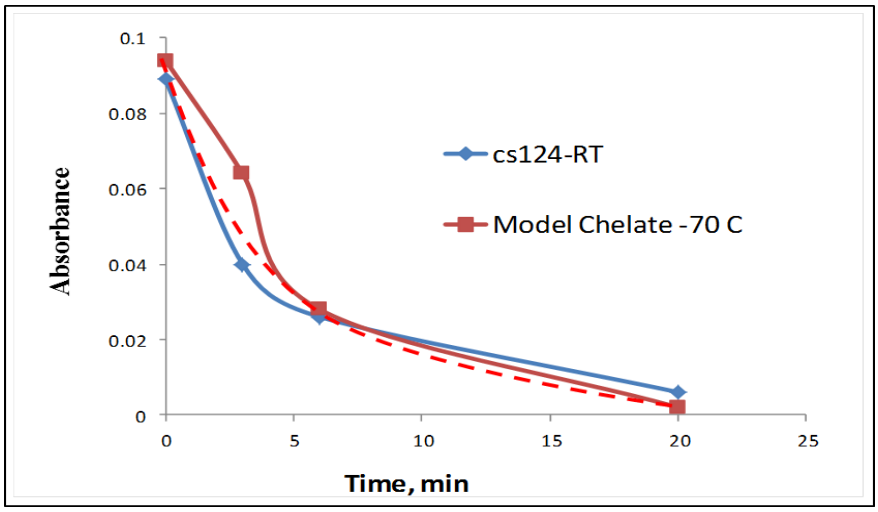

Figure 4.5 Comparative acylation reaction kinetics for cs124 (Reference Compound) and 7-amino monomethyl cs124 (Model Chelate).

4.2.5 Lanthanide Complexes of DTPA-cs124-CF_3-(N)N_3 and DTPA-cs124-CF_3(O)N_3 (Probe 1 and 2), ITC modifications (Probe 3 and 4) and Model Chelate

Thirty milligrams (0.1 mmol) of probe compound, precursor was added to a solution of 80 mg (0.3 mmol) of DTPA dianhydride in 0.8 mL of DMSO. After incubation at 50 °C, the mixture was supplemented with 10 mL of ether, and the resulting precipitate was collected by centrifugation, washed with ether, air-dried, dissolved in 1 mL of DMF, and mixed with 0.3 mL of water. After incubation for 10 min at 45°C, the mixture was diluted with 5 mL of water and extracted with 40 mL of butanol. The organic phase was separated and divided into four equal parts. Each portion was mixed with 0.3 mL of a 0.1 M solution of a lanthanide trichloride (Tb^3, Eu^{3+}, Dy^{3+}, or Sm^{3+}). After vigorous agitation, the organic phase was collected and concentrated by co-evaporation with water in *vacuo* at 30 °C.

Ln^{3+} complexes of DTPA-cs124-CF_3 (O) N_3, 3-$CH_2C(O)NH(CH_2)_4NH$-Tr cs124CF_3 and model chelated (7-amino monomethyl cs124) were obtained using the same protocol. All the Ln-chelates are listed in Chart 4.1.

4.3 Reactivity of Lanthanide Chelates

4.3.1 Click Reactions

Nucleophilic opening of strained ring systems (97) and 1,3-dipolar cycloadditions (98) are the two extensively studied click reactions. Of particular interest is 1.3 cycloaddition between a terminal alkyne and an azide to generate substituted 1,2,3-triazoles.

The formation of triazoles via the cycloaddition of azide and acetylene was first reported by Dimroth in the early 1900's. However, the scope, and mechanism of click reaction based on 1,3 cycloaddition was not fully understood until the 1960's (99). The reaction generates a mixture of 1,4- and 1,5-disubstituted triazoles (Scheme 4.5). While the copper (I)-catalyzed reaction exclusively yields the 1,4-disubstituted 1,2,3-triazole (100,101). The *in situ* reduction of copper(II) salts such as $CuSO_4 \bullet 5H_2O$ with sodium ascorbate in aqueous alcoholic solvents allows the formation of 1,4-triazoles at room temperature in high yield with less than 2 mol % catalyst loading.

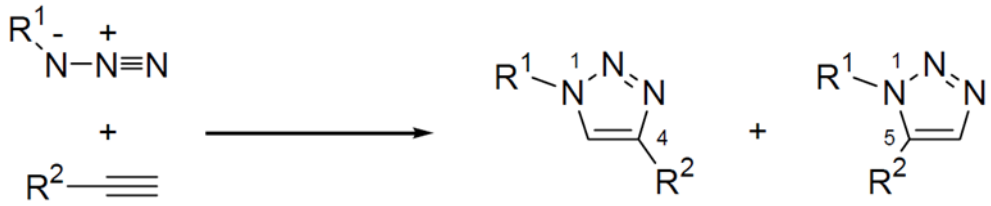

Scheme 4.5 Triazole formation by 1,3-dipolar cycloaddition.

The copper-catalyzed reaction is thought to proceed in a stepwise manner starting with the generation of copper (I) acetylide (98) (Figure 4.6). The copper(I)-catalyzed reaction selectively produces the 1,4-isomer in < 90 % yield after 8 hours (100).

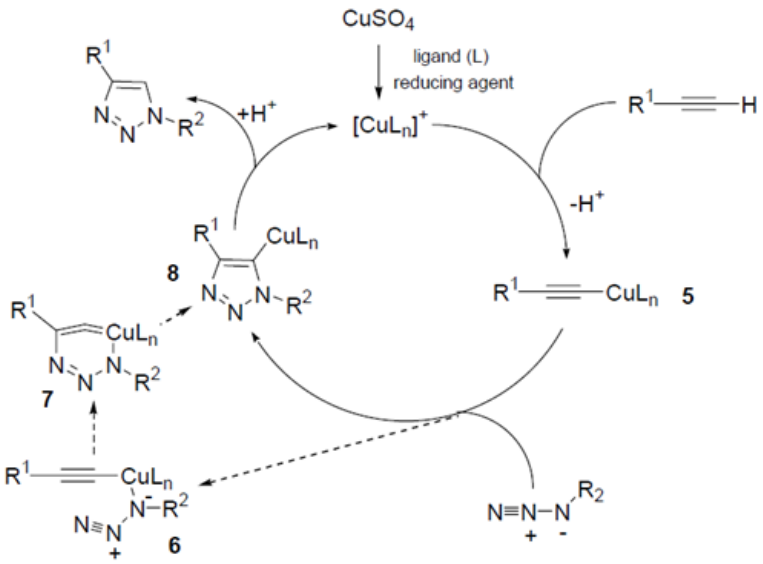

Figure 4.6 Postulated catalytic cycle for alkyne-azide coupling.

Protocol: Three microliters of 2M triethylammonium acetate buffer, pH 7.0 and 15 μl of DMSO were mixed with 5 μl of 0.5 mM alkyne-modified oligonucleotide possessing, or lacking a quencher. One microliter of the 10 mM click reactive probe 1 or probe 2, 3 μl of 5mM ascorbic acid solution; and 3 μl of 10 mM Copper (II) – TBTA stock in 55% DMSO, were consequently added to the solution. After overnight incubation at room temperature, the mixture was supplemented with 3 μl of 3 M NaAc pH 5.5 and oligonucleotide material precipitated by addition of 300 μl of ethanol. The residue was additionally washed by 80% ethanol (2 x 0.3 ml), dissolved in water and subjected to reverse phase HPLC. The click reaction of luminescent azido complex with DNA oligonucleotide is shown in Scheme 4.6.

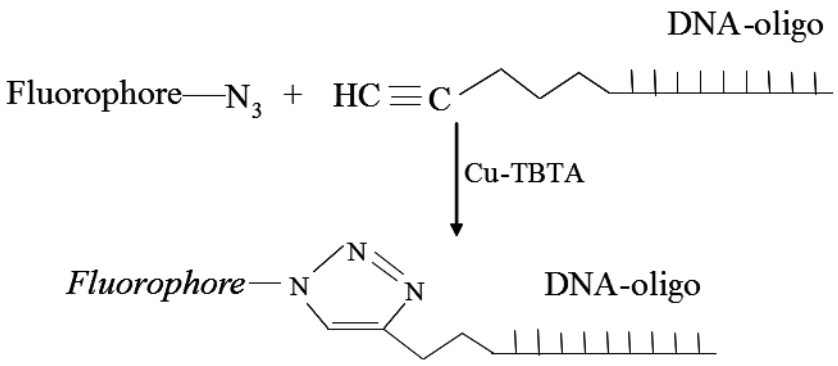

Scheme 4.6 Click reaction of luminescent azido complex with DNA-oligonucleotide.

4.3.2 Reaction of Isothiocyano-Compound with Cysteine and Ethylenediamine

The reaction mixture contained 0.1 M sodium-borate pH 9.5, 10 mM cysteine solution, and 0.1 – 1 mM of isothiocyano (ITC) probe 3 or probe 4. The mixture was incubated 5 min at room temperature and the reaction products analyzed by TLC using acetonitrile-water (3:1) as developing solvent. The reaction with ethylenediamine was performed with 0.1 M ethylenediamine pH 8.0 at 50 ^{o}C for 1 h. The products were analyzed as described for cysteine reaction.

4.4 Physical Methods

4.4.1 Steady State Fluorescence Measurements

Excitation and emission fluorescence spectra in a steady-state mode were recorded using a Quanta-Master 1 (Photon Technology International, PTI) digital fluorometer at ambient temperature and Felix^{TM} Software is used with the system configured for steady state applications.

The Fluorescence emission is measured in 10 mM sodium borate buffer, pH 8.0 at 1μM probe concentration. The antenna is excited at 347 nm for probe 1, 340 nm for probe 2 and, 346 nm and 323 nm for model chelate and reference compound cs124.

Lanthanide emission intensities are recorded for the probes 1, probe 2, model chelate and the reference compound in both water and heavy water (D_2O).

4.4.2 Time Resolved Luminescence

Time-resolved and gated luminescence measurements were performed using a home-built experimental setup (Figure 4.7). A Suprasil fluorescence cell filled with sample solutions was irradiated by pulsed (ca. 15 ns) UV light from an excimer laser (351 nm, XeF). Before passing through the cell, the laser beam was formed by a rectangular aperture 0.5 cm × 1.0 cm (width × height). Fluorescence from the cell collected at an angle of 90 degrees was focused onto the entrance slit of a grating spectrograph (SpectraPro-300i, Acton Research Corporation, diffraction grating 150 grooves/mm blazed at 500 nm) using a fused silica lens with a focal distance of 2.5 cm. The spectrograph was equipped with a gated intensified CCD Camera (ICCD-MAX, Princeton Instruments) to record transient spectra. A slit width of 0.5 mm was used for time-resolved luminescence measurements, which corresponds to a spectral resolution of 5 nm. Time gated spectra were recorded with a spectral resolution of 0.3 nm (a slit width of 0.01 mm in combination with a pixel size on the ICCD camera of 0.026 mm). ICCD gating, with a delay after the laser pulse, was used to determine the temporal behavior of the transient fluorescence. For measurements of luminescence lifetimes, the light was diverted to a photomultiplier tube mounted on the exit slit of the spectrograph. The PMT signal was pre-amplified and averaged, using a digital storage oscilloscope (LeCroy 9310A).

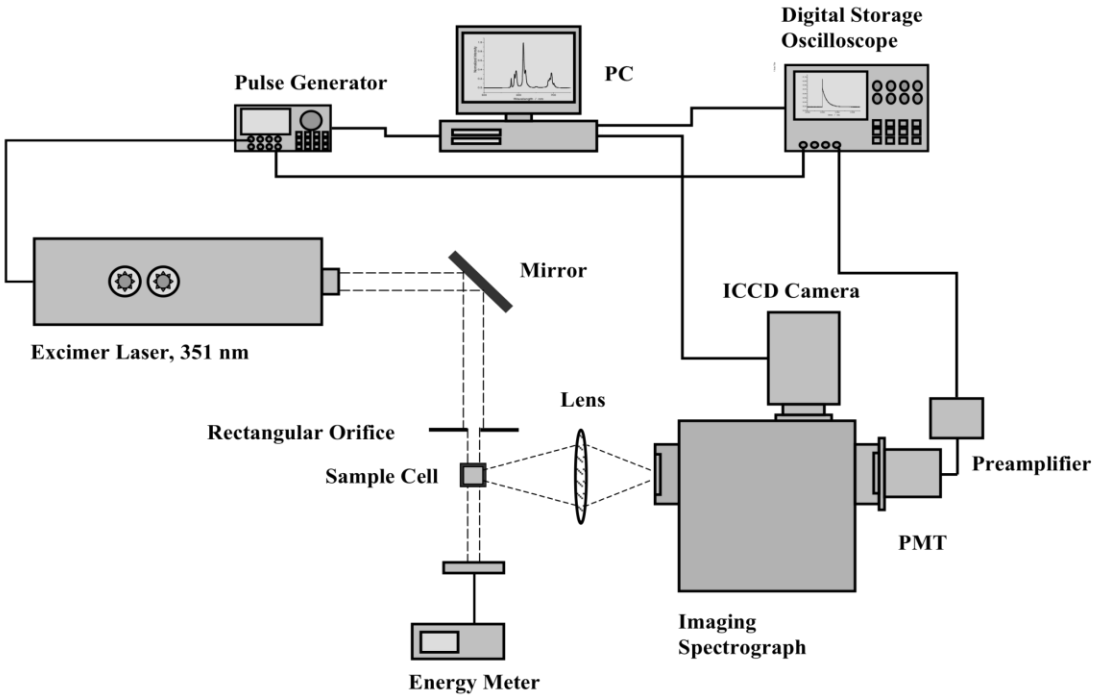

Figure 4.7 Home-built experimental setup for time-resolved luminescence measurements.

4.4.3 Quantum Yield Measurements

Quantum yield of the chelated lanthanide is measured using the single-point method. The quantum yield is calculated using the integrated emission intensities from a single sample and reference pair at identical concentration. This method is fast and easy and gives a good approximation of quantum yield. Hence, a simple ratio of the integrated fluorescence intensities of the two solutions (recorded under identical conditions) will yield the ratio of the quantum yield values. Since Φ_F for the standard sample is known, it is trivial to calculate the Φ_F for the test sample.

4.5 Results

4.5.1 Fluorescence Emission of Lanthanide Complexes

All complexes displayed narrow emission spectrum typical of luminescent lanthanide chelates (Figure 4.8 – Figure 4.10). The process of antenna mediated lanthanide emission includes the transfer of energy from the antenna fluorophore to the coordinated metal and the subsequent emission of photon by the excited lanthanide. The first step is the most crucial part of the process, because even slight modification in the chromophore-antenna structure dramatically affects lanthanide luminescence (52). In this chapter, is discussed synthetic approach that allows the introduction of crosslinking group in position 1 (probe 1 and probe 3), position 2 (probe 2) and position 3 (probe 4) of the quinolone and quinolone based antenna fluorophore. Comparison with the reference fluorophores and a methyl-substituted quinolone derivative at position 7 (model chelate) demonstrates that the structural modifications affected the brightness of the lanthanide chelaes in different ways.

Steady state fluorescence emission of Probe 1 with varying lanthanide metals, Eu^{3+}, Tb^{3+}, Sm^{3+} and Dy^{3+} and with no metal are shown in Figure 4.8. The emission was measured in water and heavy water for a given known concentration, 1µM of the probe 1.

The antenna emission was observed at 392 nm. Europium emission is much more prominent for probe 1 followed by for terbium. Relatively small emission is observed for samarium and dysprosium. The energy transfer process can be seen from drop in the emission intensity of the antenna and corresponding increase in the lanthanide emission.

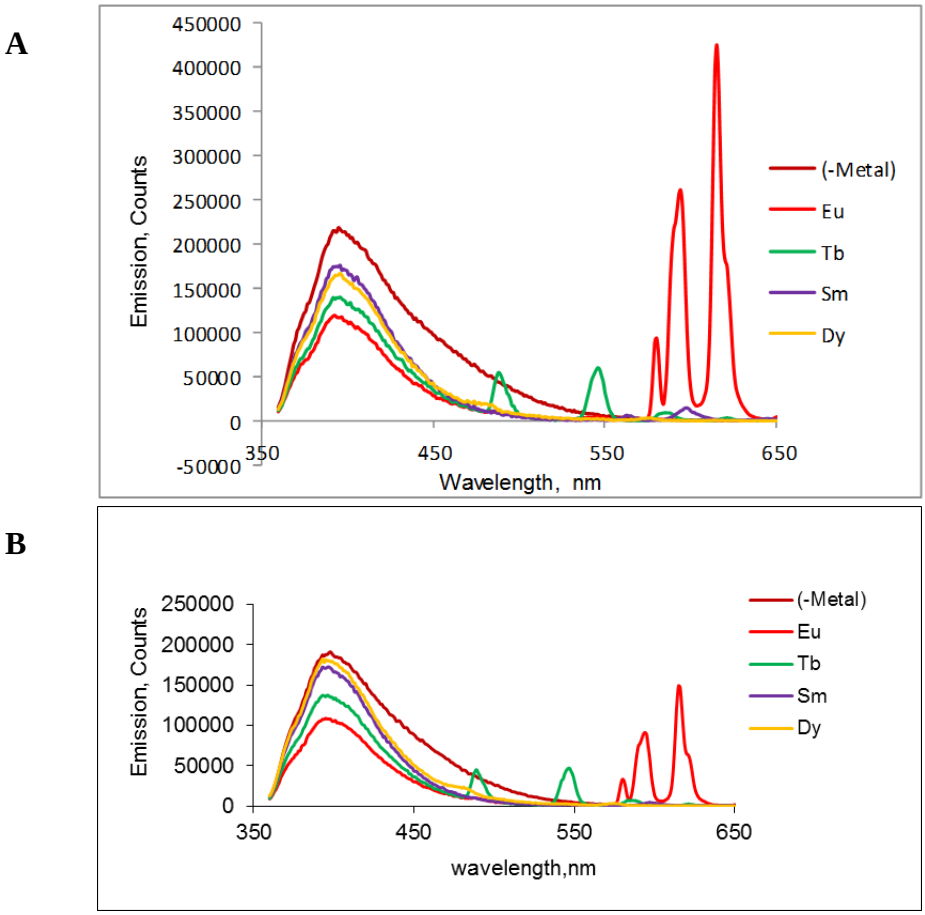

Figure 4.8 Normalized time-resolved emission of 1 μM solutions of probe 1 (no Me) and its lanthanide complexes: terbium (Tb), europium (Eu), dysprosium (Dy), samarium (Sm); in (A) Water and (B) Heavy water, excited at 347 nm.

Emission spectrum of probe 2 is illustrated in Figure 4.8. Steady state fluorescence emission of probe 2 with varying lanthanide metals, Eu^{3+}, Tb^{3+}, Sm^{3+} and Dy^{3+} and with no metal are shown in Figure 4.9. The emission was measured in water and heavy water for a given known concentration, 1µM of the probe 2.

The antenna emission was observed at 402 nm. Terbium emission is much more prominent for probe 2 followed by for europium. Sm and Dy exhibits relatively small emission. The energy transfer process can be seen from drop in the emission intensity of the antenna and corresponding increase in the lanthanide emission. The emission

intensities are further enhanced in the presence of heavy water. In heavy water both terbium and europium emission is comparable.

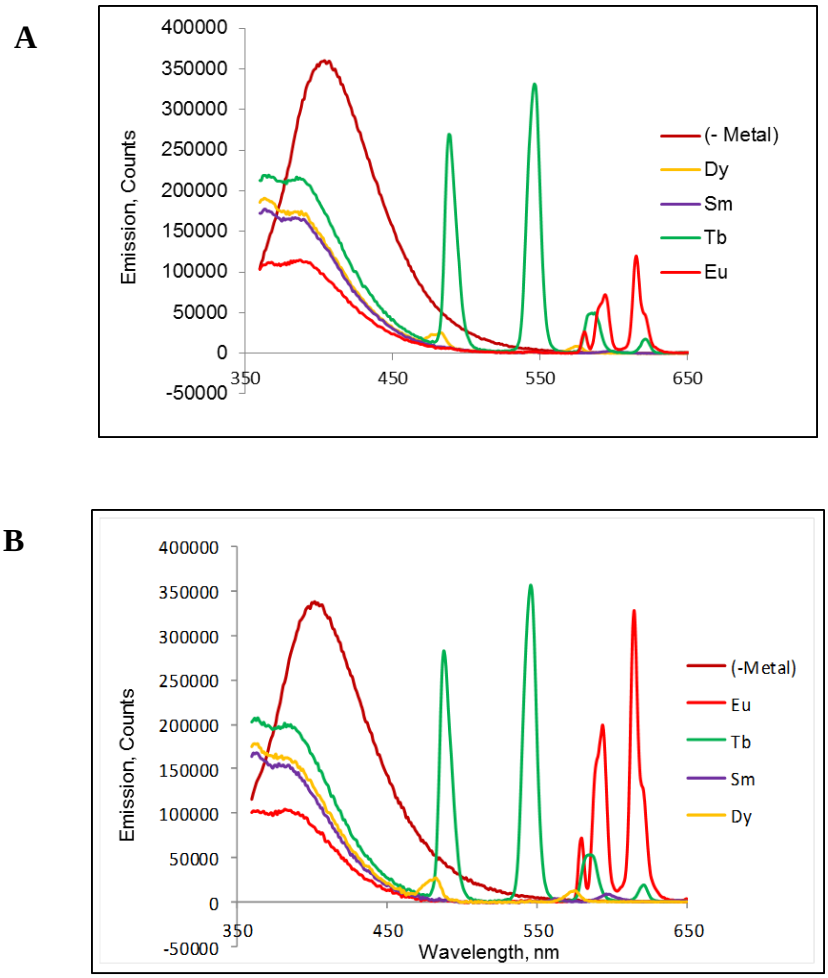

Figure 4.9 Normalized time-resolved emission of 1 μM solutions of probe 1 (no Me) and its lanthanide complexes: terbium (Tb), europium (Eu), dysprosium (Dy), samarium (Sm); in (A) Water and (B) Heavy water, excited at 340 nm.

Steady state fluorescence emission of Model chelate with varying lanthanide metals, Eu^{3+}, Tb^{3+}, and Dy^{3+} and with no metal are shown in Figure 4.10. The emission was measured in water and heavy water for a given known concentration, 1µM of the probe. It was observed that the Sm^{3+} complex of the model chelate did not show any measurable emission signal

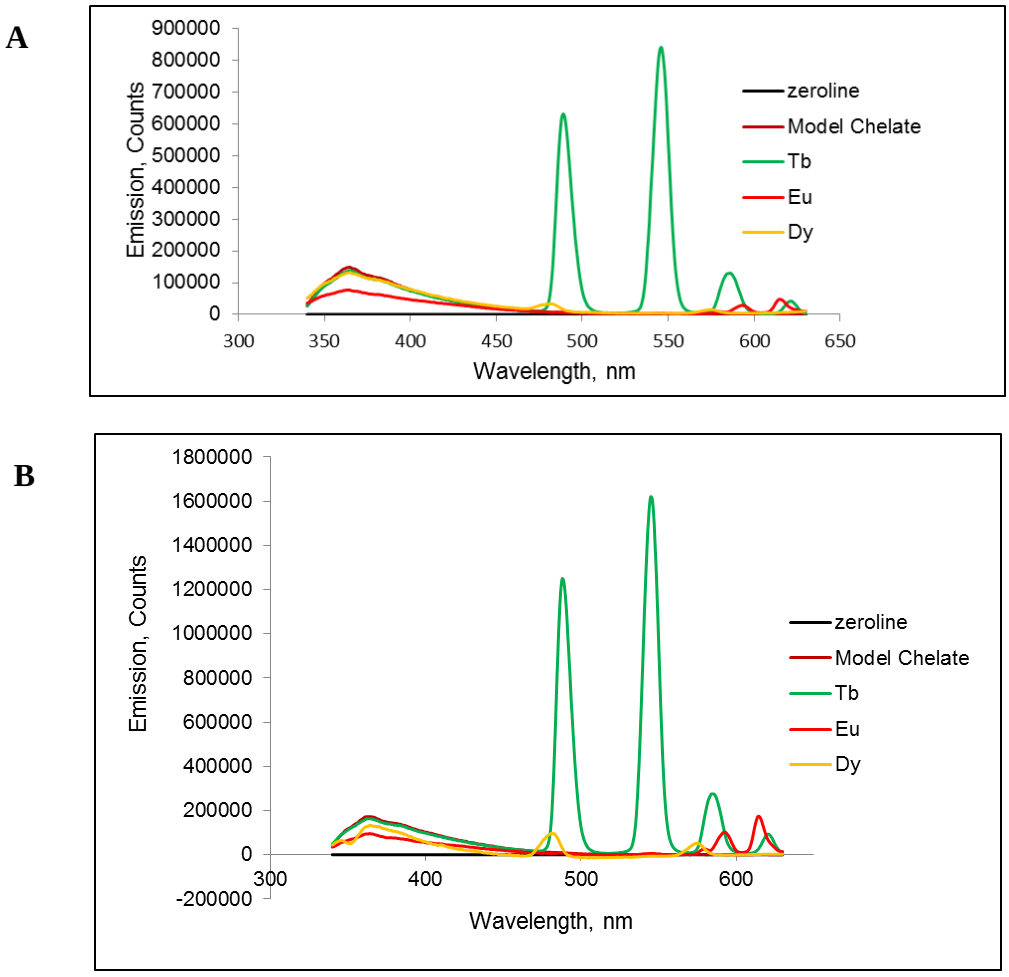

Figure 4.10 Normalized time-resolved emission of 1 μM solutions of Model Chelate (no Me) and its Lanthanide Complexes: terbium (Tb), europium (Eu), and dysprosium (Dy) in (A) Water and (B) Heavy Water, excited at 346 nm.

The antenna emission was observed at 360 nm. Terbium emission is quite prominent followed by Europium. Dysprosium exhibits relatively small emission while Samarium signal is too weak and therefore not presented in the plot. The energy transfer process looks very efficient which is evident from the fact that small drop in the emission intensity of the antenna corresponds to significant increase in the lanthanide emission. As expected, emission intensities were enhanced in the presence of heavy water. A detailed comparison of spectral properties of various lanthanide chelates are shown in Table 4.1.

Table 4.1 Emission and Relative Brightness of Lanthanide Chelates under Various Conditions

Compound	Emission		Relative brightness	% Relative brightness	
	H_2O	D_2O	D_2O/H_2O	H_2O*	D_2O*
	Tb^{+3} complexes (emission at 545 nm,counts)				
DTPA-cs124CF_3*	12200	14170	1.16	100	100
DTPA-cs124CF_3-(N)-N_3 (probe1)	4560	4700	1.03	37	33
DTPA-cs124CF_3-(O)-N_3 (probe 2)	18700	19680	1.05	153	140
DTPA-cs124CF_3-3-NCS (probe 4)	15500	18700	1.21	130	132
DTPA-cs124*	124000	195000	1.57	100	100
DTPA-cs124-Me chelate	85600	164000	1.92	69	84
	Eu^{+3} complexes (emission at 615 nm,counts)				
DTPA-cs124CF_3*	10350	41000	3.96	100	100
DTPA-cs124CF_3-(N)-N_3 (probe1)	9770	36700	3.76	94	90
DTPA-cs124CF_3-(O)-N_3 (probe 2)	11760	47780	4.06	113	117
DTPA-cs124CF_3-3-NCS (probe 4)	5300	13800	2.6	51	34
DTPA-cs124*	4700	15200	3.23	100	100
DTPA-cs124-Me chelate	4800	17300	3.60	102	114
	Dy^{+3} complexes (emission at 482 nm,counts)				
DTPA-cs124CF_3*	567	1000	1.77	100	100
DTPA-cs124CF_3-(N)-N_3 (probe1)	1930	2450	1.27	340	245
DTPA-cs124CF_3-(O)-N_3 (probe 2)	2540	2670	1.05	448	266
DTPA-cs124CF_3-3-NCS (probe 4)	NA	NA	NA	NA	NA
DTPA-cs124*	4600	15300	3.33	100	100
DTPA-cs124-Me chelate	3550	9600	2.70	77	63
	Sm^{+3} complexes (emission at 598 nm,counts)				
DTPA-cs124CF_3*	$2.02\ 10^2$	$7.49\ 10^2$	3.71	100	100
DTPA-cs124CF_3-(N)-N_3 (probe1)	$4.57\ 10^2$	$1.44\ 10^3$	3.15	226	192
DTPA-cs124CF_3-(O)-N_3 (probe 2)	$2.79\ 10^2$	$8.34\ 10^2$	3.00	138	111
DTPA-cs124CF_3-3-NCS (probe 4)	NA	NA	NA	NA	NA
DTPA-cs124*	NA	NA	NA	NA	NA
DTPA-cs124-Me chelate	NA	NA	NA	NA	NA

*reference compound

4.5.2 Effect of Heavy Water on Lanthanide Chelate Emission

The quantum yield of the excited lanthanide ion (defined as the probability of the excited state emitting a photon) in the antenna-chelate complex depends strongly on the number of coordinated water molecules (96), due to non-radiative dissipation of the energy of the excited state through the vibration of O-H bonds. This process does not occur with heavy water due to the different frequency of O-D bond vibration. This effect accounts for the

enhanced brightness of lanthanide luminescence in heavy water. As seen from Table 4.1 for DTPA ligands in D_2O, the brightness of the Tb^{3+} chelates was 1.2- to 1.9-fold higher than in H_2O-based solutions. As expected, the effect was more pronounced for DTPA-Eu^{3+} chelates (~2.7- to 4.2-fold), as well as for Dy^{3+} (~1.0- to 1.7-fold), and Sm^{3+} complexes (~ 3.0 fold).

4.5.3 Time-resolved Emission Lifetimes

Time-resolved measurements indicate that there is a single exponential decay mode for the luminescence signal which is indicative of homogeneity of the complexes, shown in Figure 4.11. Emission lifetimes for the lanthanide chelates are shown in Table 4.2.

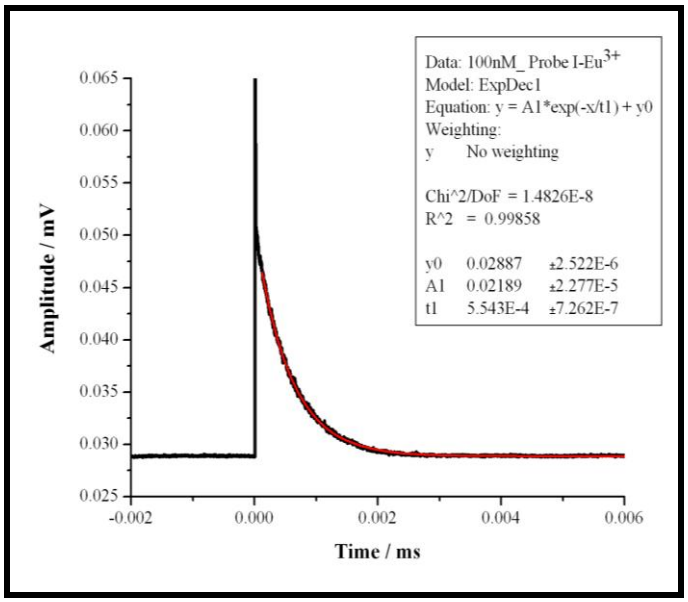

Figure 4.11 Kinetic lifetime decay.

It is evident from the data that the emission lifetime for Europium and Terbium chelates are in millisecond (ms) order, while Samarium and Dysprosium complexes are in the order of microsecond (μs). For reasons not known, the model chelate of Terbium showed impressive emission decay of about 1.68 ms. Also, it can be generalized that the

luminescence lifetime can be considerably improved when emission is measured in deuterium oxide solution.

Table 4.2 Emission Lifetimes of Lanthanide Chelates in Water and Heavy Water

Europium (Eu^{3+}) Maximum Emission at 615 nm

Probe	Conc. (nM)	Luminescence Lifetime(ms) in H_2O	Luminescence Lifetime(ms) in D_2O
Probe 1	100	0.52	1.82
Probe 2	100	0.58	1.88
Model Chelate	100	0.61	-

Terbium (Tb^{3+})Maximun Emission at 545 nm

Probe	Conc. (nM)	Luminescence Lifetime(ms) in H_2O	Luminescence Lifetime(ms) in D_2O
Probe 1	100	0.07	0.11
Probe 2	100	0.12	0.19
Model Chelate	100	1.68	-

Dysprosium (Dy^{3+}) Maximum Emission at 482 nm

Probe	Conc. (μM)	Luminescence Lifetime(μs) in H_2O	Luminescence Lifetime(μs) in D_2O
Probe 1	1	1.52	4.8
Probe 2	1	1.87	5.6
Model Chelate	1	-	-

Samarium (Sm^{3+}) Maximun Emission at 598 nm

Probe	Conc. (μM)	Luminescence Lifetime(μs) in H_2O	Luminescence Lifetime(μs) in D_2O
Probe 1	1	1.96	5.1
Probe 2	1	6.05	13.2
Model Chelate	1	-	-

4.5.4 Quantum Yield

Quantum yield of probe 1 and 2 are shown in Table 4.3. On comparing the quantum yield of probe 1 and 2, it was found that Terbium complexes of probe 2 had higher quantum yield than the Terbium complex of probe 1. However, Europium complex of probe 1 and

2 showed similar quantum yield. Similar observations were made with Samarium and Dysprosium complex of probe 1 and 2. When the experiments were performed in deuterium water solution, enhancement of quantum yield was noticed with Europium, while with rest of the other metal no major improvement observed.

In case of reference compound and model chelate, Figure 4.3, profound improvement in quantum yield was noticed in deuterium oxide solution. Of the three metals chelates studied, Terbium displayed highest quantum yield.

Table 4.3 Quantum Yield of Probe 1 and Probe 2 in Relation to Tryptophan as Reference Standard

	Quantum Yield (Φ_F) in water		Quantum Yield (Φ_F) in D_2O	
	Probe 1	Probe 2	Probe 1	Probe 2
-metal (Trp)	**0.12**	**0.43**	**0.134**	**0.432**
Eu	0.024	0.03	0.083	0.08
Tb	0.01	0.12	0.013	0.13
Dy	0.001	0.0056	0.0013	0.005
Sm	0.001	0.001	0.003	0.003

Table 4.4 Quantum Yield of cs124 and Model Chelate in Relation to Tryptophan as Reference Standard

	Quantum Yield (Φ_F) in water		Quantum Yield (Φ_F) in D_2O	
	Model Chelate	cs124	Model Chelate	cs124
-metal (Trp)	**0.101 (± 0.008)**	**0.14 (± 0.035)**	**0.13 (± 0.0097)**	**0.15 (± 0.023)**
Eu	0.01	0.005	0.031	0.018
Tb	0.2	0.16	0.36	0.27
Dy	0.008	0.0046	0.028	0.023

4.5.5 Reactivity of Synthesized Amine, and Click Reactive Probes

Click reactivity of probe 1 and 2 was confirmed by incubation with alkyne-derivatized oligonucleotides in the presence of copper complex and ascorbate. Results in Figure 4.12 suggest suitability of the synthesized compounds for fluorescent DNA labeling.

The reactivity of ITC modified probes, 3 and 4 were examined with cysteine at weakly alkaline conditions favoring ionization of thiol group. The reaction proceeded quickly and quantitatively at room temperature, yielding dithiocarbamate derivatives as was evidenced by strongly reduced mobility of the reaction products on TLC. The same effect was observed in reaction of ITC compounds with ethylenediamine at 50 °C.

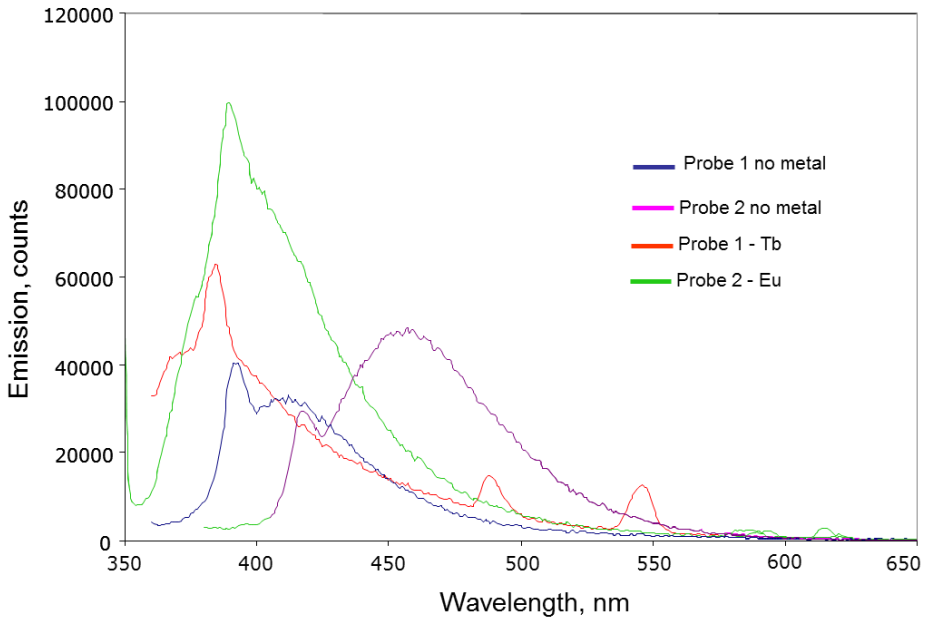

Figure 4.12 Click reactivity of lanthanide chelates of probe 1 and probe 2 and their respective antennae without metal.

4.6 Discussion

Due to unique photon emission properties of lanthanide based probes, they are suitable for a wide variety of applications that require ultrasensitive detection of biomolecules. Currently the progress in this field depends on the availability of efficient probes. The energy pathways in luminescent lanthanide chelates are not fully understood yet, which complicates the rational design of the probes living room for trials and fails. Even though the first probes of this class were synthesized more than three decades ago, not many of them have been commercialized. The development of new more efficient probes is still in great demand due to emerging challenging applications (design of environment-sensitive probes, single molecule detection, etc.).

In the present research to improve the existing probes, new synthetic strategies were employed to obtained bright luminescent probes with high yield. The obtained amine-, and click-reactive probes can be efficiently coupled to biological molecules. The synthesized probes are ready-to-use since they contain pre-bound lanthanide, unlike those described in the previous applications, in which the biomolecule of interest was first modified with metal free chelates, followed by addition of a lanthanide. Photophysical properties of the synthesized probes are characterized in great detail. Comparing to the existing probes of this class the new compounds are more bright and possess stronger metal retention, which enables their use in the media containing high concentration of metal scavengers (e.g., inside the living cell). The brightness of the probes significantly increased in heavy water suggesting the use of this medium to increase the sensitivity of detection. Synthesized probes are suitable for amine, thiol and click reaction.

CHAPTER 5

SIMPLE NO-CHROMATOGRAPHY PROCEDURE FOR AMINE-REACTIVE Eu^{3+} LUMINESCENT PROBES OPTIMAL FOR BIOCONJUGATION

5.1 Introduction

Lanthanide luminescence has long life time enabling highly sensitive detection in time-gated mode. The synthesis of reactive lanthanide probes for covalent labeling of the objects of interest is cumbersome task due to large size of the probe, complex multi-step procedures and the presence of sensitive groups, which often prevents introduction of reactive crosslinking functions optimal for conjugation. This chapter discloses simple synthetic protocol for luminescent Europium lanthanide chelates possessing acylating function, whose reactivity is comparable to that of commonly used N-hydroxysuccinimide (NHS) esters. The probes react with proteins at pH 7.0 within several minutes at ambient temperature displaying high coupling efficiency. The resulting conjugates survive electrophoretic separation under denaturing conditions, which makes these labels useful in proteomic studies that rely on high detection sensitivity.

Lanthanide luminescence has long life time, allowing time-gated detection mode, which greatly increases detection sensitivity comparing to conventional fluorophores, whose light emission is short-lived (79-87). Also, lanthanide emission has sharply spiked fingerprint-like spectra enabling easy discrimination from background fluorescence. Large Stokes shift (the spectral distance between excitation and emission maxima) provides excellent spectral discrimination between excitation and emission light further contributing to high detection sensitivity. All these factors make lanthanide luminescent probes ca. 1000 times more sensitive comparing to regular fluorescent counterparts,

providing the detection sensitivity 10^{-13}-10^{-14} M. Due to small molar extinction of a lanthanide ion it has to be sensitized, which is achieved by tethering (through a chelating group) to an antenna (organic fluorophore) that absorbs the light and transfers the energy to the lanthanide. The excited lanthanide finally emits the light, which can be sensitively detected. Besides keeping a lanthanide close to an antenna fluorophore, chelating group prevents coordination of water by the metal, thereby strongly increasing the quantum yield of the emission. A luminescent probe also contains crosslinking group for conjugation of the label to a biomolecule of interest. The necessity to combine three functional units in the same probe and the presence of chemically sensitive groups in the synthetic intermediates complicates the procedure, thereby preventing introduction of convenient crosslinking groups, active under physiological conditions. The present study describes a simple protocol for the synthesis of amine-reactive acylating Eu^{3+} luminescent chelates, which does not require chromatographic purification steps and can be achieved in one – two working days. The resulting probes are highly soluble in water and react with proteins in neutral media at ambient temperature within 1-2 min. The probes are especially useful for labeling of sensitive biological material, not stable at elevated pH, or temperatures. Chart 5.1 shows the structures of probe 5 and probe 6.

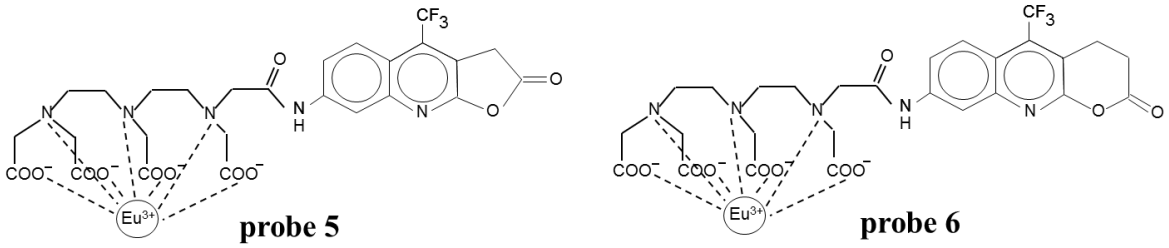

Chart 5.1: Structure of synthesized luminescent lanthanide probes.

5.2 Synthesis of Probe 5 and Probe 6

The following reagents were purchased from Aldrich:

diethylenetriaminepentaacetic acid dianhydride (DTPA), triethylamine, 1,3-phenylene diamine, ethyl 4,4,4-trifluoroacetoacetate, ethylacetoacetate, 1,3-dicyclo hexyl carbodiimide (DCC), ethylenedianime, N-trityl-1,6-diaminohexane, methylbromacetate, anhydrous dimethylformamide and dimethylsulfoxide, 1-butanol, ethylacetate, chloroform, acetonitrile, ethanol, sodium and potassium hydroxide, Na_2SO_4, Na_2CO_3, acetic acid, citric acid, thiocarbonyldiimadazole, $TbCl_3$, $EuCl_3$, $SmCl_3$ and $DyCl_3$, silica gel TLC plates on aluminum foil (200 μm layer thick with a fluorescent indicator). Only distilled and deionized water (18 MΩ cm^{-1}) was used. All experiments, including the preparation and use of lanthanide complexes, were performed either in glassware washed with mixed acid solution and rinsed with metal-free water or in metal-free plastic ware purchased from Bio-Rad. All chemicals were the purest grade available.

5.2.1 Synthesis of Probes 5

5.2.1.1 7-Amino-4-trifluoromethyl-3-carboxymethyl-2(H) quinolone (cs124CF_3-CH_2COOH, Compound II of Scheme 5.1), improved protocol. To a mixture of 2.2 ml (mmol) of 4,4,4-trifluoroacetoacetate and 1.5 ml of methylbromoacetate in 5 ml of DMF, 1 g of powdered KOH was slowly added under rigorous agitation. The mixture was agitated for 30 more min and then kept for 1 h at 60^o C. 50 ml water was added and the mixture was extracted with chloroform. Organic layer was dried over anhydrous sodium sulfate and evaporated in *vacuo* first at room temperature and then at 80 °C until the remaining 4,4,4-trifluoroacetoacetate is completely removed leaving behind ca. 2 g of crude trifluoroacetylmethylethylsuccinate (compound **II** of Scheme 5.1). This residue

was dissolved in 5 ml of DMSO and supplemented with 0.8 g (mmol) of 1,3-phenylenediamine and 200 mg of anhydrous $ZnCl_2$. The mixture was heated for 1 h at 110 °C, combined with 1.5 ml of 10 M KOH and incubation continued at 80 °C for another 15-20 min under agitation. The residue was separated by centrifugation, and the resulting solution mixed with 70 ml of water, followed by extracted with ethylacetate (2 x 100 ml). Water layer was acidified by 8 ml of 1 M citric acid to pH ca. 3 and re-extracted with EtAc (3 x 100 ml). Organic layers were combined and after drying over Na_2SO_4 evaporated to dryness. The residue was washed with hot acetonitrile (3 x 7 ml) and dried under reduced pressure. Yield 420 mg.

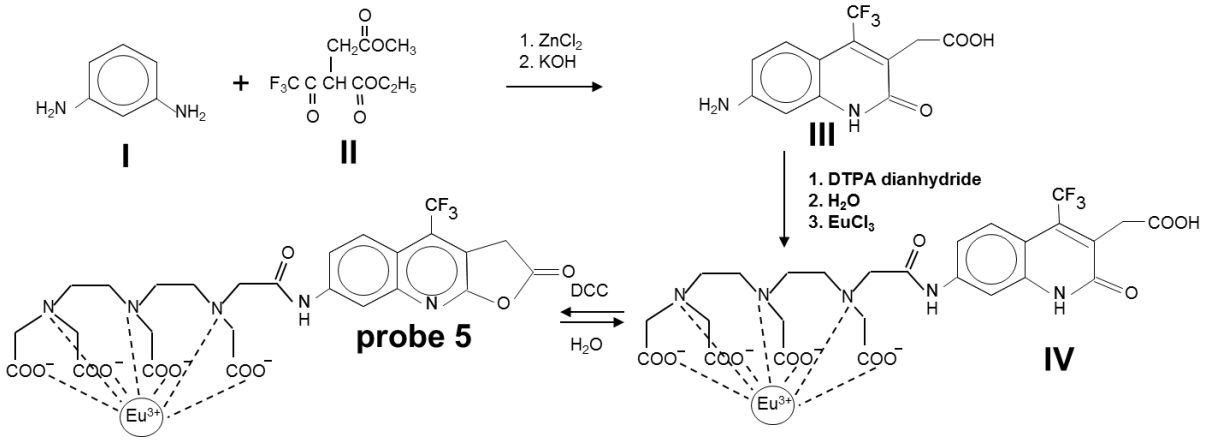

Scheme 5.1 Synthetic route for probe 5.

5.2.1.2 Synthesis of Probe 5 Chelate. DTPA dianhydride (25 mg) was dissolved in 0.2 ml of DMSO under heating (80 ^{o}C). This solution was added to 11.8 mg of compound II and the mixture rigorously agitated. After incubation for 10 min at 70 °C the mixture was poured into 4 ml of ether. The residue was dissolved in 0.3 ml of dioxane followed by addition of 0.2 ml of water. After 10 min incubation at room temperature the solution was subsequently supplemented with 10 ml of butanol and 4 ml of water. After extraction the organic layer was collected and titrated with 0.1 M solution of $EuCl_3$ until the

maximum level of luminescence at 615 nm was achieved under excitation at 349 nm. Butanol phase was collected and evaporated in *vacuo* to the volume of about 1 ml and the solution left for 20 min at 4 °C. The precipitate was collected, subsequently washed with butanol and ether and dried in *vacuo* to afford 6 mg of the product V of Scheme 5.1. The residue was dissolved in 0.1 ml of DMSO and supplemented with 20 mg of DCC. After 20 min incubation at room temperature the residue was removed by centrifugation and the solution was poured in 1 ml of ether, the product collected by centrifugation, washed by ether, re-dissolved in 0.1 ml of DMSO and precipitated by another 1 ml of ether. The residue was washed by acetonitrile and dried in *vacuo* yielding 4.5 mg of probe **5** chelate. MS: Compound **IV** (Eu-DTPA-cs124-CF_3CH_2COOH) (-1) 809.1 (found, traces), (809 calcd); -Eu, $+4H^+$ 662.2 (found, main signal), 662.0 (calculated). Probe **5** after reaction with butylamine (Eu-DTPA-cs124-$CF_3CH_2C(O)$-NHBu) (-1) 864.01 (found, traces), 864.0 (calcd); -Eu, $+4H^+$ 716.12 (found, main signal), 716.0 (calcd).

5.2.2 Synthesis of Probes 6

5.2.2.1 7-Amino-4-trifluoromethyl-3-carboxyethyl-2(H) quinolone (cs124CF_3-CH_2CH_2COOH, Compound X of Scheme 5.2). To 2.2 ml (mmol) of 4,4,4-trifluoroacetoacetate 1 g of powdered KOH was slowly added under rigorous agitation and refrigeration by ice. To this mixture 1.9 ml of ethyl-3-bromopropionate was added and incubation continued for 3 h at 60 °C. The residue (KBr) was removed by centrifugation, followed by addition of 0.5 g of KOH and 0.9 ml of ethyl-3-bromopropionate. After overnight incubation at 60°C the mixture was supplemented with 5 ml of water and extracted with chloroform. Organic layer was dried by anhydrous sodium sulfate and evaporated under reduced pressure to remove volatile and unreacted

components affording 1 g of crude trifluoroacetyldiethylglutarate (compound **VIII** of Scheme 5.2). This residue was dissolved in 2 ml of DMSO and supplemented with 0.4 g (mmol) of 1,3-phenylenediamine and 100 mg of anhydrous $ZnCl_2$. The mixture was heated for 1.5 h at 110 °C, combined with 0.75 ml of 10 M KOH and incubation continued at 60 °C for another 30 min under agitation. The precipitated zinc hydroxide was separated by centrifugation, and the resulting solution mixed with 20 ml of water, followed by extraction with ethylacetate (2 x 40 ml). Water layer was acidified by 4 ml of 1 M citric acid to pH ca. 3 and re-extracted with ether (3 x 50 ml). Organic layers were combined and after drying over Na_2SO_4 evaporated to dryness. The residue was heated with 3-4 ml of acetonitrile under agitation and left at 4 °C. The precipitate was collected, washed with hot acetonitrile (3 x 1 ml) and dried in *vacuo*. Yield 90 mg. ^{1}H NMR chemical shifts (*d*) in DMSO were as follows: 2.31 (t 2H, -C**H**$_2$COOH, J = 7.5 Hz), 2.91 (2H broad, -C**H**$_2$CH$_2$COOH), 6.02 (s 2H, 7N**H**$_2$), 6.42 (1H, 8H), 6.53 (dd 1H, 6H, J_1 = 9 Hz, J_2 = 2.4 Hz). 7.40 (m 1H, 5H).

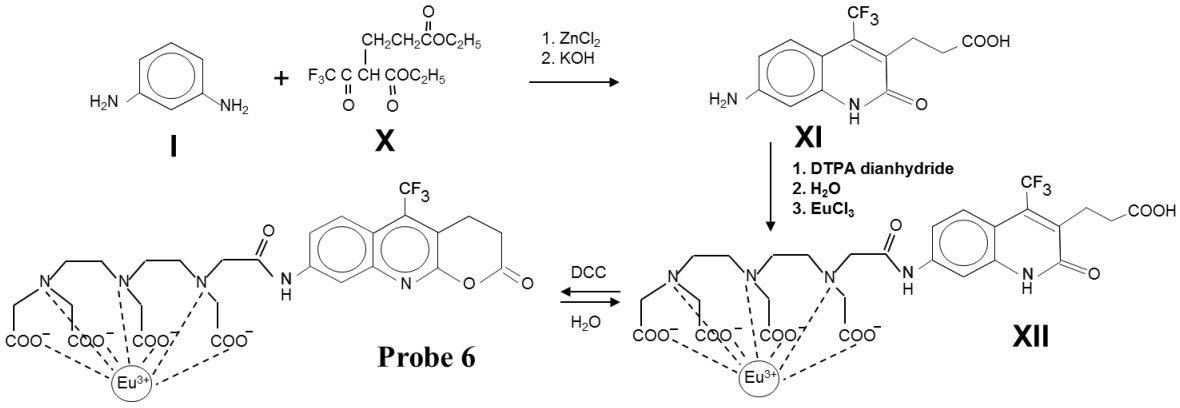

Scheme 5.2 Synthetic route for probe 6.

5.2.2.2 Synthesis of Probe 6 Chelate. DTPA acylation of compound **IX** and obtaining of corresponding Eu^{3+} chelate was performed essentially as in the case of probe **5** starting from 20 mg of compound **IX**. Yield – 20 mg. Reaction of the resulting compound **X** with DCC was performed in the mixture (1:1) of anhydrous DMF and DMSO (2 mg, ~3 μmol of the compound in 0.1 ml of the mixture) at 0 °C in the presence of 25 mg of DCC and 10 μmol of pyridine hydrochloride. After 30 min incubation the precipitated dicyclohexylurea was separated by centrifugation the residue washed with DMSO, and combined solution mixed with 1 ml of ether. After centrifugation the residue was washed with ether (3 x 1 ml), air dried, dissolved in desired volume of DMSO and stored at -80 °C. MS: Compound **XII** (Eu-DTPA-cs124-$CF_3CH_2CH_2COOH$) (-1) 823.1 (found, traces), 823.0 (calcd); -Eu, $+4H^+$ 676.2 (found, main signal), 676.0 (calculated). Probe **6** after reaction with butylamine (Eu-DTPA-cs124-$CF_3CH_2C(O)$-NHBu) (-1) 878.2 (found, traces), 864.0 (calcd); -Eu, $+4H^+$ 731.12 (found, main signal), 731.0 (calcd).

5.3 Reaction of Probes 5 and 6

5.3.1 Reaction with Ethylenediamine HCl and Butylamine HCl

One – two microliters of 20-40 mM solution of a probe was mixed with 9 μl of 0.1 M butylamine –HCl pH 10.5, or 0.1 M ethylenediamine-HCl pH 8.0. After 5 min incubation at ambient temperature the mixtures were analyzed by TLC in acetonitrile – water (3:1) developing system.

Suspension of 12 mg of compound **IIIa** in 1 ml of THF was supplemented with 25 mg of DCC. After 30 min incubation under rigorous agitation the TLC analysis in the system chloroform- ethanol (2:1) revealed fluorescent reaction product with R_f = 0.8. A

small portion of the reaction mixture was applied on silicagel plate and compound **VIa** was purified in the system hexane – acetone (2:1). The product was eluted by acetonitrile and the solution kept at -20 ^{o}C. The rest of the reaction mixture was supplemented with two fold molar excess of butylamine and the reaction product **VIIIa** purified by silicagel column chromatography in hexane-acetone (1:1) solvent system, Scheme 5.3. Yield 10 mg.

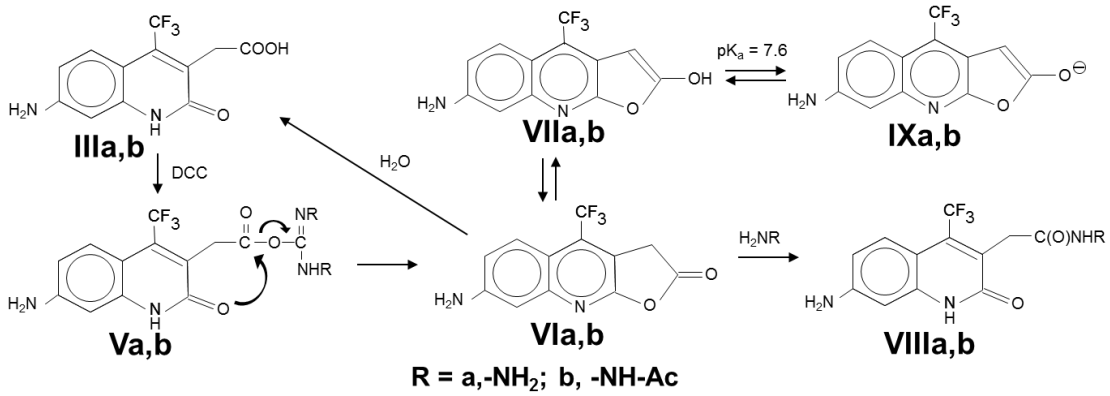

Scheme 5.3 Reaction of model compounds of probe 5.

5.3.2 Other Reactions

The solution of 20 mg of compound III in 0.2 ml of DMF was supplemented with 20 µl of acetic anhydride and the mixture kept at 37 ^{o}C. After 2 h incubation the acylation product (deep blue fluorescence) was purified by TLC in ethylacetete developing system. Yield 15 mg. Similarly compounds VIb and **VIIIb** were obtained as described above for compounds VIa and **VIIIa** of Scheme 5.3.

Compound XIII was obtained essentially as compound V, but at 0 °C. The reaction time course was monitored by TLC in hexane – acetone (2:1 developing system), Scheme 5.4. The compound was purified by preparative TLC in the same solvent system. Compound XIV is obtained as described above for compounds **VIII.**

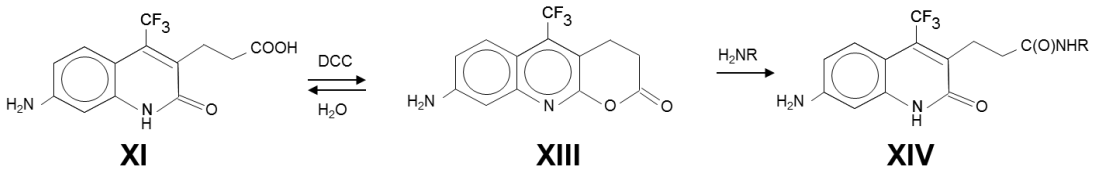

Scheme 5.4 Reactions of model compound.

5.3.3 Time Course Hydrolysis

Time course for hydrolysis of compounds **VIa,b** and **XIII** was performed in fused silica cells in water. UV spectra of the solution were recorded at time intervals indicated in legends, Figures 5.1, 5.2 and 5.3.

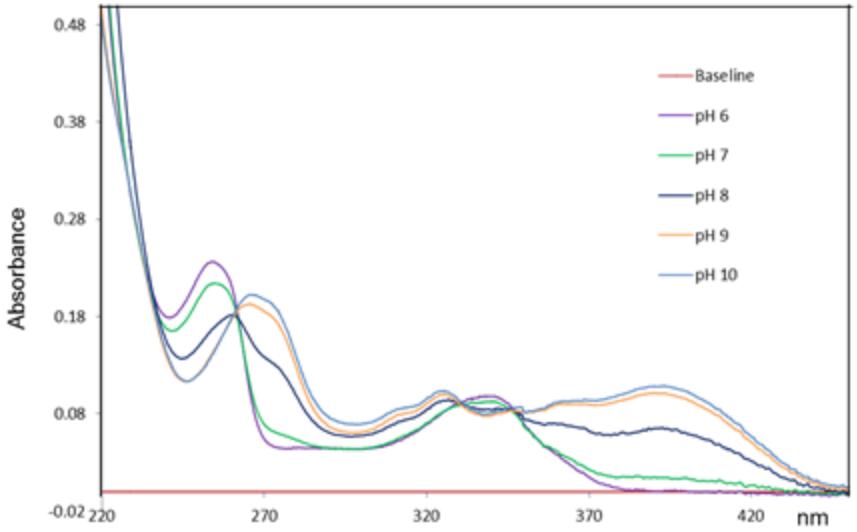

Figure 5.1 Light absorbance spectra for model compound **VIb** at various pH.

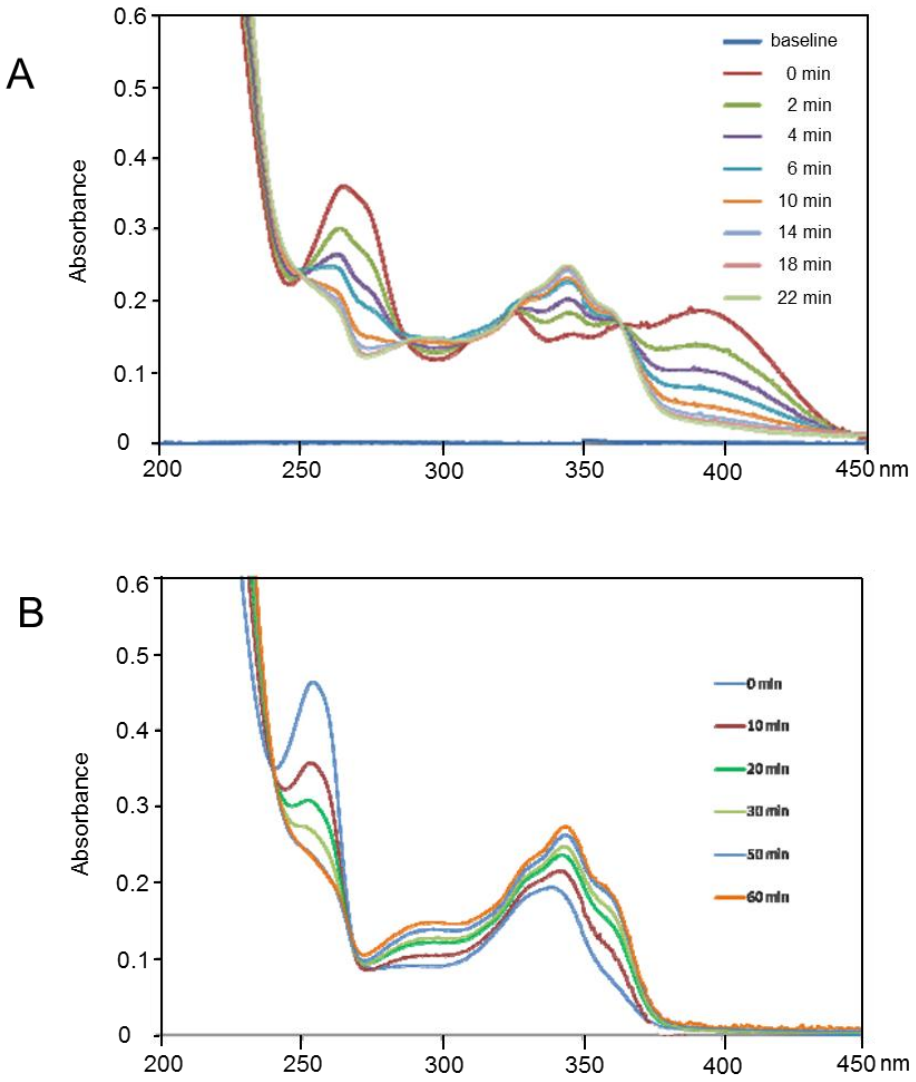

Figure 5.2 Light absorbance spectra recorded upon hydrolysis of model compound **VIb** at pH 9.0 **(A)** and pH 5 **(B).**

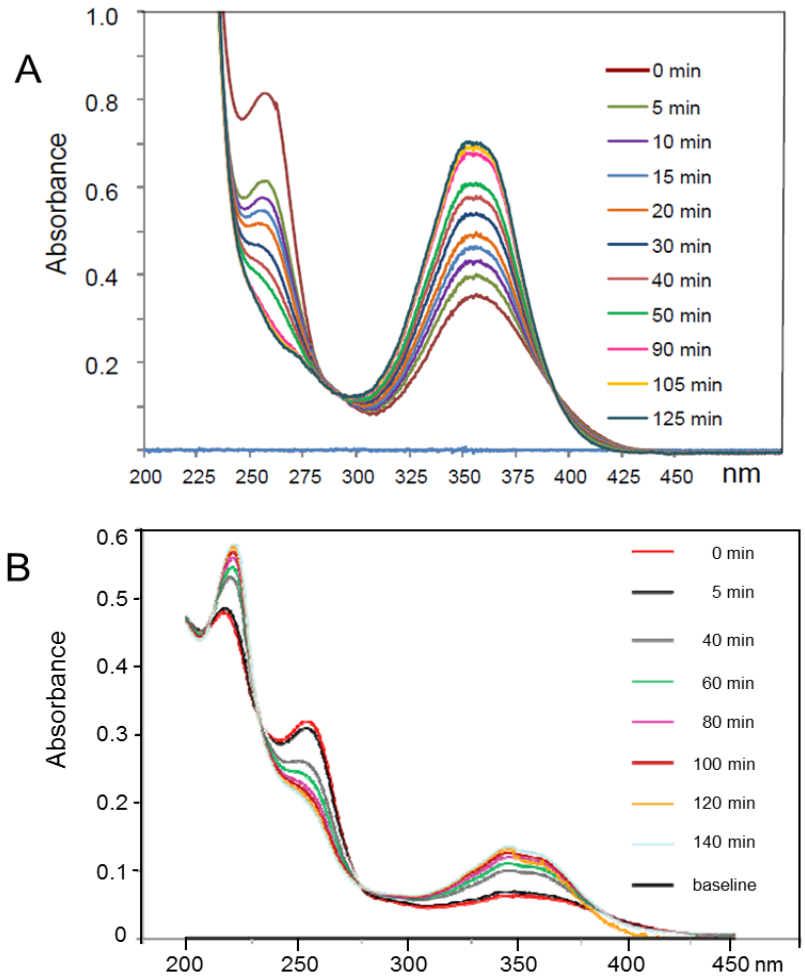

Figure 5.3 Change in light absorption spectra accompanying hydrolysis of compound **VIa** (**A**) and compound **XIII** (**B**).

5.3.4 Modification of Avidin and BSA by Probes 5 and 6

One of the ways to significantly increase the detection sensitivity of light-emitting probes is to bundle them onto a carrier molecule, which then can be attached to an object of interest. Parent protein, avidin possesses 32 lysine residues at which luminescent labels can be attached, which makes it a superior scaffold for multiple label attachment as shown in Figure 5. 4.

With conventional fluorophores this approach gets complicated due to self-quenching, facilitated by the fluorescence resonance energy transfer (FRET) from an

excited to nearby non-excited dye molecule that efficiently absorbs the energy, Figure 5.5. The degree of quenching is highly dependent on the spectral overlap between the excitation (absorption) and emission of a particular fluorophore. The majority of conventional fluorophores have a small (10-30 nm) Stokes shift (a distance between emission and absorption maxima) causing a significant spectral overlap. High molar extinction of the common fluorescent dyes contributes to quenching. On the contrary, lanthanide luminescent probes possess an extremely large Stokes shift (150-250 nm), which should prevent the energy transfer between excited and non-excited fluorophore molecules thereby allowing to attached multiple lanthanide probes to the single carrier molecule like avidin as seen in Figure 5.5.

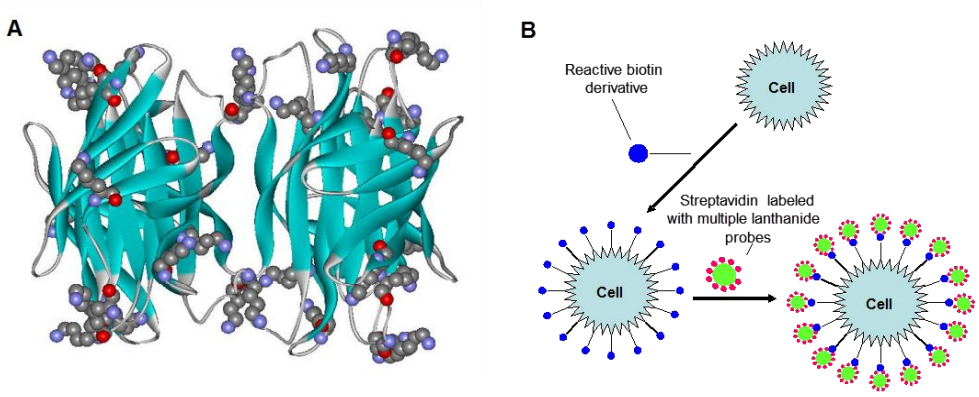

Figure 5.4 The scheme for luminescent labeling of living cells. A) X-ray structure of avidin with lysine residues to which reactive light-emitting probes can be attached. B) The strategy for cell labeling. The cells are treated with reactive biotin derivative, followed by attachment of the luminescent labeled avidin conjugates to biotinylated cells.

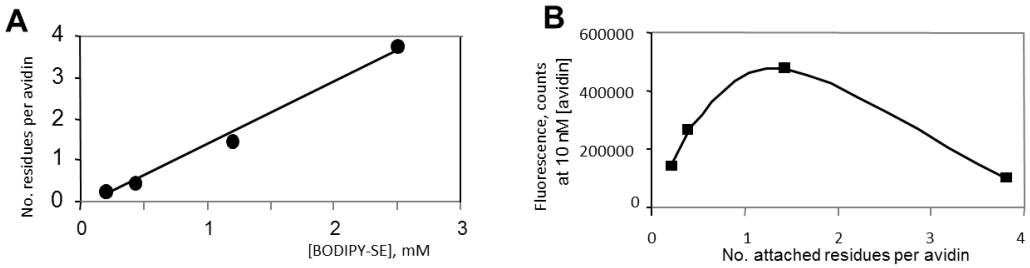

Figure 5.5 Modification of avidin with BODIPY residues A) number of attached residues per avidin molecule and B) fluorescence quenching effect.

Protocol: The reaction cocktails (10-16 µl) were composed by mixing of 7 µl of avidin (20 mg/ml), or BSA (10 mg/ml), 1 µl of 1 M sodium borate buffer with pH 7-10, and 1-8 µl of a reactive probe at concentrations specified in figure legends. After incubation for 1-20 min at 20 °C the mixtures were diluted to 100 µl by water and subjected to size-exclusion chromatography on Sephadex G-50 "medium" in 10 mM Hepes-HCl buffer pH 8.0 containing 50 mM NaCl. The fractions corresponding to modified avidin were collected by visual detection using UV monitor (365 nm light).

5.3.5 Electrophoretic Separation of Modified Proteins

The modified proteins were denatured by addition of SDS to final concentration 1 % and subjected to separation by DISC electrophoresis in Laemmly system (102) using 10 % polyacrylamide gel.

5.4 Methods

5.4.1 Physical Methods

Excitation and emission fluorescence spectra in a steady state mode were recorded using QuantaMaster 1 (Photon Technology International) digital fluorimeter at ambient temperature. UV absorption spectra were recorded on Cary 300 Bio UV-Visible spectrophotometer (Varian). Mass spectra were obtained at the Center for Advanced Proteomics Research (UMDNJ) using MALDI-TOF detection mode. NMR spectra were recorded by Process NMR Associates on Varian Mercury-300 superconducting NMR spectrometer operating at 300 MHz.

5.4.2 Preparation of SDS-Polyacrylamide Gel Electrophoresis

Almost all analytical electrophoresis of proteins is carried out in polyacrylamide gels under conditions that ensure dissociation of the proteins into their individual polypeptide subunits and that minimize aggregation. In general, the strongly anionic detergent, SDS is used in combination with a reducing agent and/or heat to dissociate the proteins before they are loaded on the gel.

Polyacrylamide gels are composed of chains of polymerized acrylamide that are cross-linked by a bifunctional agent such as N, N'-methylenebisacrylamide. The effective range of separation of SDS-polyacrylamide gels depends on the concentration of polyacrylamide used to cast the gel and on the amount of cross-linking. Table 5.1 shows the linear range of separation obtained with gels cast with concentrations of acrylamide that range from 5% to 15%. Most SDS-polyacrylamide gels are cast with a molar ratio of bisacrylamide:acrylamide of 1:29, which has been shown empirically to be capable of resolving polypeptides that differ in size by as little as 3%.

Table 5.1 Effective Range of Separation of SDS-Polyacrylamide Gels

Acrylamide concentration (%)	Linear range of separation (kD)
15	12-43
10	16-68
7.5	36-94
5.0	57-212

In most cases, SDS-polyacrylamide gel electrophoresis is carried out with a discontinuous buffer system in which the buffer in the reservoirs is of a different pH and ionic strength from the buffer used to cast the gel. The SDS-polypeptide complexes in the

sample that is applied to the gel are swept along by a moving boundary created when an electric current is passed between the electrodes. After migrating through a stacking gel of high porosity, the complexes are deposited in a very thin zone on the surface of the resolving gel. The ability of discontinuous buffer systems to concentrate all of the complexes in the sample into a very small volume greatly increases the resolution of SDS-polyacrylamide gels.

5.4.3 Time-resolved Imaging of the Protein after SDS PAGE Separation

The scheme of the imaging device is shown in Figure 5.4. The excitation light from eximer laser controlled by pulse generator was directed to the gel slab using concave lens. The light from the gel was collected through an objective to the entrance of imaging spectrograph after 50 µsec delay and further amplified using ICCD camera. The signal was accumulated from 1000 frames and displayed on the computer screen.

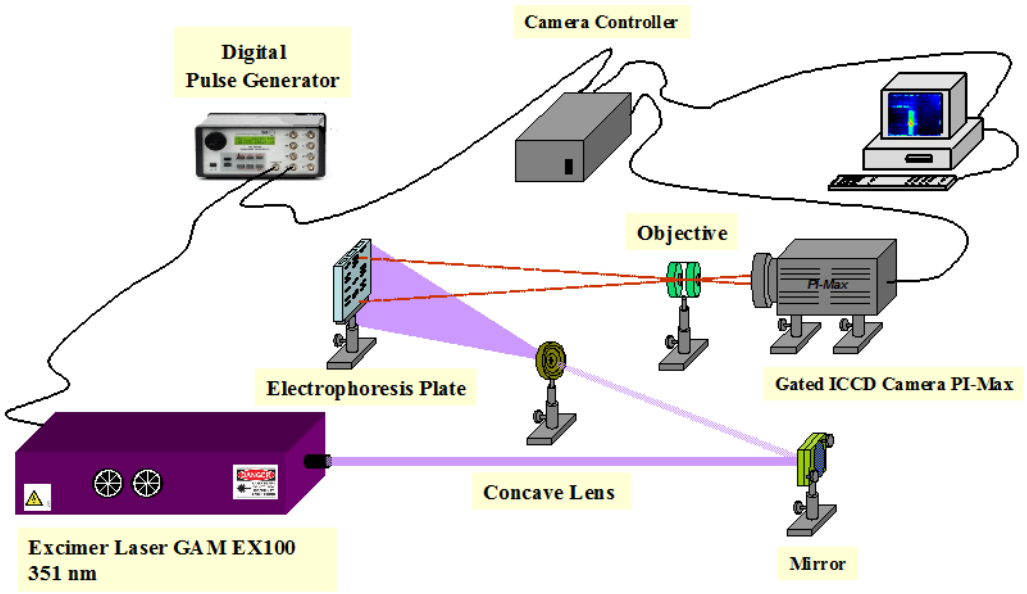

Figure 5.6 The scheme of Home-Built device for time-resolved imaging of protein slab gels.

5.5 Results

5.5.1 The Synthesis and Properties of the Reactive Probes and Synthetic Intermediates

Lanthanide chelates of carbostyril fluorophores (cs124 and cs124CF_3) represent attractive luminescent labels due to high quantum yield and high solubility in water (90-95). In previous studies (52) discusses how the probes were perfected by increasing retention of coordinated lanthanide, which also enhanced the probes brightness by elimination of water from metal coordination sphere (96). However, these probes required elevated temperatures and/or prolonged incubation for coupling to biomolecules. This could be an issue for unstable proteins or their complexes. Introduction of more reactive crosslinking groups in lanthanide luminescent probes is problematic due to complex synthetic protocols and possible side-reactions. One of the convenient classes of reactive groups commonly used for attachment of the probes is acylating function, represented by cyclic anhydrides or activated esters of carbonic acids, such as N-hydroxysuccinimide esters. Previously described anhydride acylating compounds with the reactive group at the chelating part of the luminescent probe (89) are quite active, but they are not optimal since the attachment of these probes to the molecule of interest is followed by lanthanide addition, that can result in the metal binding to the other metal chelating sites of a biomolecule. Also, in these compounds crosslinking eliminates a carboxylate chelating group from lanthanide coordination sphere that weakens metal retention and decreases the brightness of the probe. In the present study we set up to synthesize reactive lanthanide probes free of the above shortcomings. The strategy takes advantage of previously described by us intermediate compound **IIIa** (Scheme 5.3). Using sirendipitive catalytic effect of strong base on the reaction producing compound **IIIa**

from the precursor (103) significant improvement in the yield and simplification of the synthesis of this compound were achieved. Further it was noticed that treatment of compound **IIIa** with DCC yields an active acylating intermediate. The present research examined this reaction in more details. It was found that reaction of **IIIa** with DCC yields product **VIa** (Scheme 5.3), evidently through intramolecular attack of fluorophore's 2-oxo group on activated carbon of intermediate acylisourea derivative **Va**. The same reaction was observed with model compound in which 7-aminogroup was acetylated (compound **IIIb**). The reaction product (**VIb**) possessed distinctive UV absorption spectrum (Figure 5.1), which was strongly pH dependent (Figure 5.1), suggesting tautomeric equilibrium with enole form (structure **VIIb** of Scheme 1B), capable of ionization. Apparent pKa value inferred from UV spectrum recorded at various pH was 7.9, which is expected for this compound. Compound **VIb** reacted with water with half-reaction time ca. 15 min at 20 °C at pH 5, and 4 min at pH 9 (Figure 5.2) producing the original product **IIIb** as judged by characteristic transition of UV absorption spectrum and TLC analysis. Compound **VIa** displayed the same spectral behavior upon reaction with water with half-life time equal to 20 min at pH 6 (Figure 5. 3A). Incubation of compounds **VIa,b** with amines yielded acylation products, corresponding amides **VIIIa,b**. Next, it was investigated whether analogous cyclization reaction can proceed with DTPA-acylated derivative of compound **III** chelated with lanthanide (compound **IV**). It was reasoned that chelation would protect carboxylate groups of DTPA residue from reaction with DCC, while 3-carboxymethyl group of quinolone moiety should retain reactivity. Indeed, incubation of Eu^{3+} chelate **IV** with DCC in DMSO yielded expected compound, probe **5** (Scheme 5.1). Like model compound **VIb** probe **5** displayed

characteristic changes in light absorption spectrum upon hydrolysis with nearly the same rate.

For the synthesis of probe **6**, analogous strategies was used. 4,4,4-trifluoroacetoacetate was alkylated by ethyl-3-bromopropionate in the presence of a base to obtain trifluoroacetyldiethylglutarate (compound **X** of Scheme 5.2). The yield of the compound was lower than for corresponding synthetic intermediate for probe **5,** trifluoromethylmethylethylsuccinate (compound **II**) obviously due to lower reactivity of an alkylating compound and its side reaction leading to ethylacrylate. As expected, incubation of compound **X** with a phenylenediamine afforded reaction intermediate, which rapidly converted to desired fluorophore **XI** upon subsequent treatment with KOH. By analogy with compound **IIIa**, incubation of product **XI** with DCC resulted in accumulation of the derivative **XII** with increased mobility on TLC. The product **XIII** had UV absorption spectrum similar to that of **VIa**. Like compound **VIa** this product reacted with water (with half-reaction time 40-45 min at 20 °C) yielding the original compound **XI** (Figure 5.2B), or with an amine, producing corresponding amide (compound **XIV**). In contrast to compound **VIa**, light absorption spectrum for compound **XIII** was pH-independent indicating the absence of tautomeric form.

DTPA acylation of compound **XI** followed by $EuCl_3$ addition produced corresponding chelate **XII** with high yield. Reaction of **XII** with DCC resulted in cyclization by analogy with the synthesis of probe **5** producing probe **6**.

5.5.2 Conjugation of Probes 5 and 6 to Avidin and BSA

The dependence of the conjugation efficiency of probe **6** to BSA at pH 7 as function of time is shown in Figure 5.5. It is seen that reaction was complete in 5 min, reflecting high

rate of acylation. Remarkably, coupling efficiency for probe **6** remained the same in wide pH range (from 7 to 10), suggesting high reactivity of the probe towards BSA lysine residues (Figure 5.6) comparing to hydrolysis rate. Essentially the same reactivity was displayed by probe **5**.

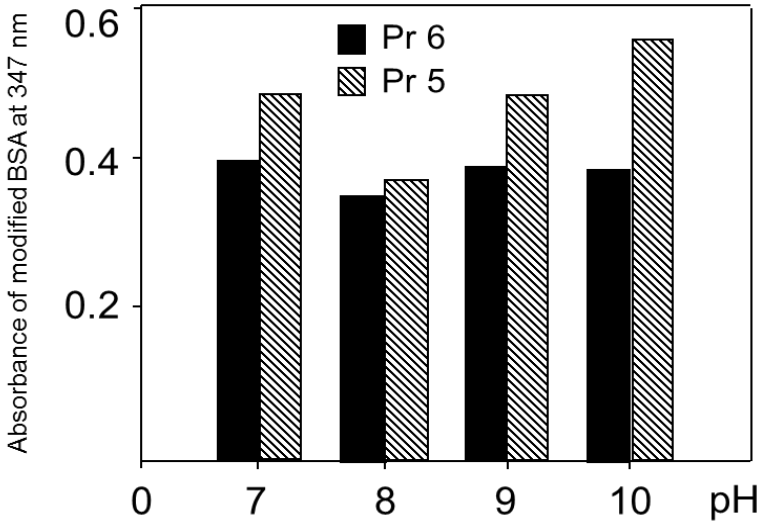

Figure 5.7 Absorbance of BSA modified by probes 5 and 6 at various pH at concentration of the probes 8 mM.

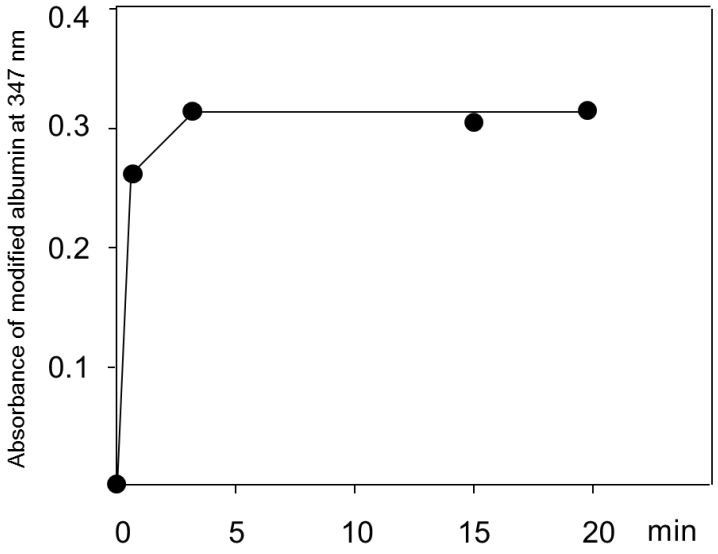

Figure 5.8 Time course for modification of BSA by probe 6 at probe concentration 8 mM.

Figure 5.7 (A) shows the number of conjugated residues for probes **6** and **5** as function of probe concentration. It is seen that ca. 23-24 luminescent residues can be attached to the protein at 16 mM probes concentration, which is close to the number of accessible Lys residues in BSA.

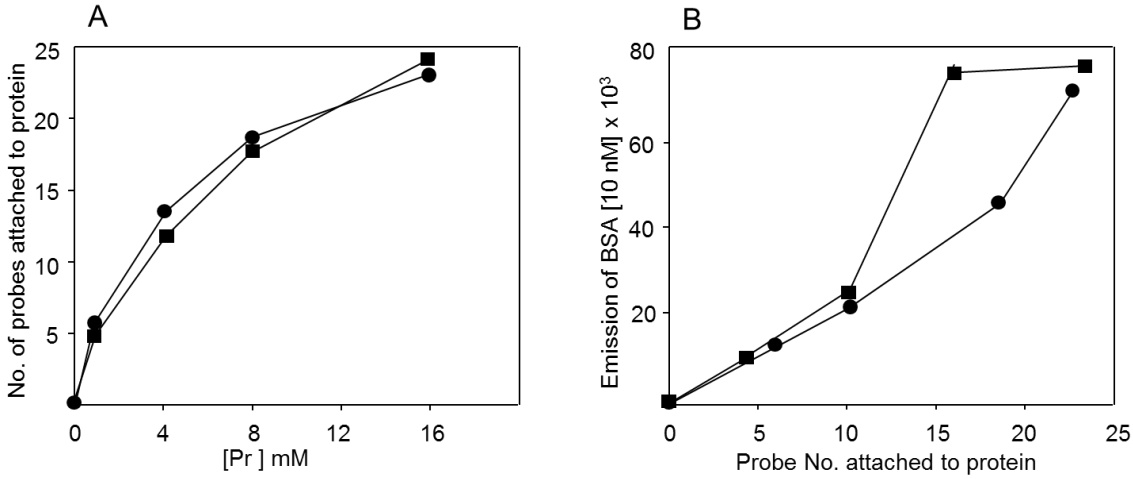

Figure 5.9 Dependence of the number of the attached probes on the probes concentration in the reaction of BSA modification (A). Dependence of the BSA luminescence on the number of attached probes (B).

5.5.3 Fluorescent Properties of the Reactive Probes and their Conjugates.

As follows from the luminescence intensity the dependence of the light emission on the number of probes **5** and **6** attached to BSA displayed non-linear enhancement, suggesting synergistic effect (92,104). This effect was due to enhanced efficiency of the energy transfer as follows from the ratio of antenna-to-lanthanide emission (Table 5.2). Light emission of the labeled protein further increased in deuterium oxide (Table 5.2) due to prevention of non-radiant energy dissipation (96) caused by coordinated water.

Table 5.2 Luminescence for BSA [10 nM] Modified with Probe 6 and for Hydrolyzed Free Probe

No. of attached probes	Antenna emission	Eu^{3+} emission	Ratio
6.5	4 700	12 000	2.55
13	7 500	32 000	4.3
18	8 900	45 000	5.0
	9 500*	96 000*	10.1*
22.4	16 400	74 600	4.6
	Non-attached probe **6**		
	4700	12 000	2.55

* Recorded in heavy water

5.5.4 Stability of the Lanthanide Chelates Attached to Proteins Under Condition of Denaturing Electrophoretic Separation

Next, the light emitting properties of protein conjugates at the conditions of electrophoretic separation in the presence of SDS were examined. To this end BSA – probe **6** conjugate was incubated in separation buffer for disc-electrophoresis containing 0.125 M Tris, 0.4 M glycine and 0.1 % SDS. As seen from Figure 5.8, prolonged incubation (80 min) only slightly reduced the brightness of the conjugate (by ca. 15%), suggesting the possibility of electrophoretic separation of the proteins modified with our luminescent probes.

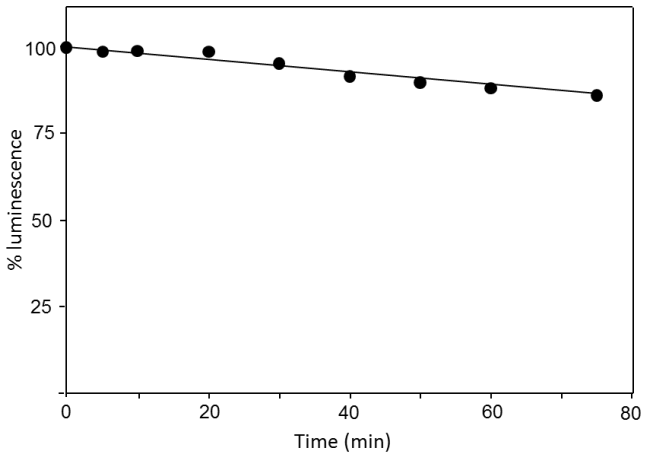

Figure 5.10 Light emission of the BSA modified with probe 6 after incubation in electrophoresis buffer for various times.

This was further confirmed by separation of purified *E.coli* RNA polymerase and *E.coli* whole cell lyzate labeled by luminescent Eu^{3+} chelate (Figure 5.9).

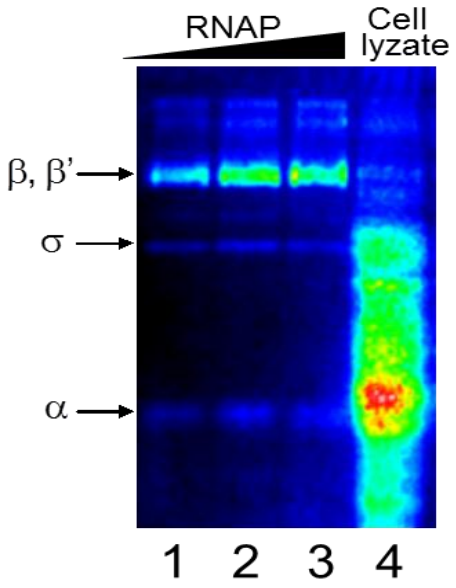

Figure 5.11 Time-resolved gel image of the gel containing labeled *E. coli* RNA polymerase subunits (lanes 1-3) and whole cell *E.coli* lyzate (lane 4).

The labeled proteins were imaged in time-resolved mode by acquisition of the signal from multiple pulsed excitations using home built device shown in Figure 5.4. In

this setup the excitation light from eximer laser was directed to the gel using concave lens. The emitted light from the gel was collected through an objective to the entrance of imaging spectrograph and enhanced by ICCD camera. As expected, the image was highly contrasted.

5.6 Discussion

The present research discusses the development of simple synthetic protocol for highly reactive luminescent Eu chelates based on serendipitive reaction. This strategy takes advantage of intra- molecular conversion of pre-formed lanthanide complex to active acylating quinoline derivative by DCC in non-aqueous medium. This reaction involves exclusively carboxylate group in position 3 of fluorophore ring, while DTPA carboxylates are protected by coordination with a lanthanide. Resulting compounds represent cyclic esters and display acylating activity comparable with that of widely used N-hydroxysuccinimide (NHS) esters, which is evident from their hydrolysis rates. Thus, half-hydrolysis times at ambient temperature are ca. 10 min for Probe **5** and ca. 40 min for probe **6**, while for NHS esters it is 6 min at the same conditions. Both probes can be coupled to biomolecules with high efficiency in physiological conditions, as exemplified by modification of avidin and BSA. Generally, upon conjugation probe **6** gave more reproducible strong emission signal, while the signal for probe **5** conjugates was sensitive to slight changes in reaction conditions. Thus, in some cases less efficient energy transfer from antenna to lanthanide was observed. Also, the emission maximum for antenna fluorophore in such conjugates displayed detectable red shift. Most likely this was due to partial oxidation of the reactive fluorophore form at the conjugation conditions. Indeed, isomeric enole form of fluorophore (compound **VII** of Scheme 5.1) is expected to be

prone to oxidation, especially in ionized state **IX**. This was confirmed by studies of model compound, N7-acetyl derivative of fluorophore **VIb** (**VIIb**), which quickly turned dark at the conditions of conjugation reaction due to oxidation. However, this side reaction can be suppressed by using oxygen scavengers (e.g., pyrogallol). Remarkably, probe **6** always displayed stable reproducible signal upon conjugation, since the probe does not exist in oxygen-sensitive enolic form.

The suggested protocols for probes **5**, and **6** are simple, since they do not include chromatographic purification steps and can be accomplished in 1-2 working days. The probes react under extremely mild conditions (pH 7.0, 20 °C, 1-2 min), which makes them especially valuable for labeling of sensitive biological molecules. Stability of the luminescent probes under the conditions of denaturing electrophoretic separation opens the possibility of using the probes in proteomic studies, especially in the cases in which hyper-sensitive detection is required. High detection sensitivity was demonstrated by using home-built device for time-resolved imaging.

Finally, the developed synthetic protocols may be used to obtain analogous reactive chelates of cs124 antenna fluorophore (containing methyl instead of trifluoromethyl group in position 4 of quinolone ring), which are highly luminescent when complexed with Tb^{3+}.

CHAPTER 6

FLUORESCENT DERIVATIVE OF CASPOFUNGIN AND POSACONAZOLE FOR DIAGNOSTIC IMAGING OF INVASIVE FUNGAL PATHOGENS

6.1 Introduction

Invasive fungal infections (IFI) are a growing threat to human health due to increase in the number of immune-compromised patient population (105). In most situations where IFI diagnosis is considered, the clinical presentation is often non-specific and can be caused by a wide range of infectious organisms, underlying illness, or complications of treatment. Furthermore, successful laboratory diagnosis of fungal infections is highly dependent on appropriate clinical specimen collection and selection of the appropriate microbiological test (105). Microbiological tests differ from mycosis to mycosis, are dependent on clinical symptoms and the site of infection and often diagnosis is problematic. For example, in sterile sites such as blood or other CSF fluids, the discovery of such organisms is indicative of infection. However, in non-sterile material, such as pus, sputum and other respiratory fluids, the results can be equivocal unless there is an additional evidence of infection (106).

Successful IFI diagnosis is further complicated due to uncertainties and controversies in disease definition and in selecting the standardized methods for establishing the diagnosis. Recently, the European Organization for Research and Treatment of Cancer/Mycoses Study Group (EORTC/MSG) proposed criteria for the classification of invasive fungal infections. A consensus was reached for defining opportunistic IFI in immune-compromised patients that improves not only IFI diagnosis on a particular patient but also allows epidemiologists to make generalizations, prognosis,

and accurate treatment guidelines for IFI. This included criteria for defining a proven, probable, or possible IFI based on host factors, clinical features, and mycological evidence (107). Their definition of a proven IFI is a positive histopathologic or cytopathologic examination showing hyphae or yeast. Concurrently, the criterion to establish a proven fungemia is a positive blood culture for fungi. For probable IFI, the definition includes isolation of fungi by culture in combination with other host or clinical features. Probable IFI diagnoses are difficult make since cultures of respiratory tract fluids lack sensitivity. In patients with proven invasive aspergilosis, *Aspergillus* spp. can be isolated from sputum and BAL specimens in fewer than 30% and 60% of the cases, respectively (108). In most cases, the confirmation of an invasive aspergillosis diagnosis requires positive histopathology. However, lung biopsies often difficult due to profound neutropenia and thrombocytopenia associated with patients at risk for invasive aspergillosis.

Fungal cell wall components such as glucans and galactomannans, which are actively shed during growth and development, are the basis of antigen assays for rapid diagnostic testing (109). These assays include commercial products such as the Glucatell (1-->3)-beta-D-glucan (BG) detection assay (Associates of Cape Cod) (110) or the Platelia *Aspergillus* galactomannan antigenemia assay (111). These antigen-based detection assays assist in making decisions using other clinical and diagnostic factors. Yet, their value is limited by the potential for false-positive and false-negative results due to an assortment of factors, which include interference due to contaminating antigen resulting from treatment with antibiotics (112-114).

In recent years, standardization of protocols for PCR amplification of organisms, such as *Aspergillus* spp. from blood and respiratory samples (113) has aided in the diagnosis of these infections, especially since cultures are often negative (114).

Diagnostic imaging is an important part of the diagnosis of invasive aspergillosis. Characteristic images from computed tomography (CT) can be used to identify disease lesions in neutropenic patients and help manage invasive fungal infection. Importantly, the CT halo sign is a transient finding that provides a probable diagnosis of early invasive pulmonary aspergillosis. Patients with a halo sign at baseline are more likely to have a satisfactory treatment response than those without this indicator (115). Diagnostic imaging is inherently non-specific and must be used in combination with other clinical and microbiological factors.

The diagnosis of invasive aspergillosis continues to be a major challenge, despite several improvements such as diagnostic imaging techniques and antigen tests. The European Organization for Research and Treatment of Cancer/Invasive Fungal Infections Cooperative Group and the National Institute of Allergy and Infectious Diseases Mycoses Study Group (EORTC/MSG) concluded that that early diagnosis can be improved by combining different diagnostic techniques (116,117).

This work, discloses the development of novel fungal-specific probes that have the potential to be used for diagnostic imaging. As a first step toward increasing specificity, this chapter describe the development of a broad-spectrum fungal-specific targeting molecule, which when modified with a fluorescent label fully retains its targeting properties, and provides a basis for future imaging applications. This new approach (fungal-specific probe) takes advantage of highly specific and sensitive antifungal drugs with known safety properties as targeting molecules. By coupling a

fluorophore that can be visualized, the new probe would be able to detect the presence of fungal pathogens.

Prominent antifungal drugs include the polyene macrolides (amphotericin B and nystatin) that target fungal plasma membrane ergosterol; the azoles (fluconazole, itraconazole, voriconazole) that target the 14 α-sterol demethylase enzyme; and the echinocandins that target 1,3-β-D-glucan synthase. An important feature of these molecules is that they display strong affinity for their cellular targets with high specificity. The exception is the polyene drugs amphotericin, which partitions into cellular membranes and interacts with ergosterol in an undefined manner. However, it accumulates in the kidneys where it shows cross-reactivity with mammalian cholesterol leading to its toxicity. The high degree of specificity of azoles and echinocandins reflects their high affinity binding to targets that are only present on fungi and are not present in the host. These are ideal features for diagnostic targeting molecules. By labeling drugs with various reporter molecules, they should be highly suitable for specific pathogen detection. In addition, since the targets are present in high abundance in each cell (thousands to hundred thousands of copies), they have the potential to show an amplified signal per cell interaction.

Among the current antifungal drugs, the most suitable for this purpose are the echinocandin and the azole classes. The advantages of these inhibitory molecules are; broad and high specificity to fungal pathogens, high affinity to cellular targets demonstared by sub-micromolar MICs and nanomolar enzyme inhibition constants, small molecules which are optimized for penetration but large enough (FW 900-1300 Da) to allow derivatization without significantly affecting their anti-fungal properties and excellent safety profile.

In this research, echinocandin drug, caspofungin (CSF) and azole class of drug, posaconazole (POS) have been studied. They bind with high affinity to its fungal target glucan synthase (116, 117) and 14-α-demethylase respectively which is not found in humans. This fungal specificity potentially makes it a powerful and highly discriminating diagnostic tool for the sensitive detection and visualization of fungal pathogens, when coupled with a suitable label (108). The antifungal molecule caspofungin (CSF) shows broad activity against clinically important *Candida* and *Aspergillus* spp. (116). It contains two aliphatic primary amino groups that are convenient sites for chemical modification, which facilitate the engineering of broad-spectrum labeled probes. Similarly the fluorescent derivative of triazole antifungal drug, posaconazole is been studied as well. Chart 6.1 displays structure of fluorescent derivatives of the anti-fungal drugs.

A

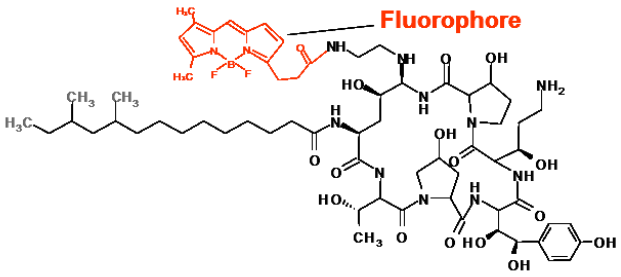

B

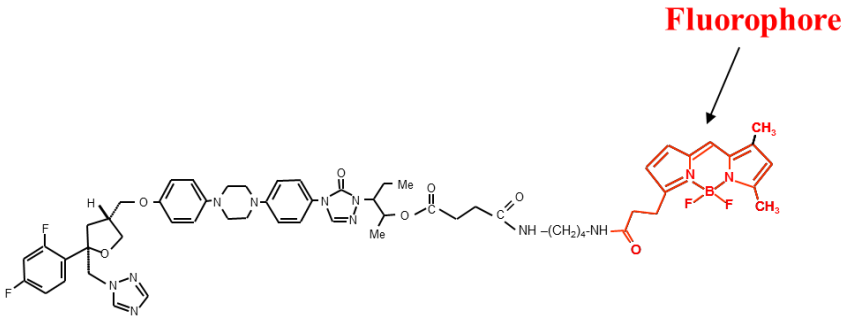

Chart 6.1 Bodipy fluorescent derivative of A) Caspofungin and B) Posaconazole.

6.2 Synthesis of Fluorescent Derivative of Posacoazole and Caspofungin

6.2.1 Bodipy-Fluorescent Derivative of Posaconazole

Compound I: Solution of 38 mg of posaconazole in 0.3 ml of DMSO was supplemented with 70 mg of succinic anhydride and 60 ml of methylimidazole. After 5 h incubation at 45o C TLC analysis in chloroform – ethanol – 20 % ammonium hydroxide (100:10:1) revealed ca. 95 % conversion of posaconazole to acylation product. The mixture was poured drop wise into 3 ml of 1 M citric acid and left for 30 min at 4o C. The precipitate was collected by centrifugation, washed with water (4 x 3 ml) and dried in vacuo under gentle heating. Yield 30 mg. High resolution MS (MALDI) *m/z:* anal, calc. for $C_{41}H_{46}N_8O_7F_2$ is 800.87; found, 799.3.

Compound II: To the solution of 30 mg of I in 0.3 ml of THF 10 mg of 4-nitrophenole and 25 mg of DCC were added. After 30 min incubation at 20° C TLC analysis in Chloroform ethanol (3:1) developing system revealed nearly quantitative conversion of compound I to reaction product. The precipitate was removed by centrifugation and the reaction mixture evaporated to dryness under reduced pressure. High resolution MS (MALDI) *m/z:* anal, calc. for $C_{47}H_{49}N_9O_9F_2$ is 921.97; found 923.4.

Compound III: Solution of 20 mg of succinimidyl ester of BODIPY-fluoresceine in 0.3 ml of DMSO was poured drop wise into a solution of 50 µl 1,4-diaminobutane monoacetate in 0.5 ml of 80% aqueous DMSO under rigorous agitation. The mixture was diluted by 4 ml of water and quickly extracted by ethylacetate (2 x 5 ml). The organic layer was extracted by 2 ml of water, dried over anhydrous sodium sulfate, evaporated to dryness and dissolved in 0.3 ml of DMSO. Yield, 70 %.

Compound IV: The residue of compound II was dissolved in the solution of compound III (see above) and supplemented with 3 µl of triethylamine. After 5 min incubation at 37 °C

TLC showed ca. quantitative conversion of II to fluorescent reaction product. The product was precipitated by addition of 5 ml of water, collected by centrifugation and purified on silicagel column (2.5 x 40 cm) in chloroform – ethanol (15:1) developing system. Yield – 21 mg. High resolution MS (MALDI) m/z: anal, calc. for $C_{59}H_{70}N_{12}O_7F_4B$ ($M - F + H^+$) is 1127.1; found, 1126.5.

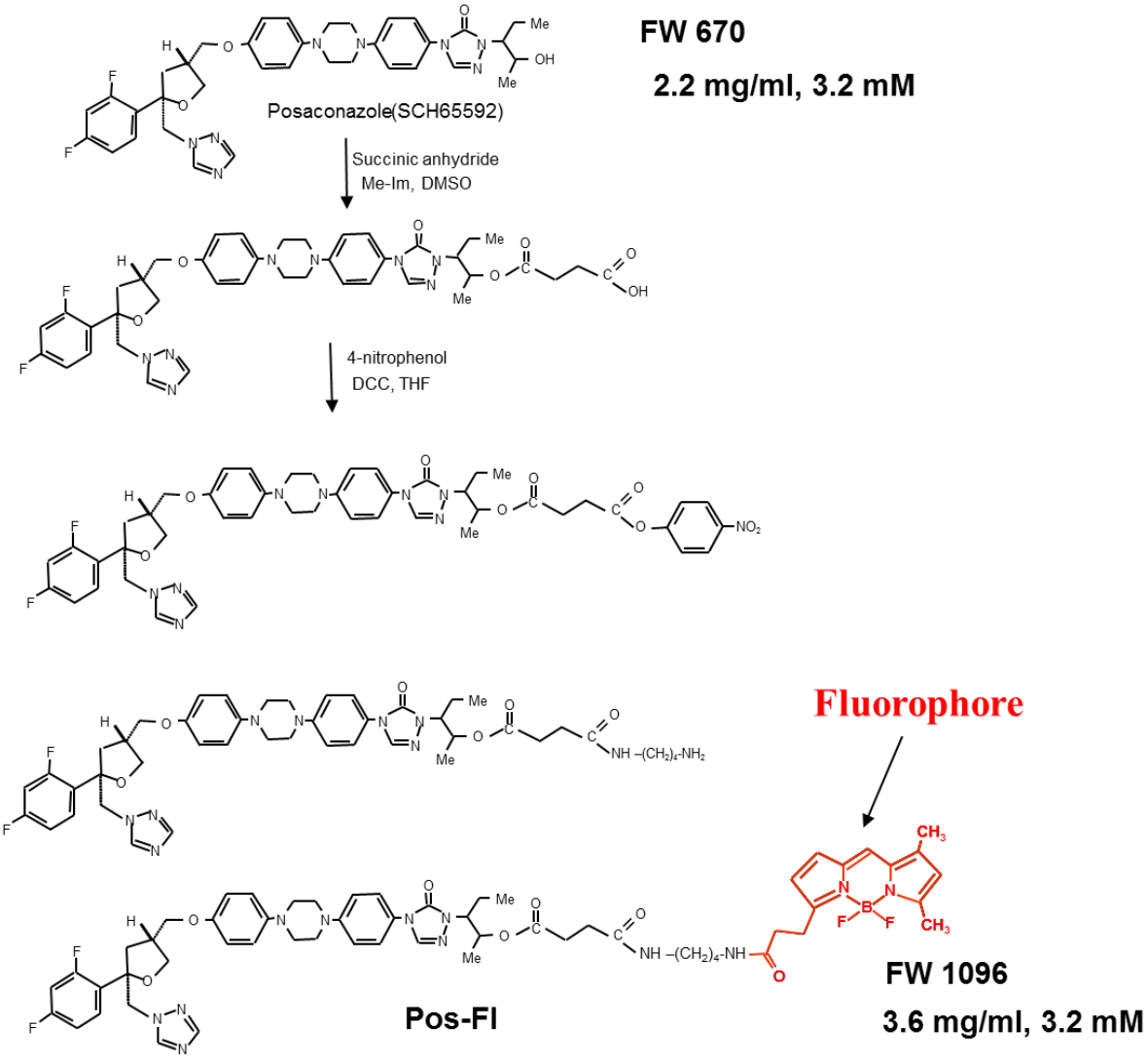

Scheme 6.1 Synthetic route for posaconazole fluorescent derivative.

6.2.2 BODIPY-Fluorescent Derivative of Caspofungin

Solution of 3 µmol of BODIPY-fluoresceine succinimidyl ester in 50 ml of DMF was added by 10 µl portions to the solution of 3 µmol of caspofungin and 2 µl of triethylamine in 100 µl of DMF under rigorous agitation. TLC analysis of the reaction mixture in acetonitrile – water (6:1) system detected two major fluorescent products. Fluorescence of faster migrating product was strongly quenched. The most likely this spot corresponds to double modification product at both aliphatic amino groups of the drug. The coupling reaction product is shown in Chart 6.1 (A). Slower migrating product was purified by preparative TLC in the same system. Yield – 1 µmol. High resolution MS (MALDI) *m/z:* anal, calc. for $C_{66}H_{102}N_{12}O_{16}F_2B$ is 1368.43; found, 1368.8.

6.3 Properties

6.3.1 Absorbance of Fluorescent Posaconazole Adduct

Incubation of activated ester **II** compound with ethylenediamine resulted in appearance of characteristic absorption at 405 nm of nitrophenolate anion (Figure 6.1), which was indicative for acylation of the diamine by posaconazole activated ester. Incubation of the ester with aminobutane derivative of BODIPY fluorophore (compound **III**) afforded desired fluorescent posaconazole –BODIPY adduct **IV**, with expected light absorption spectrum (Figure 6.2). The comparison of absorption spectra of the posaconazole adduct with the reference compounds indicate presence of both the drug and the fluorophore moieties in the final synthesized compound.

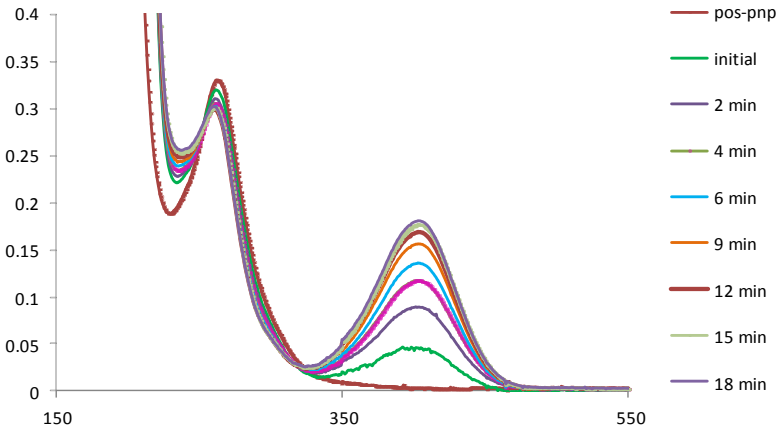

Figure 6.1 UV absorption spectra of the reaction mixture containing reactive posaconazole acylating derivative and ethylenediamine.

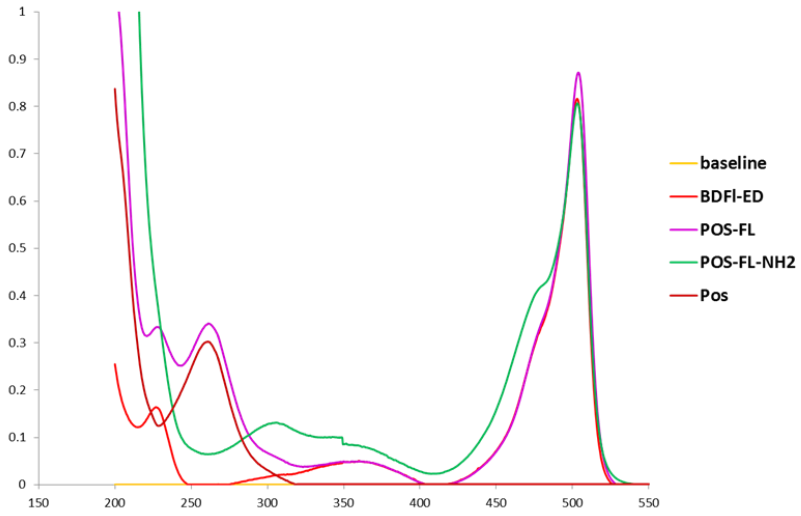

Figure 6.2 UV absorption spectra for fluorescent (Posaconazole) drug derivatives and reference compounds.

6.3.2 Absorbance of Fluorescent Caspofungin Adduct

The UV absorbance of the caspofungin adduct was compared with reference compounds, Figure 6.3. The product was highly fluorescent and had UV absorption spectrum (Figure 6.3) close to superposition of the spectra of BODIPY and caspofungin. pH shift from 7 to

11 caused characteristic spectral change due to ionization of caspofungin tyrosine residue. Mass spectrum of the compound indicated the presence of one fluorophore residue per caspofungin molecule.

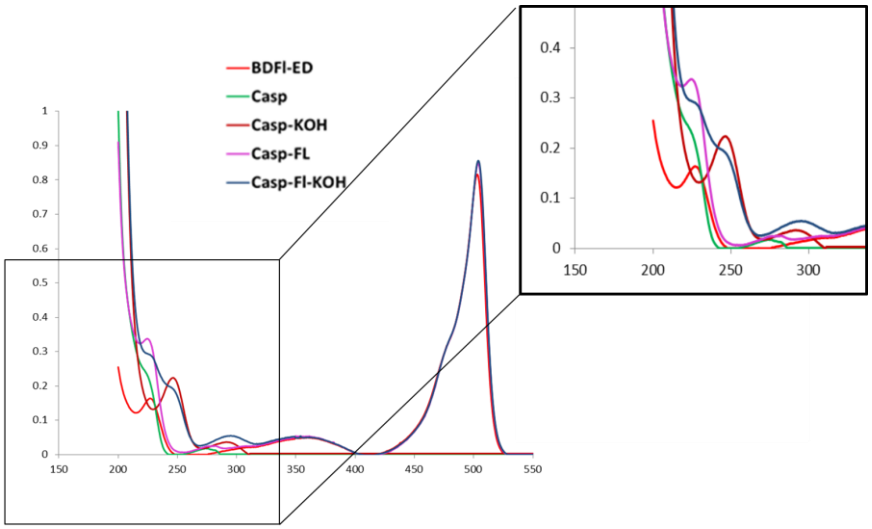

Figure 6.3 UV absorption spectra for fluorescent (Caspofungin) drug derivatives and reference compounds.

6.3.3 Vitro Test Model

The behavior of the fluorescent drug was studies under various solvent conditions to predict the performance under real-time circumstance. Figure 6.4 shows fluorescence intensity of the synthesized compounds under various conditions. It is seen that the posaconazole derivative is weakly fluorescent in water, which can be explained by contact quenching of BODIPY fluorophore by light absorbing moiety of the drug. Indeed, the fluorescence dramatically increased in organic solvents in which stacking interaction is broken. At the same time, the fluorescence of BODIPY was not affected by the solvents. A similar, but much smaller effect was seen for caspofungin derivative (Figure 6.4). Strong increase of the fluorescence of posaconazole derivative suggests that binding of the drug to its target should produce the same effect, since the binding should also

destroy stacking interaction of the fluorophore with the drug. The *vitro* model depicts that the principle can very well be used for design of "signaling" molecules, which represent quenched fluorescent derivatives of the drugs. Such compounds can "light" a pathogen cell when they bind to their cellular target.

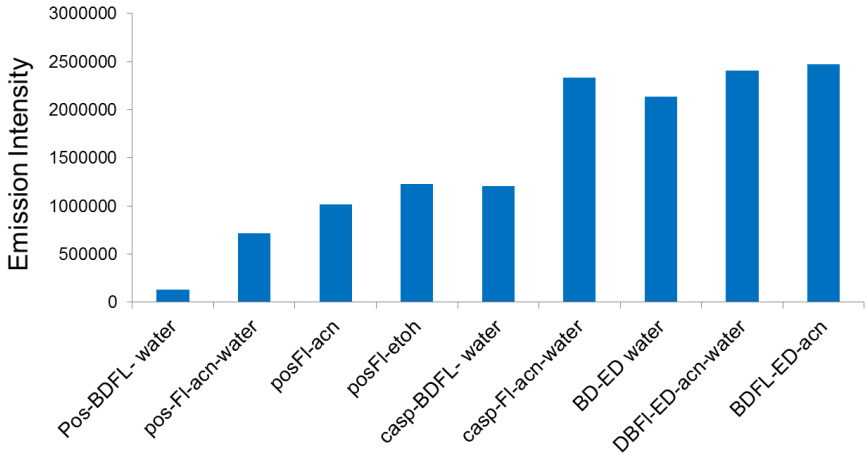

Figure 6.4 Fluorescence of the drugs derivatives and BODIPY fluorophore in various media.

6.4 Results

6.4.1 The Synthesis of Fluorescent Derivatives of Caspofungin

Caspofungin has two reactive aminogroups to which fluorescent groups can be attached through acylation. Since these two groups have similar reactivity the resulting products of mono-modification contain the dye molecule attached to an either group of the drug. Incubation of the drug with acylating derivative of BODIPY resulted in accumulation of two reaction products. The first product with lower chromatographic mobility has highly fluorescent. UV absorption spectra the product (Figure 6.3) was close to superposition of those for BODIPY fluorophore and caspofungin. pH shift from 7 to 11 caused

characteristic spectral change due to ionization of caspofungin tyrosine residue. Mass spectrum of the compound indicated the presence of one fluorophore residue per caspofungin molecule. The product with higher chromatographic mobility most likely represented caspofungin derivative containing two dye molecules attached to both amino groups of the drug.

6.4.2 The Synthesis of Fluorescent Derivatives of Posacanozole

The coupling of fluorophore to posaconazole molecule represented a challenging task since the drug does not have reactive groups suitable for the attachment. We were able to modify single hydroxyl group of posaconazole by succinic anhydride (Scheme 6.1). Surprisingly this reaction was very selective allowing nearly quantitative conversion. As expected the modification detectably reduced the mobility of the product due to introduction of a carboxylate (product **I**). Subsequent incubation of the acylation product with 4-nitrophenol in the presence of DCC yielded a new compound with greater chromatographic mobility whose UV absorption spectrum was close to the sum of that for acylated nitrophenol and posaconazole suggesting the formation of activated ester **II**. Incubation of this compound with ethylenediamine resulted in appearance of characteristic absorption at 405 nm of nitrophenolate anion, which was indicative for acylation of the diamine by posaconazole activated ester. Incubation of the ester with aminobutane derivative of BODIPY fluorophore (compound **III**) afforded desired fluorescent posaconazole –BODIPY adduct **IV**, with expected light absorption spectrum (Figure 6.2).

6.4.3 Light Emission Properties of Fluorescent Caspofungin and Posaconazole Compounds

It is seen that the posaconazole derivative is weakly fluorescent in water, which can be explained by contact quenching of BODIPY fluorophore by light absorbing moiety of the drug. Indeed, the fluorescence dramatically increased in organic solvents in which stacking interaction is broken. At the same time the fluorescence of BODIPY was not affected by the solvents. The same, but much smaller effect was seen for caspofungin derivative (Figure 6.4). Strong increase of the fluorescence of posaconazole derivative suggests that binding of the drug to its target should produce the same effect, since the binding should also destroy stacking interaction of the fluorophore with the drug.

6.5 Discussion

Highly fluorescent derivatives of antifungal drugs caspofungin and posaconazole, with preserved antimicrobial activity have been synthesized and characterized using fluorescent, light absorbing, and mass spectroscopy. Obtained anti-fungal fluorescent derivatives could render the microbial cells fluorescent allowing sensitive detection and imaging of fine distribution of the targeted enzymes within the elements of living growing cells. The pathogens' imaging was highly specific since common pathogenic bacteria were not stained by the compounds. Such an approach when coupled with existing high resolution imaging modalities has the potential to decrease morbidity and mortality in the immune-compromised patients by facilitating the implementation of appropriate antifungal therapy**.** This pilot study establishes a basis for fungal-specific targeting molecules that with the appropriate labels can be used for prompt diagnosis of invasive fungal infections.

Overall, this pilot study establishes a preliminary basis for fungal-specific targeting molecules that with the appropriate labels can be used as an adjunct to support the diagnosis of invasive fungal infections. Validation of the probes as viable clinical diagnostic tools will require *in vivo* efficacy studies and an assessment of serum and other host factors. Such an approach when coupled with existing high resolution imaging modalities using radiographically-visible labels has the potential to decrease morbidity and mortality in immune-compromised patients by facilitating more accurate diagnostics.

APPENDIX A

NUCLEAR MAGNETIC RESONANCE (NMR) RAW DATA

NMR data interpretation on some of the fluorescent compounds described in Chapters 3 and 5.

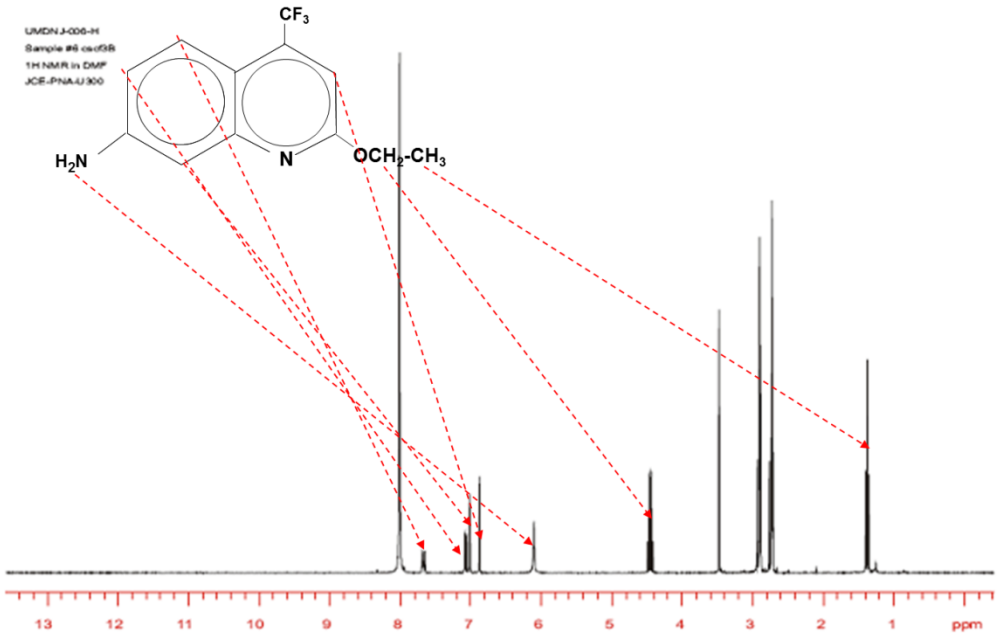

Appendix A.1 NMR spectrum of 7-amino-4-triflurомethyl-2-ethoxy quinoline (Qin124-CF_3).

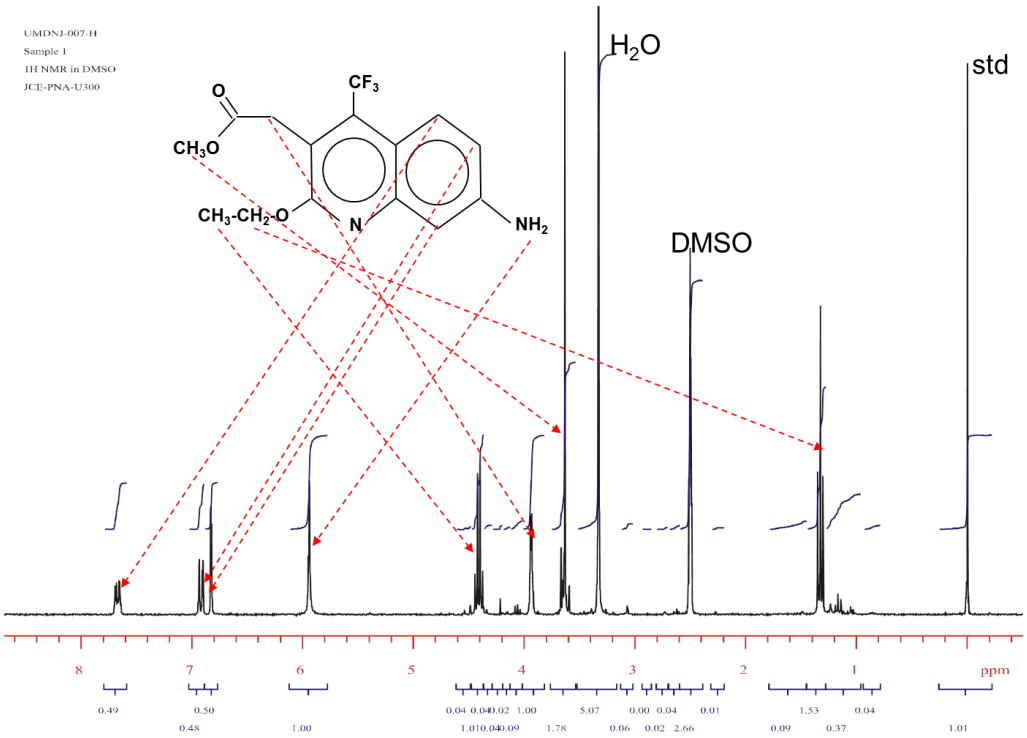

Appendix A.2 7-amino-4-ethoxy-3-carbomethoxymethyl-2-trifluoro methyl Quinolone.

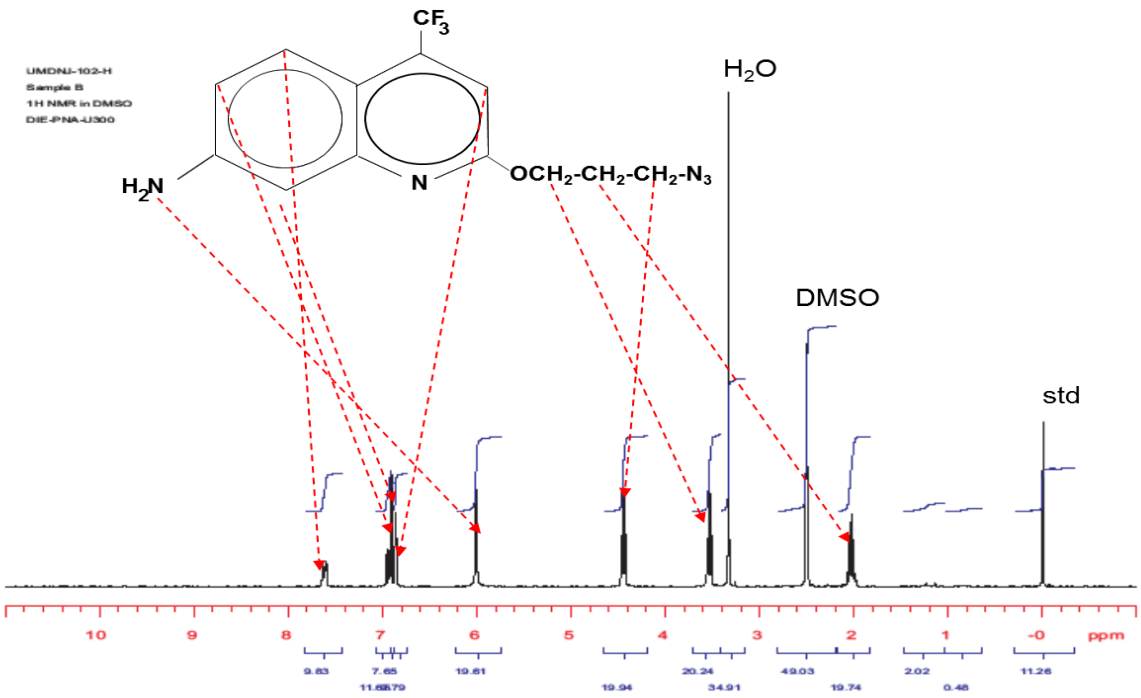

Appendix A.3 NMR spectrum of 7-amino-4-trifluoromethyl-2-(3-azidooxypropyl).

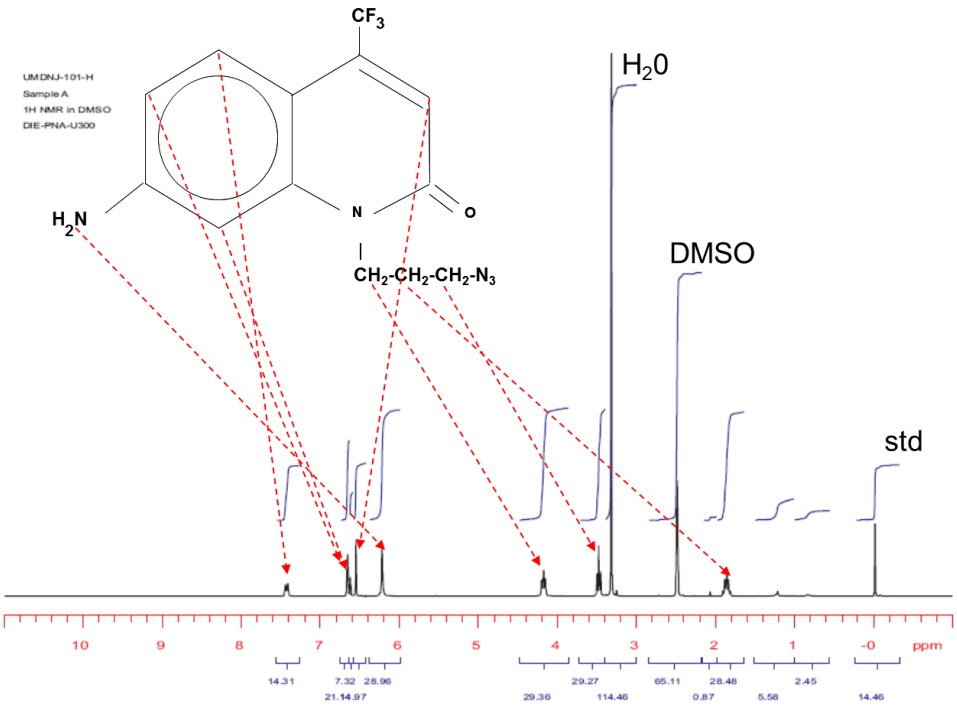

Appendix A.4 NMR spectrum of 1-(3-azidopropyl)-cs124-CF_3.

APPENDIX B

MASS ANALYSIS DATA

Mass analysis of compounds described in Chapter 4, 5 and 6

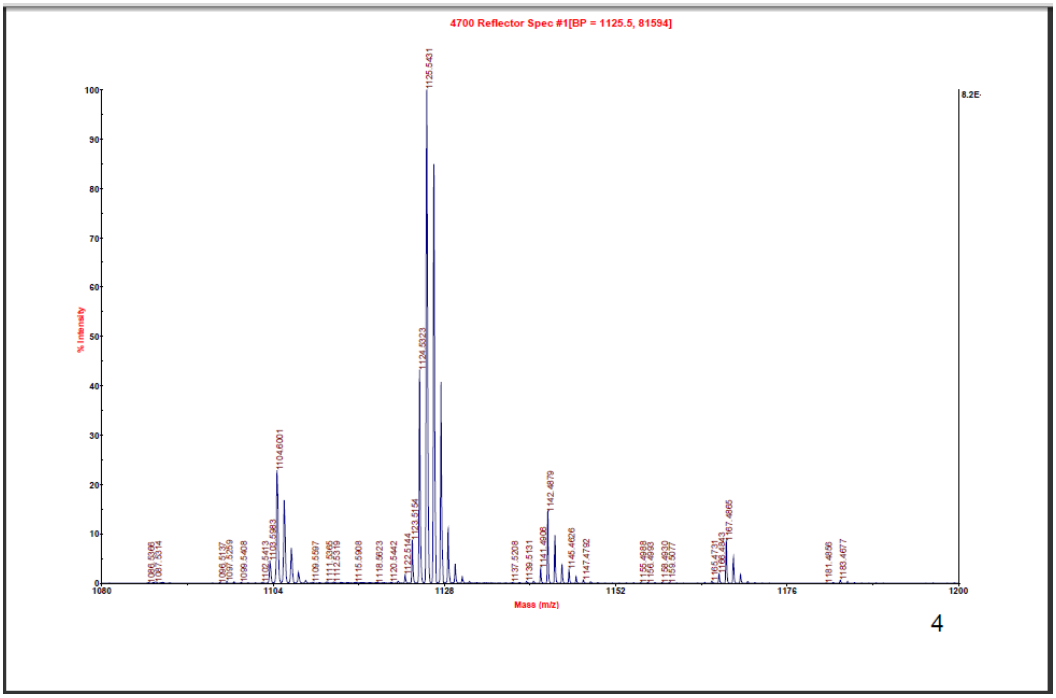

Appendix B.1 Mass spectrum of Posaconazole – Bodipy Fl Adduct.

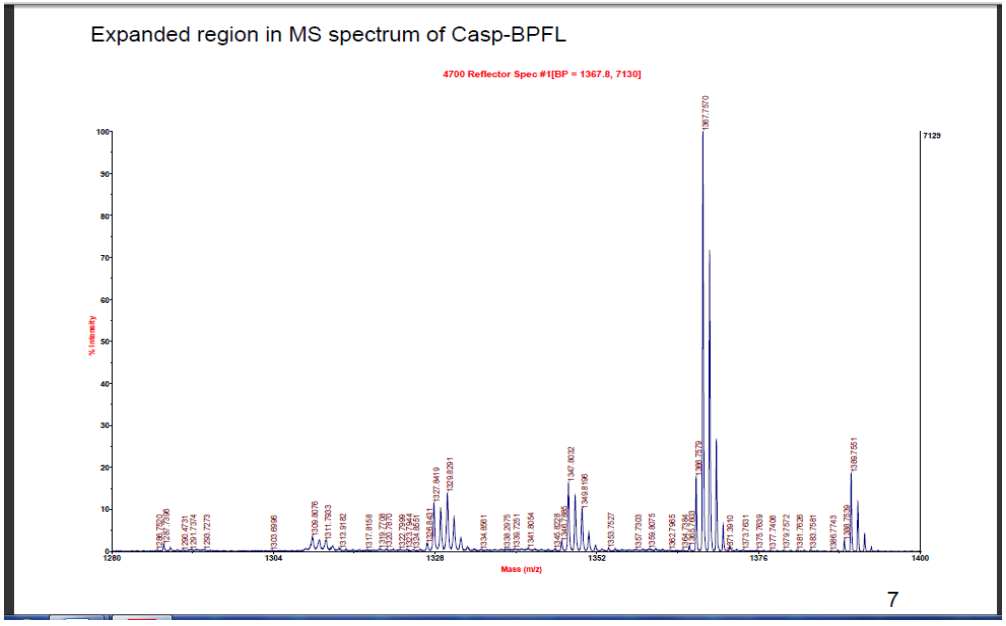

Appendix B.2 Mass spectrum of Caspofungin – Bodipy Fl Adduct.

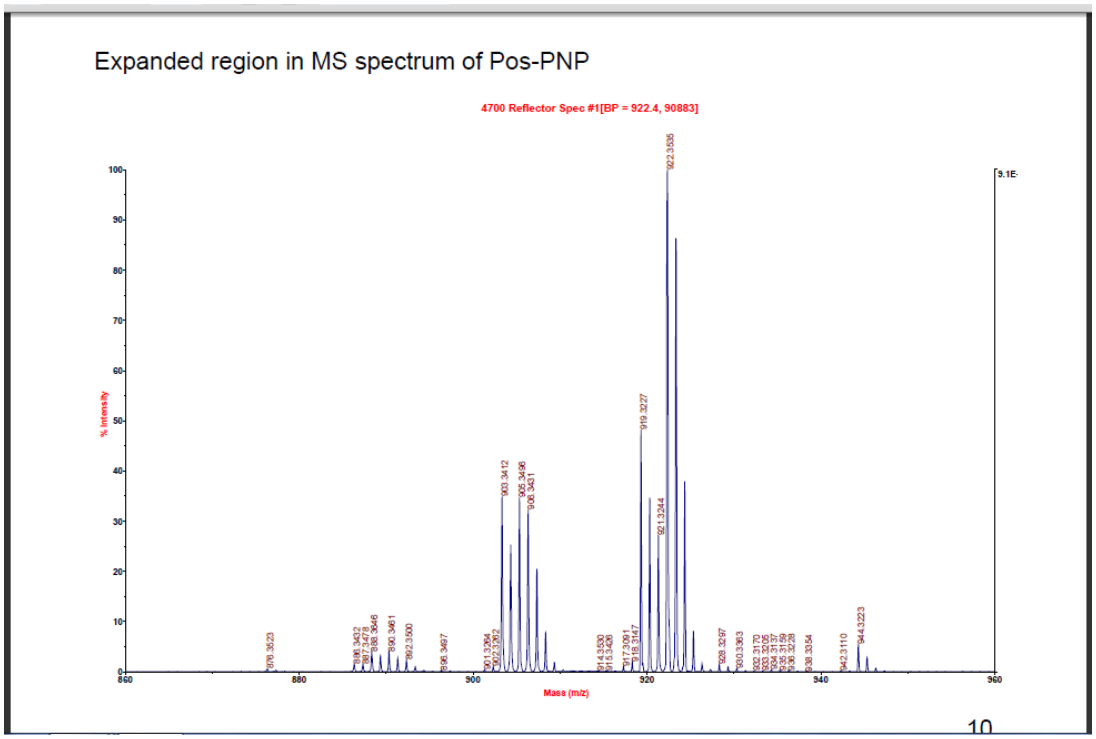

Appendix B.3 Mass spectrum of posaconazole p-nitrophenol derivative.

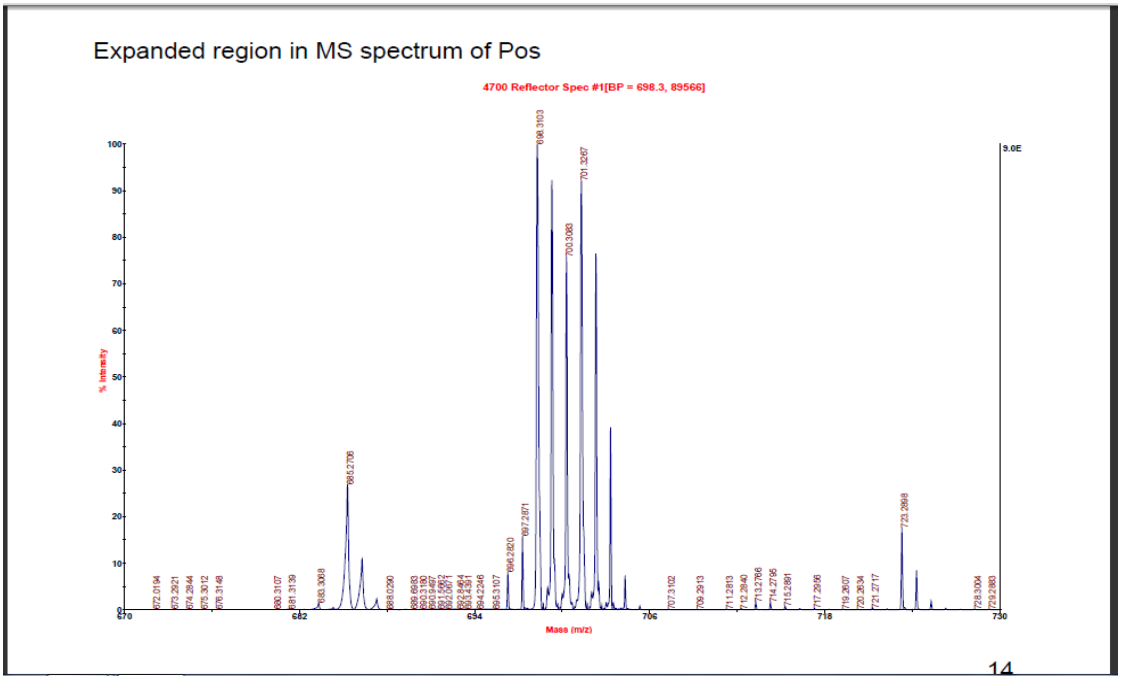

Appendix B.4 Mass spectrum of Posaconazole.

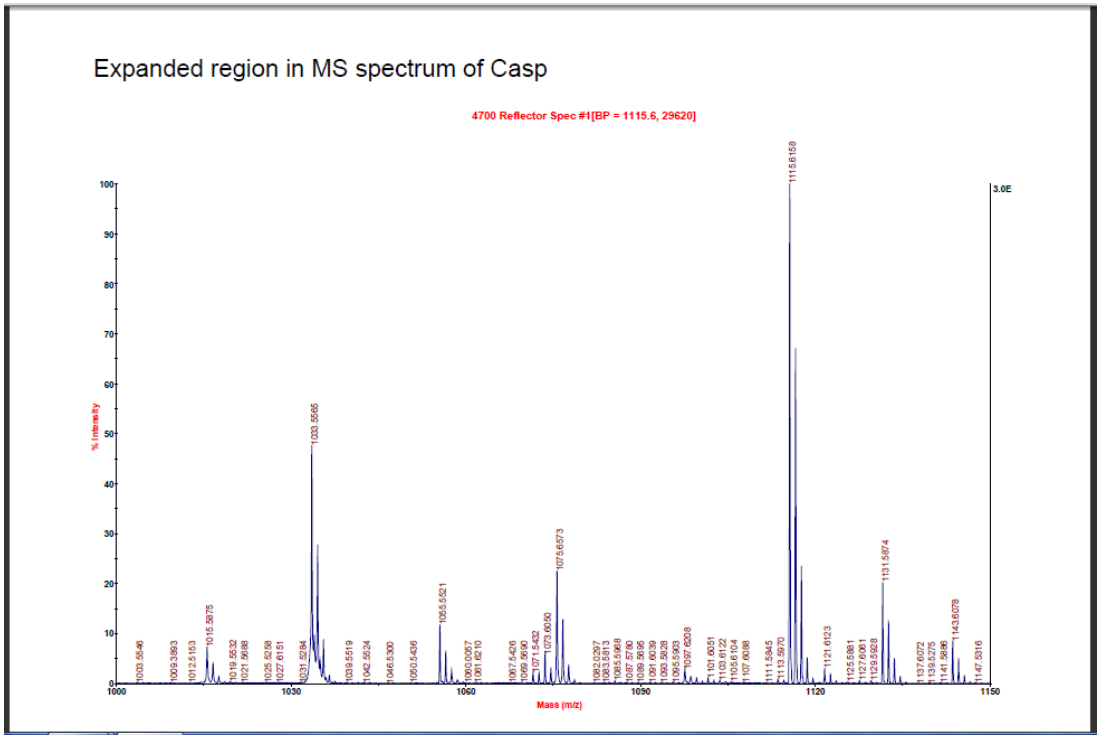

Appendix B.5 Mass spectrum of Caspofungin.

REFERENCES

(1) Lakowicz, Joseph R. Principles of Fluorescence Spectroscopy. Baltimore : Springer, (2006) Third edition.

(2) Bunzli, J. C. (2006) Benefiting from the unique properties of lanthanide ions. *Acc. Chem. Res.* 39, 53-61.

(3) Selvin, P.R., and Ming, X. (2001) Quantum Yields of Luminecent lanthanide Chelates and Far-Red Dyes Measured by Resonance Energy Transfer. *J.Am. Chem. Soc.* Vol. 123, pp. 7067-7073.

(4) Sammes, P.G., and Yahioulu, G. (1996) *Nat. Prod. Rep.* Vol. 13, pp. 1-28.

(5) Cooper M.E., and Sammes, P.G. (2000) Synthesis and properties of a new luminescent europius (III) terpyridyl chelates. *J.Chem. Soc. Perkin Tran.* Vol. 28, pp. 1675-700.

(6) Helmamila, I., Dakubu, S., Mukkal V. M., Siitari, H., and Lovgren, T. (1984) Europium as a label in time-resolved immunofluorometric assays. *Anal. Biochem.* Vol. 137, pp. 335-43.

(7) Mathis, G., Socquet, F., Viguier, M., and Darbouret, B. (1997) Homogeneous immunoassay using rare earth cryptates and time-resolved fluorescence: principles and specific markers for tumor markers. *Anticancer Res.* Vol. 17, pp. 3011-14.

(8) Saha, A.K., Kross, K., Kloszewski, E.D., Upson, D.A., and Toner, J. L. (1993) Time-resolved fluorescence of a new europium chelate complex: demonstration of highly sensitive detetion of protein and DNA samples. *J.Am.Chem Soc.* Vol. 115, pp. 11032-33.

(9) Siitari, H., Hemmila, I., Soini, E., Lovgren, T., and Koistenen, V. (1983) Detection of Hepatitis B surface antigen using time-resolved fluoriimminoassay. *Anal. Biochem.*Vol. 301, pp. 258-260.

10) Vamosi, G., Gohlke, C., and Clegg, R. (1996) Fluorescence characteristics of 5-carboxtetramethylrhodamine linked covalently to 5' end of oligonucleotide: multiple conformers of single stranded and double stranded dye-DNA complexes. *J. Biophys.* Vol. 71, pp. 972-974.

(11) Eaton, D.F. (1988) Reference material for fluorescence measurements - Pure and applied chemistry. Vol. 60, 7, pp. 1107-1114.

(12) Richardson, F.S. (1982) Terbium (III) and europium (III) ions as luminescent probes and stains for biomolecular systems. *Chem Rev.* Vol. 82, pp. 541-552.

(13) Becker, R.S., Chakravorti, S., Gartner, C.A., and de Graca, M. (1993) *J. Chem. Soc., Faraday Trans.* Vol. 89, p. 1007.

(14) *Lambdachromew Laser Dyes, Lambda.* U. Brackmann. (1986).

(15) Snavely, B.B. in: J.B. Birks (Ed.). *Organic Molecular Photophysics, chapter 5.* s.l. : John Wiley and Sons, London, 1973.

(16) Shank, C.V., Dienes, A., Trozzolo, A.M., and Myer, J.A. (1970) *Appl.Phys. Lett.* Vol. 16, p. 405.

(17) Reynolds, G.A., and Drexhage, K.-H. (1975) *Opt. Commun.* Vol. 13, p. 222.

(18) Fletcher, A.N., Bliss, D.E., and Kauffman, J.M. (1983) *Optics Communications.* Vol. 47, pp. 57-61.

(19) Grunhagen, H.H., Witt, H.T., and Naturforsch, Z. (1970) *European Journal of Biochemisry.* Vol. 25b, pp. 373-386.

(20) Haughland, R.P., and Larison, K.D. *Handbook of Fluorescent Probes and Research Chemicals.* Eugene : Molecular Probes Inc, (1992).

(21) Wolfbeis, O.S. in: S.G. Schulman (Ed.),. *Molecular Luminescence Spectroscopy: Methods and Applications, chapter 5.* s.l. : Wiley, (1985).

(22) Williams, R.T., and Roy, J. (1959) *Inst. Chem.* Vol. 83, p. 611.

(23) Yakatan, G.J., Juneau, R.J., and Schulman, S.G. (1972) *Anal. Chem.* Vol. 44, p. 1044.

(24) Zinsli, P.E. (1974) *J. Photochemistry.* Vol. 3, p. 55.

(25) Bauer, R.K., Kowalczyk, A., Balter, A., and Naturforsch, Z. (1977) Vol. 32 a, p. 560.

(26) Beddard, G.S., Carlin, S., and Davidson, R.S. (1977), *J. Chem. Soc. Perkin Trans.*Vol.2, p. 266.

(27) Song, P.-S., and Gordon III, W.H. (1970) *J. Phys. Chem.* Vol. 74, p. 4234.

(28) Song, P.-S., Harter, M.L., Moore, T.A., and Herndon, W.C. (1971) *Photochem Photobiol* Vol. 14, p. 521.

(29) Mantulin, W.W., Song, P.-S. (1973) *J. Am. Chem. Soc.* Vol. 95, p. 5122.

(30) Kirkiacharian, B.S., Santus, R., and Helene, C. (1972) *J. Photochem. Photobiol*. Vol. 16, p. 455.

(31) Lai, T., Lim, B.T., and Lim, E.C. (1982) *J. Am. Chem. Soc.* Vol. 104, p. 7631.

(32) Sakhno, T.V., Konoplev, G.G., Valkova, G.A., Shigorin, D.N., and Khim, Zh. Fiz. (1982) Vol. 56, p. 878.

(33) Wolfbeis, O.S., and Naturforsch, Z. (1977) *J. Chemical Pysics.* Vol. 32a, p. 1065.

(34) Wolfbeis, O.S. (1981) *Phys. Chem. N.F.* Vol. 125, p. 15.

(35) Wolfbeis, O.S., and Uray, G. (1978) *Monatsh. Chem.* Vol. 109, p. 123.

(36) Forster, Y., and Haas, E. (1993) Anal. *Biochem* Vol. 209, p. 9.

(37) Rechthaler, K., and Kohler, G. (1994) *Chem. Phys.* Vol. 189, p. 99.

(38) Sanghi, S., and Mohan, D. (1996) *Spectrochim. Acta 52A.* Vol. 52A, p. 1299.

(39) Ponomarev, O.A., Vasina, E.R., Yarmolenko, S.N., Mitina, Zh, V.G., and Obshch. Khim., (1988) *J. Molecular Structure.* Vol. 58 , p. 438.

(40) Ponomarev, O.A., Yu.F., Pedash,O.V., and Zh. Fiz. Khim. (1989) *J. Molecular Structure.* Vol. 63, p. 456.

(41) Walter, M.F., Fabian, K., Niederreiter, S., Georg, U., and Wolfgang, S. (1999) Substituent effects on absorption and fluorescence spectra of. *Journal of Molecular Structure.* Vol. 477, pp. 209-220.

(42) Rieutord, A., Prognon, P., Brion, F., and Mahuzier, G. (1997) *Analyst.* Vol. 59R.

(43) Tzougraki, C., Noula, C., Geiger, R., and Kokotos, G. (1994) *Liebigs Ann Chem*. p. 365.

(44) Selvin,P.R., and Pinghua. Ge., (2004) Carbostyril Derivatives as Antenna Molecules for Luminescent. *Bioconjugate Chem.* Vol. 15 (5), pp. 1088-1094.

(45) *J Am Chem Soc.* (1994) Vol. 116, pp. 7801.

(46) *Anal Biochem.* (1991) Vol. 198, pp. 228.

(47) Chen, J., and Selvin, P.R. (2000) Synthesis of 7-amino-4-trifluoromethyl-2-(1H)-quinolinone and its use as an antenna molecule for luminescent europium polyaminocarboxylates chelates. *J. Photochem.Photobiol A.* Vol. 135, pp. 27-32.

(48) Moniva, R., Van Beek, T., and Zuilhof, H. (2001) Surface functionalization by strain promoted alkyne-azide click reactions. *Angew Chem. Int.* Vol. 50, pp. 2-5.

(49) Best, M. (2009) Click Chemistry and Bio-orthogonal reactions: Unprecedental selectivity in the labeling of biological molecules. *Biochemistry.* Vol. 48, pp. 6571-6584.

(50) Hein, C., Liu, X-M., and Wang, D. (2008) Click Chemistry, a powerful tool for pharmaceutical sciences. *Pharmaceutical Research.* Vol. 25, pp. 2216-2230.

(51) Karsnoperov, L., Marras S., Kozlov, M., Wirpza, L., and Mustaev, A. (2010) Luminescent Probes for ultra-sensitive detection of nucleic acids. *Bioconjugate Chem.* Vol. 21, pp. 319-327.

(52) Bissell, E., Mitchel, A., and Smith, R. (1980) Synthesis and chemistry of 7-amino-4-(trifluoromethyl) coumarin and its amino acid and peptide derivatives. *J.Org.Chem.* Vol. 45, pp. 2283-2287.

(53) Lewis, F., Reddy, D., Elbert, J., Tillberg, B., and Kojima, M. (1991) Spectroscopy and Photochemistry of 2-quinolones and their Lewis acid complexes. *J.Org.Chem.* Vol. 56, pp. 5311-5318.

(54) Uray, G., Neiderreiter, K., Begaj, F., and Fabian, W. (1999) Long wavelength Absorbing and Emitting Carbostyrils with High fluorescence Quantum Yields. *Helvetica Chimica Acta.* Vol. 82, pp. 1408-1417.

(55) Schiller, D.S., and Fung, H.B. (2007) Posaconazole: an extended-spectrum triazole antifungal agent. *Clin Ther.* Vol. 29, pp. 1862-1886.

(56) Rachwalski, E.J., Wieczorkiewicz, J.T., and Scheetz, M.H. (2008) Posaconazole: an oral triazole with an extended spectrum of activity. *Ann Pharmacother* Vol. 42, pp. 1429-38.

(57) Brunton, L., Lazo, J., and Parker, K. (2006) Goodman and Gilman's. *The Pharmacological Basis of Therapeutics.* 11th ed. San Francisco : McGraw-Hill.

(58) Clinical Pharmacology Posaconazole. [Online] http://www.clinicalpharmacology-ip.com/Forms/Monograph/monograph.aspx?cpnum=2811&sec=monmech. Accessed in February, 2012.

(59) Undenfriend, S. (1995) Development of the spectrofluorometer and its commercialization. *Protein Sc.* Vol. 4, pp. 542-551.

(60) Berlman, I.B. (1971) *Handbook of fluorescence spectra of aromatic molecules.* end ed. s.l. : Academic Press.

(61) Rolinski Antonie, J.W.G., Visser and Olaf. *J. photobiology.info.* [Online guide] http://www.photobiology.info/Visser-Rolinski.html. Accessed in December, 2011.

(62) Williams, A. T. R., Winfield, S. A., and Miller, J. N. (1983) Relative fluorescence quantum yields using. *Analyst.* Vol. 108, p. 1067.

(63) *J.Phys.Chem.* (1979) Vol. 83, p. 696.

(64) *J.Phys.Chem.* (1980) Vol. 84, p. 1871.

(65) *J.Phys.Chem.* (1961) Vol. 65, p. 229.

(66) *J.Am.Chem.Soc.* (1945) Vol. 16, p. 1099.

(67) *Trans.Faraday.Soc.* (1957) Vol. 53, pp. 646-655.

(68) *J.Chem.Phys.* (1971) Vol. 55, p. 4131.

(69) *J.Phys.Chem.* (1970) Vol. 74, p. 4480.

(70) *J.Phys.Chem.* (1968) Vol. 68, p. 2680.

(71) *J.Phys.Chem.* (1961) Vol. 65, p. 229.

(72) *J.Phys.Chem.* (1983) Vol. 87, p. 83.

(73) Phillips, S.R., Wilson, L.J., and Borkman, R.F. (1986) Acrylamide and iodide fluorescence quenching as a structural probe of tryptophan microenvironment in bovine lens crystallins. *Curr Eye Res*. Vol. 8, pp. 611-619.

(74) O'Reilly, James E. (1975) Fluorescence experiments with quinine. *J. Chem. Educ.* Vol. 52, p. 610.

(75) LouAnn, S., Ballew, R., Elizabeth, M., Brown, A., Demas, J., Nesselrodt, N., and DeGraff, B. A. (1990) Photophysics in a disco: Luminescence quenching of quinine . *J. Chem. Educ.* Vol. 67, pp. 1065-1071.

(76) Gutow, J. H. (2005) Halide (Cl-) Quenching of Quinine Sulfate Fluorescence: A Time-Resolved Fluorescence Experiment for Physical Chemistry. *J. Chem. Educ*. Vol. 82, pp. 302-305.

(77) Kitai, A. (2008) Luminescent Materials and Applications. s.l. : *John Wiley and Sons.* Vol. 32.

(78) Bunzil, J.C. (2006) Benefiting from the unique properties of lanthanide ions. *Acc Chem Res.* Vol. 39, pp. 53-61.

(79) Dickson, E.F., Pollak, A., and Diamandis, E.P. (1995) Time-resolved detection of lanthanide luminescence for ultrasensitive bioanalytical assays. *J. Photochem Photobiology.* Vol. B 27, pp. 3-19.

(80) Dickson, E. F., Pollak, A., and Diamandis, E. P. (1995) Ultrasensitive bioanalytical assays using time-resolved fluorescence detection. *Pharmacol Ther.* Vol. 66, pp. 207-235.

(81) Hemmila, I., and Laitala, V. (2005) Progress in lanthanides as luminescent probes. *J. Fluorescence.* Vols. 15, pp. 529-542.

(82) Heyduk, T. (2001) Luminescence resonance energy transfer analysis of RNA polymerase complexes. *Methods.* Vols. 25, pp. 44-53.

(83) Parker, D. (2004) Excitement in f block: structure, dynamics and function of nine-coordinate chiral lanthanide complexes in aqueous media. *Chem Soc Rev.* Vols. 33, pp. 156-165.

(84) Selvin, P. R. (2001) Principles and biophysical applications of lanthanide-based probes. *Annu Rev Biophys Biomol Struct.* Vols. 31, pp. 275-302.

(85) Werts, M. H. (2005) Making sense of lanthanide luminescence. *Sci Prog*. Vol. 88, pp. 101-131.

(86) Yuan, J., and Wang, G. (2005) Lanthanide complex-based fluorescence label for time-resolved fluorescence bioassay. *J. Fluorescence*. Vol. 15, pp. 559-568.

(87) Selvin, P. R., Rana, T., and Hearst, J. (1994) Luminescence resonance energy transfer. *J Am Chem Soc*. Vol. 115, pp. 11032-11033.

(88) Li, M., and Selvin, P. R. (1997) Amine-reactive forms of a luminescent ethylenetri -aminepentaacetic acid chelate of terbium and europium: attachment to DNA and energy transfer measurements. *Bioconjug Chem*. Vol. 8, pp. 127-132.

(89) Ge, P., and Selvin, P. R. (2003) Thiol-reactive luminescent lanthanide chelates: part 2. *Bioconjug Chem*. Vol. 14, pp. 870-876.

(90) Ge, P., and Selvin, P. R. (2008) New 9- or 10-dentate luminescent lanthanide chelates. *Bioconjug Chem*. Vol. 19, pp. 1105-1111.

(91) Diamandis, E. (1991) Multiple labeling and time-resolvable fluorophores, *Clin. Chem.* Vol. 104, pp. 1486-1491

(92) Chen, J., and Selvin, P. R. (1999) Thiol-reactive luminescent chelates of terbium and europium. *Bioconjug Chem*. Vol. 10, pp. 311-315.

(93) Chen, J., and Selvin, P. R. (2000) Synthesis of 7-amino-4-trifluoromethyl-2-(1H)-quinolinone and its use as an antenna molecule for luminescent europium polyaminocarboxylates chelates. *J Photochem Photobiol A.* Vol. 135, pp. 27-32.

(94) Ge, P., and Selvin, P. R. (2004) Carbostyril derivatives as antenna molecules for luminescent lanthanide chelates. *Bioconjugate Chem*. Vol. 15, pp. 1088-1094.

(95) Selvin, P. R., and Hearst, J. E. (1994) Luminescence energy transfer using a terbium chelate: improvements on fluorescence energy transfer. *Proc Natl Acad Sci U S A.* Vol. 91, pp. 10024-10028.

(96) Li, M., and Selvin, P. R. (1995) Luminescent polyaminocarboxylate chelates of terbium and europium: The effect of chelate structure. *J. Am. Chem. Soc.* Vol. 117, pp. 8132–8138.

(97) Stein Henerson, R. B., Elderfield, R. C., and Fruton, J. S. (1950) In Heterocyclic Compounds. Ed.; Wiley & Sons, Inc.: London, Vol.1.

(98) Huisgen, R. (1984) 1,3-Dipolar Cycloadditions – Introduction, Survey, Mechanism. In 1,3-Dipolar Cycloaddition Chemistry. Padwa, A, Ed.; Wiley: New York, pp.1-176.

(99) Huisgen, R. (1961) *Proc. Chem. Soc*.Vol. 122, pp. 357-369.

(100) Rostovtsev, V., Green, L. G., Fokin, V. V., and Sharpless, K. B. (1967) *Angew. Chem.* Vol 102, pp. 2596-2599.

(101) Tornøe, C. W., Christensen, C., and Meldal, M. (2002) *J. Org. Chem.* Vol. 67, pp. 3057-3064.

(102) Laemmli UK (1970) Cleavage of structural proteins during the assembly of the head of bacteriophage T4". *Nature*, Vol.259, pp. 680–685.

(103) Pillai, S., Kozlov, M., Marras, S.A.E., Krasnoperov, L., and Mustaev, A. (2012) New Cross-linking Quinoline and Quinolone Derivatives for Sensitive Fluorescent Labeling. *J. Fluorescence.* Vol. 22, pp. 1021-1032.

(104) Wirpsza, L., Pillai, S., Batish, M., Marras, S.A.E., Krasnoperov, L., Mustaev, A. (2012) Highly Bright Avidin-based Affinity Probes Carrying Multiple Lanthanide Chelates. *J. Photochem. Photobiol.).* Vol. 116, pp. 22-29.

(105) Chamilos, G., Luna, M., Lewis, R.E., et al. (2006) Invasive fungal infections in patients with hematologic malignancies in a tertiary care cancer center: an autopsy *Haematol*. Vol. 91, pp. 986-989.

(106) Singh, N., Avery, R.K., Munoz, P. et al. (2003) Trends in risk profiles for and mortality associated with invasive aspergillosis among liver transplant recipients. *Clin Infect Dis*. Vol. 36, pp. 46-52.

(107) Wheat, L.J. (2003) Rapid diagnosis of invasive aspergillosis by antigen detection. *Transpl Infect Dis*. Vol. 5, pp. 158-166.

(108) Odabasi, Z., Mattiuzzi, G., Estey, E. et al. (2004) Beta-D-glucan as a diagnostic adjunct for invasive fungal infections: validation, cut off development, and performance in patients with acute myelogenous leukemia and myelodysplastic syndrome. *Clin Infect Dis*. Vol. 39, pp. 199-205.

(109) Maertens, J., Verhaegen, J, Lagrou, K., et al. (2001) Screening for circulating galactomannan as a noninvasive diagnostic tool for invasive aspergillosis in prolonged neutropenic patients and stem cell transplantation recipients: a prospective validation. *Blood*. Vol. 97, pp. 1604-10.

(110) Maertens, J., Theunissen, K., Verbeken, E. et al. (2004) Prospective clinical evaluation of lower cut-offs for galactomannan detection in adult neutropenic cancer patients and haematological stem cell transplant recipients. *Br J Haematol*. Vol. 126, pp. 852-860.

(111) Marr, K.A., Balajee, S.A., McLaughlin, L. et al. (2004) Detection of galactomannan antigenemia by enzyme immunoassay for the diagnosis of invasive aspergillosis: variables that affect performance. *J Infect Dis*. Vol. 190, pp. 641-9.

(112) Viscoli, C., Machetti, M., Cappellano, P. et al. (2004) False-positive galactomannan platelia *Aspergillus* test results *Clin Infect Dis*. Vol. 38, pp. 913-916.

(113) White, P.L., Mengoli, C., Bretagne, S., et al. (2011) Evaluation of Aspergillus PCR Protocols for Testing Serum Specimens. *J Clin Microbiol.* Vol. 49, pp. 3842-3845.

(114) Denning, D.W., Park, S., Lass-Florl, et al. (2011) High frequency triazole resistance found in non- culturable *Aspergillus fumigatus* from lungs of patients with chronic fungal disease. *Clin Infect Dis*. Vol. 52, pp. 1123-1129.

(115) Greene, R. (2005) The radiological spectrum of pulmonary aspergillosis. *Med Mycol*. Vol. 43 Suppl 1:S147-S154.

(116) Perlin, D.S. (2011) Echinocandin-resistant Candida: molecular methods and phenotypes. *Curr Fungal Infect Rep*. Vol. 5, pp. 113-119.

(117) Denning, D.W. Enchinocandin antifungal Drugs. (2003) *Lancet*. Vol. 362, pp. 1142-1151.